Artemis over-expression and radiosensitivity in human cell lines

A thesis submitted for the degree of Doctor of Philosophy

By

Gonul Ulus-Senguloglu

Brunel Institute for Cancer Genetics and Pharmacogenomics
Division of Biosciences
School of Health Sciences and Social Care

November 2012

Abstract

The cellular radiosensitivity of two fibroblast cell lines derived from a breast cancer patient that “over-reacted” to radiotherapy (84BR) and a patient with multiple independent tumours (175BR) was examined. Both patients had not been previously diagnosed with a mutation in any known DNA repair gene.

The clonogenic assay revealed the 84BR and 175BR cell lines were hypersensitive to gamma radiation when compared to repair normal NB1 and 1BR.3 fibroblast cells. In addition, DNA DSB repair was found to be defective in both patient cell lines due to the abnormal persistence of γ-H2AX foci over a 24 hour time point in the nuclei of gamma irradiated cells when compared to normal fibroblasts. Also normal response to the cross-linking agent nitrogen mustard in a clonogenic assay was observed in 84BR and 175BR cell lines indicating a normal homologous recombination (HR) DNA repair pathway (since HR is essential for DNA crosslink repair). From these data it was concluded that these cells were defective in one or more components of the Non Homologous End Joining (NHEJ) pathway.

The *Artemis* gene which has an endonuclease activity in the NHEJ repair pathway trims the ends of the double strand breaks before the two ends are ligated. Quantitative real time PCR analysis detected approximately 1.5 to 2 fold over-expression in *Artemis* gene in 84BR and 175BR cell lines compared to normal cells. Also an increase in the level of apoptosis before and following radiation exposure and a failure to efficiently repair DNA DSB were observed in the patient cell lines.

Consequently, it was demonstrated in the cell lines described in this study that increased expression of Artemis endonuclease leads to abnormal and illegitimate DNA DSBs due to unregulated action of the protein thus, contributing to increased radiosensitivity and elevated apoptosis.

Publications

1. Elevated expression of Artemis in human fibroblast cells is associated with cellular radiosensitivity and increased apoptosis. **G Ulus-Senguloglu**, CF Arlett, PN Plowman, J Parnell, N Patel, EC Bourton and CN Parris. British Journal of Cancer (2012) 107, 1506–1513. 2012.

2. Multispectral imaging flow cytometry reveals distinct frequencies of γ-H2AX foci induction in DNA double strand break repair defective human cell lines. Emma C. Bourton, Piers N. Plowman, Sheba Adam Zahir, **Gonul Ulus-Senguloglu**, Hiba Serrai, Graham Bottley, Christopher N. Parris, Cytometry Part A, Volume 81A, Issue 2, pg. 130-137, 2012.

Acknowledgement

I would like to express my sincere gratitude towards my supervisor Dr. Christopher Parris for his guidance, support and understanding especially during my pregnancy. His supervision was paramount for the completion of this project. I must extend my thanks to my group members, Hiba, Sheba and Dr. Emma Bourton for being an excellent team.

In addition, some members of the Institute have been very kind to extend their help at various phases of my research, so I want to thank Dr. Sahar Al-Mahdawi, Dr. Chiranjeevi Sandi and Dr. Rana Hassan on various helpful discussions, guidance and moral support, Dr. Hemad Yasaei and Dr. Terry Roberts for their valuable suggestions with quantitative PCR and Dr. Evgeny Makarov for his professional support during my pregnancy.

I like to thank all my friends Dr. Mengya Liu, Dr. Aycan Cinar, Maryam, Punam, Azadeh, Vahid, Yaghoub, Seda, Hassan, Chetana and Ane, for being great friends during my research.

I want to thank my husband, Mustafa Hayri, for his love, support, encouragement and patience which were undeniably the only drive that kept me going throughout my research. In addition, I want to extend my gratitude towards my in-laws. Finally, and most importantly, I would like to say a ‘big thank you’ to my beautiful daughter, Ezo Dilara, for putting a smile on my face every day.

Last but not the least, I want to humbly thank my parents Suleyman and Elif, and my dearest sister Belgin, for their faith in me and allowing me to be as ambitious as I want to be. It was under their watchful eye, especially from my mother, that I gained so much drive and an ability to tackle challenges head on. For these reasons and more, I would like to dedicate this project to my lovely mother.

Table of contents

Abstract ii
Publications iv
Acknowledgement v
Table of contents vi
List of Figures x
List of Tables xii
Abbreviations xiii
Chapter 1 - General Introduction 1
1.1 - DNA damage and repair 1
1.1.1 - Direct repair (DR) 4
1.1.2 - Base Excision repair (BER) 6
1.1.3 - Nucleotide excision repair (NER) 9
1.1.4 - Mismatch repair (MMR) 11
1.2 - DNA Strand breaks 14
1.2.1 - DSBs initiated by Oxidative Damage 15
1.2.2 - DSBs initiation in B and T cell development 19
1.3 - DSB repair mechanisms 20
1.3.1 - Non-Homologous End Joining (NHEJ) Pathway 20
1.3.1.1 - Ku Heterodimer 23
1.3.1.2 - DNA-Dependent Protein Kinase (DNA-PK) 25
1.3.1.3 - Artemis 26
1.3.1.4 - XRCC4, XLF and DNA Ligase IV complex 29
1.3.2 - Homologous Recombination (HR) Pathway 31
1.3.3 - Single-Strand Annealing (SSA) 33
1.4 - Radiosensitivity and human syndromes 36
1.4.1 - RS-SCID 37
1.4.2 - Ataxia Telangiectasia (A-T) 39
1.4.3 - Nijmegen Breakage syndrome (NBS) 41
1.4.4 - Bloom's Syndrome (BS) 43
1.5 - Over responders to radiotherapy 44
1.5.1 - 84BR and 175BR Patients 46
1.6 - Project Aim 49
Chapter 2 - Clonogenic assays 50
2.1 - Introduction 50
2.2 - Materials and Method 55

2.2.1 - Cell Lines 55
2.2.2 - Cell Culture....55
2.2.3 - Sub-culturing 56
2.2.4 - Cell Count 56
2.2.5 - Irradiation of cells 57
2.2.6 - Feeder Layers 57
2.2.7 - Clonogenic Cell Survival Assay with Gamma Radiation....58
2.2.8 - Clonogenic cell survival assay with Nitrogen Mustard 58
2.3 - Results....60
2.3.1 - Clonogenic cell survival assays - Gamma Radiation....60
2.3.2 - Clonogenic cell survival assays - Nitrogen Mustard 63
2.4 - Discussion 66
Chapter 3 - DNA DSB Assay (γ-H2AX detection)....68
3.1 - Introduction 68
3.1.1 - Techniques employed for the measurement of DNA DSBs....71
3.2 - Materials & Method 77
3.2.1 - Irradiation of cells 77
3.2.2 - Fixing of cells....77
3.2.3 - Permeabilisation and Blocking 77
3.2.4 - Immunostaning with Anti-γH2AX Antibody 77
3.2.5 - Mounting Slides....78
3.2.6 - Cell Scoring and Imaging 78
3.3 - Results....79
3.3.1 - -H2AX foci assay: DNA DSB repair....79
3.4 - Discussion 82
Chapter 4 - Quantification of NHEJ genes in radiosensitive cells by qRT-PCR....84
4.1 - Introduction 84
4.2 - Materials & Method 89
4.2.1 - RNA Extraction....89
4.2.1.1 - Cell Lysis....89
4.2.1.2 - Phase Separation....89
4.2.1.3 - RNA Precipitation....90
4.2.1.4 - RNA Wash and Re-suspension 90
4.2.2 - RNA Concentration and Purity Detection 91
4.2.3 - Deoxyribonuclease I, amplification grade treatment of RNA 91
4.2.4 - cDNA Preparation 92

4.2.4.1 - Annealing of Primers to RNA 92
4.2.4.2 - Synthesis of First Strand cDNA....92
4.2.4.3 - Determining the quality of cDNA 92
4.2.5 - Determining the quality of primers....93
4.2.6 - Determining the quality of PCR products 94
4.2.7 - Designing Primers for NHEJ repair genes....94
4.2.8 - Optimising Primer Concentration....96
4.2.9 - qRT-PCR....96
4.2.10 - qRT-PCR data analysis on SDS.3 Software 97
4.2.11 - Setting up the Dissociation Program 98
4.3 - Results....99
4.4 - Discussion 109
Chapter 5 - Artemis over-expression and Apoptosis in Radiosensitive cells 111
5.1 - Introduction....111
5.2 - Materials and Method 113
5.2.1- Transfection of NB1-Tert cells with *Artemis* cDNA 113
5.2.2- Maxi Preparation of Plasmid DNA 115
5.2.2.1 - Transformation of E.coli 115
5.2.2.2 - Growing Large Volume of Transformed Bacteria 116
5.2.2.3 - Purification of Plasmid DNA 116
5.2.3- Analysis of Purified Plasmid DNA....118
5.2.4- Agarose Gel Analysis of Purified Plasmid DNA 118
5.2.5- Co-transfection of NB1-Tert cells with pCMV6-XL5 *Artemis* cDNA 119
5.2.6- Isolation and Freezing of NB1-Tert Transfectants 119
5.2.7- Clonogenic assay – Surviving fraction at 2 Gy gamma irradiation....119
5.2.8- Quantitation of Artemis Protein Expression in Cells 120
5.2.9- Apoptosis Assay....121
5.2.10- Sample loading and data analysis....121
5.3 - Results....122
5.3.1 - Detection of plasmid Quality with Agarose gel 123
5.3.2 - Artemis Expression in Cells....123
5.3.3 - Radiation Sensitivity of *Artemis* Transfected NB1-Tert Cells....126
5.3.4 - Elevated Apoptosis in *Artemis* Transfected NB1-Tert Cells 128
5.3.5 - Apoptosis in radiation hypersensitive patient cells 130
5.4 - Discussion 133
Chapter 6 - General Discussion 136

Future Work 141
References.....143
Appendix 154

List of Figures

Figure 1.1	-	Repair of O^6 alkylguanine adducts by MGMT……	5
Figure 1.2	-	Model for BER pathway…….	8
Figure 1.3	-	Model for NER pathway…….	10
Figure 1.4	-	Human MMR……	13
Figure 1.5	-	Main steps involved in NHEJ……	22
Figure 1.6	-	Binding and bridging of DNA ends through Ku heterodimers……...	24
Figure 1.7	-	DNA-PK and Artemis mediated DNA end processing..	28
Figure 1.8	-	Main steps involved in HR…….	32
Figure 1.9	-	SSA model for repair of a two-ended DNA DSB……	34
Figure 1.10	-	Cancer Prone Kindred……	48
Figure 2.1	-	Sensitivity of 84BR and 175BR to IR Compare to Control Cell Lines…….	61
Figure 2.2	-	Sensitivity of 84BR and 175BR to HN2 Compare to Control Cell Lines……	64
Figure 3.1	-	Chromatin structure and histone-modifying enzymes..	69
Figure 3.2	-	Imagestream analysis of Gamma-H2AX foci in human cells……...	73
Figure 3.3	-	Fluorescence microscopy visualisation of comet assay……...	74
Figure 3.4	-	A model for PFGE……..	75
Figure 3.5	-	DSB repair measured by formation and disappearance of γ-H2AX foci in radiosensitive cells and controls…….	80
Figure 4.1	-	Steps in nucleic acid quantification by real time PCR..	86
Figure 4.2	-	Total RNA for NB1, 1BR.3, 84BR and 175BR samples.....	100
Figure 4.3	-	cDNA samples for GAPDH in patient and control cells	101
Figure 4.4	-	Primers at 10μM concentration……	102

Figure 4.5	-	Melting curve showing the primer dimer with GAPDH at 10μM concentration……...	103
Figure 4.6	-	Primers run at 10μM concentration on 1% agarose gel	104
Figure 4.7	-	GAPDH run at 5μM and remaining primers run at 10μM concentration……	105
Figure 4.8	-	NHEJ gene expression in 84BR radiosensitive fibroblasts…….	106
Figure 4.9	-	NHEJ gene expression in 175BR radiosensitive fibroblasts…….	107
Figure 5.1	-	Map of pCMV6-XL5……	113
Figure 5.2	-	Map of Plasmid pPur……..	114
Figure 5.3	-	Agarose gel analysis of the purified plasmids……	123
Figure 5.4	-	Representative images of NB1-Tert cells stained for Artemis……	126
Figure 5.5	-	The γ-radiation sensitivity of *Artemis* transfectants…	127
Figure 5.6	-	Apoptosis in the NB1-Tert cells transfected to over-express the Artemis protein……..	128
Figure 5.7	-	Non-apoptotic and cells at different stages of apoptosis……..	129
Figure 5.8	-	Apoptosis in patient and in control cells……..	131

List of Tables

Table 1.1 -	Principal of DNA-damaging agents, lesions & repair pathways……	2
Table 1.2 -	Review of DNA repair genes and their activity in DNA repair……..	3
Table 1.3 -	Radiosensitivity associated disorders……...	36
Table 1.4 -	NTT (Skin) following radiotherapy……..	44
Table 2.1 -	The Dose of radiation required to reduce cell survival in a clonogenic assay to 10% (D10) in patient and control cells……..	62
Table 3.1 -	The γ-H2AX foci formation following 2Gy of gamma irradiation in irradiated patient and control cells…….	81
Table 4.1 -	NHEJ repair genes and their locations on different chromosomes……..	85
Table 4.2 -	PCR amplification cycles for detection of cDNA quality…	93
Table 4.3 -	PCR amplification cycles for detection of primer quality...	93
Table 4.4 -	Primer sequences used for the amplification of NHEJ genes during qRT-PCR analysis…….. …	95
Table 4.5 -	PCR reaction conducted at 10µM primer concentration...	96
Table 4.6 -	The thermal profile set for the qRT-PCR reaction……...	97
Table 4.7 -	The thermal profile set for the dissociation curve……...	98
Table 5.1 -	Artemis expression in all cell lines determined by imaging flow cytometry…….....	124

Abbreviations

AB	Applied Biosystems
ALL	Acute lymphoblastic leukemia
ALS	Alkali site
AP	Apurinic/apyrimidinic
APE1	AP endonuclease 1
A-T	Ataxia telangiectasia
ATM	Ataxia telangiectasia-mutated
ATR	Ataxia and Rad3 related
BER	Base excision repair
BRCA1	Breast cancer associated gene 1
BRCA2	Breast cancer associated gene 2
BRCT	BRCA1 COOH-terminal domain
BS	Bloom's syndrome
CO_2	Carbon dioxide
cDNA	Complementary DNA
CS	Cockayne syndrome
CFA	Colony forming assay
CCD	Cooled charge-coupled device
CMP	Common myeloid progenitor
Ct	Cycle threshold
CPD	Cyclobutane pyrimidine dimer
CMV	Cytomegalovirus
DRAQ5	Deep red fluorescing bisalkylaminoanthraquinone
DAPI	4'6-diamidino-2 phenylindole
DNA	Deoxyribonucleic acid
DNA SSB	DNA single strand break
dRP	Deoxyribophosphate
DSB	Double strand break
DEPC	Diethyl pyrocarbonate
DMSO	Dimethylsulphoxide
DR	Direct repair
DDR	DNA damage response

DNA-PK	DNA-dependent protein kinase
DNA-PKcs	DNA-protein kinase catalytic-subunit
DMEM	Dulbecco modified eagle medium
dsDNA	Double strand DNA
D_{10}	Dose, required to reduce colony survival to 10%
EBV	Epstein-Barr virus
E.coli	Escherichia coli
EtBr	Ethidium bromide
EDTA	Ethylene-diamine-tetra-acetic-acid
ERCC	Excision repair cross complementing
FISH	Fluorescence in-situ hybridisation
FEN-1	Flap structure-specific endonuclease 1
Gy	Gray
GG-NER	Global genome nucleotide excision repair
GAPDH	Glyceraldehyde-3-phosphate dehydrogenase
GMP	Granulocyte/macrophage progenitors
IC_{50}	Half maximal inhibitory concentration
HTH	Helix turn helix
HNPCC	Hereditary non-polyposis colorectal cancer
HBV	Hepatitis B virus
HSPC	Hematopoietic stem cell
HCA	Heterocyclic amine
HR	Homologous recombination
OH	Hydroxyl
H_2O_2	Hydrogen peroxide
HPV	Human papilloma virus
hTERT	Human telomerase reverse transcriptase
oh'Gua	8-hydroxyguanine
IR	Ionising radiation
ICL	Interstrand cross link
IMS	Industrial methylated spirit
LENT SOMA	Late effects in normal tissues subjective, objective, management and analytic scale
LMDS	Locally multiple damaged sites

LET	Linear Energy Transfer
LB	Luria-Bertani
mTOR	Mammalian target of rapamycin
CH_3-	Methyl group
D_0	Mean lethal radiation dose
MGMT	Methylguanine-DNA metyl-transferase
MLPA	Multiplex ligation-dependent probe amplification
MSH	MutS homologue
MTT	3-(4,5-dimethylthylthiazol-2-yl)-2,5-dithenyltetrazolium
MAC	Multiple cloning site
MMR	Mismatch repair
NCBI	National Centre for Biotechnology Information
NOC	N-nitroso compounds
NHEJ	Non-homologous end joining
NO_2	Nitrogen dioxide radical
HN2	Nitrogen mustard
NBS	Nijmegen Breakage Syndrome
NTT	Normal tissue toxicity
NTC	Non template control
NER	Nucleotide excision repair
$ONOO^-$	Peroxynitrite anion
PBS	Phosphate buffer saline
6-4PPs	Photoproducts
PIKK	Phosphatidylinositol-3-kinase
PE	Plating efficiency
Pol β	Polymerase β
PCR	Polymerase chain reaction
PCNA	Proliferating cell nuclear antigen
PFGE	Pulsed field gel electrophoresis
qRT-PCR	Quantitative real time PCR
RDS	Radio- resistant DNA synthesis
RT	Radiotherapy
RS-SCID	Radiosensitive severe-combined immunodeficiency
RTOG	Radiotherapy oncology group

RAG	Recombinase activating gene
ROS	Reactive oxygen species
RFC	Replication factor C
RPLD	Repair of potentially lethal damage
RPA	Replication protein A
Rpm	Revolutions per minute
RNS	Reactive nitrogen species
RNA	Ribonucleic acid
RNAPII	RNA polymerase II
SCID	Severe-combined immunodeficiency
SDS	Sequence Detection System
SSB	Single strand break
SSA	Single strand annealing
SCGE	Single-cell gel electrophoresis
ssDNA	Single strand DNA
SDS	Sodium dodecyl sulphate
SD	Standard deviation
SE	Standard error
SEM	Standard error of mean
SMG-1	Suppressor of morphogenesis in genitalia 1
SRB	Sulforhodamine B
TFIIH	Transcription factor IIH
TCR	T cell receptor
TC-NER	Transcription-coupled nucleotide excision repair
TRRAP	Transformation/transcription domain-associated protein
TBS	Tris buffered saline
UV	Ultra violet
V (D) J	Variable (diversity) joining
XP	Xeroderma pigmentosum
WS	Werner syndrome
XRCC4	X-ray cross complementing 4
XLF	XRCC4 like factor
XP	Xeroderma Pigmentosum

Chapter 1 - General Introduction

1.1 - DNA damage and repair

To achieve a successful flow of genetic information from DNA, genetic stability and physical integrity of the DNA must be protected from DNA damaging agents. Although the DNA is a stable molecule and has sophisticated DNA repair systems to protect it from DNA damaging agents, the DNA is subject to exposure by exogenous or endogenous damage at all times which cause damage. The modifications made within the DNA, unlike some molecules such as, proteins and lipids where the damage is readily degraded and resynthesized, is permanent via the formation of mutations (Bohr and Dianov 1999). Although, all DNA lesions pose a threat to genetic integrity, DNA double strand breaks (DSBs) are considered especially deleterious as they can be potentially lethal if not repaired (Weterings and van Gent 2004). Also as Tauchi *et al.,* (2002), states even one DSB generated in a cell, if not successfully re-joined, can potentially result in cellular lethality.

Some of the main exogenously occurring DNA damaging agents have been well characterised. These are ultra violet (UV) light, ionising radiation (IR), aflatoxins (a strongly carcinogenic mould produced contaminant) found in contaminated peanuts, hetrocyclic amines (HCA) in over-cooked meats, N-nitroso compounds (NOC) found in tobacco (Wogan *et al.,* 2004; Jackson and Bartek 2009). The endogenous DNA damaging agents are reactive oxygen species (ROS), which are produced by normal oxidative metabolism and cause DNA base modification and strand breaks (reviewed in Valko *et al.,* 2007)

However, depending on the type of DNA damage, the cells have evolutionary conserved specific DNA damage recognition and repair mechanisms that are activated and put into action for the repair of vast number of DNA damage. Some of the most common DNA damaging agents, the types of DNA lesions introduced and the specific DNA damage repair pathways are summarised in Table 1.1.

Table 1.1 - Principal of DNA-damaging agents, lesions & repair pathways.

Damaging Agent	**DNA Lesion**	**Repair Pathway**
IR Anti-tumour agents	DSBs	HR NHEJ
Spontaneous reactions Oxygen radicals Alkylating agents X-rays	Abasic site Oxidised deaminated and alkylated bases ssDNA breaks	BER
UV light	6-4 photoproduct Cyclobutane pyrimidine dimer Bulky adduct	NER
Replication and recombination errors	Base mismatches Insertion Deletion	MMR

HR, Homologous Recombination; **NHEJ,** Non-homologous End Joining; **BER,** Base Excision Repair; **NER,** Nucleotide Excision Repair; **MMR,** Mismatch Repair (Scharer 2003).

As mentioned, depending on the type, extent and the location of the DNA damage, specific DNA repair mechanisms are activated within the cell to recognise, signal and repair the DNA damage. This distinctive nature of the DNA repair is gained through the presence of more than a hundred DNA repair genes whose proteins are equipped with different functions in the DNA repair process. Some of these DNA repair genes discovered since 2001 are illustrated in Table 1.2.

Table 1.2 - Review of DNA repair genes and their activity in DNA repair.

DNA repair Mechanisms	DNA repair genes	Activity	References
NHEJ	Ku70 & Ku80 DNA-PKcs Artemis XRCC4 & XLF Ligase IV	Non-specific dsDNA end binding Bridging of the DNA ends Trimming of the DNA ends Processing and gap filling Sealing the nick and repair break	(Hefferin and Tomkinson 2005)
HR	RAD50 RAD51 & RAD54 RAD52 BRCA1 & BRCA2 Mre1	Form a nuclease complex Required for homologous pairing Enhance the activity of RAD51 Recruits repair proteins to DNA damage site Forms a nuclease complex with Rad50 & NBS1	(Krejci *et al.,* 2012)
Direct repair	MGMT	O^6-meG alkyltransferase	(Hegi *et al.,* 2008)
MMR	MutSα & MutLα EXO1 RPA PCNA RFC Pol δ DNA Ligase	Binds mismatches Coordinates multiple steps in MMR Performs 3'-5' excision of ssDNA Activated by MutSα Stabilises single-stranded gap DNA repair synthesis Seals the nick to complete the repair	(Jiricny 2006; Hsieh and Yamane 2008)
NER	XPC-hHR23B XPB & XPD XPA XPG,XPF,ERCC1 DNA Pol ε δ, PCNA, RPA, RCF	Involved in damage recognition Promotes bubble formation Directs recruitment of other NER proteins Excises the damaged strand Excises and restores the nucleotide gap - generated by XPG,ERCC1,XPF	(Friedberg 2001)
BER	Glycosylase APE1 Pol β, polδ/ε Ligase III/Ligase I XRCC1 FEN1	Recognises and removes damaged bases Targets AP sites & creates a 5'dRP group Fills the gap by adding nucleotide in the gap Seals the DNA ends Seals the DNA ends Removes the flap structure	(Dianov *et al.,* 1998)

ERCC1, excision repair cross-complementing 1; **PCNA,** proliferating cell nuclear antigen; **POL**, polymerase; **RFC,** replication factor C; **RPA,** replication protein A; **TFIIH,** transcription factor IIH; **XP,** xeroderma pigmentosum; **APE1,** apurinic endoduclease 1; **XRCC1,** X-ray repair cross-complementing group 1; **FEN 1,** flap endonuclease 1, **EXO1,** Exonuclease 1; AP, apurinic/ apyrimidinic, **BRCA 1,** Breast cancer associated gene 1; **BRCA 2,** Breast cancer associated gene 2; **XRCC4,** X-ray cross complementing 4; **XLF,** XRCC4 like factor, **MGMT,** Methylguanine-DNA methyl-transferase.

1.1.1 - Direct repair (DR)

The alkylating agents (e.g. methylating and chloroethylating anticancer drugs) or naturally occurring metabolic processes damage cellular macromolecules of DNA via a unimolecular nucleophilic substitution reaction (S_N1 reaction) and thus, have a strong affinity towards oxygen atoms in DNA (Kaina *et al.,* 2010). The S_N1 reaction is where a functional group in a reaction is replaced by another group, so in this case the oxygen group in guanine, which is biologically most important position (Kaina *et al.,* 2010), may be substituted with O^6-alkylating agents such as; methyl group (CH_3-) (inserted by methylating agents) or chloroethyl group (inserted by chloroethylating agent) at the O6 position of guanine. Both of these adducts are directly repaired by the suicide enzyme, O^6-methylguanine-DNA metyl-transferase (MGMT). This DNA repair process is a single step reaction which involves direct reversal of the DNA damage into original form. The MGMT specifically removes the CH_3 group from the O6 position of guanine, thereby restoring the nucleotide to its native form without causing any DNA strand breaks (Hegi *et al.,* 2008). The adduct thymine on O4 position on DNA may also be removed by MGMT. As stated by Silber *et al.,* (2012) during this single step reaction the CH_3- group from O^6 -methyl guanine and O^{4-} thymine are transferred from the alkylated bases onto cysteine residues which results in the restoration of guanine in the DNA and irreversible activation of MGMT. This reaction is illustrated for removal of CH_{3-} group in Figure 1.1.

.

Figure 1.1 - Repair of O^6-alkylguanine adducts by MGMT.

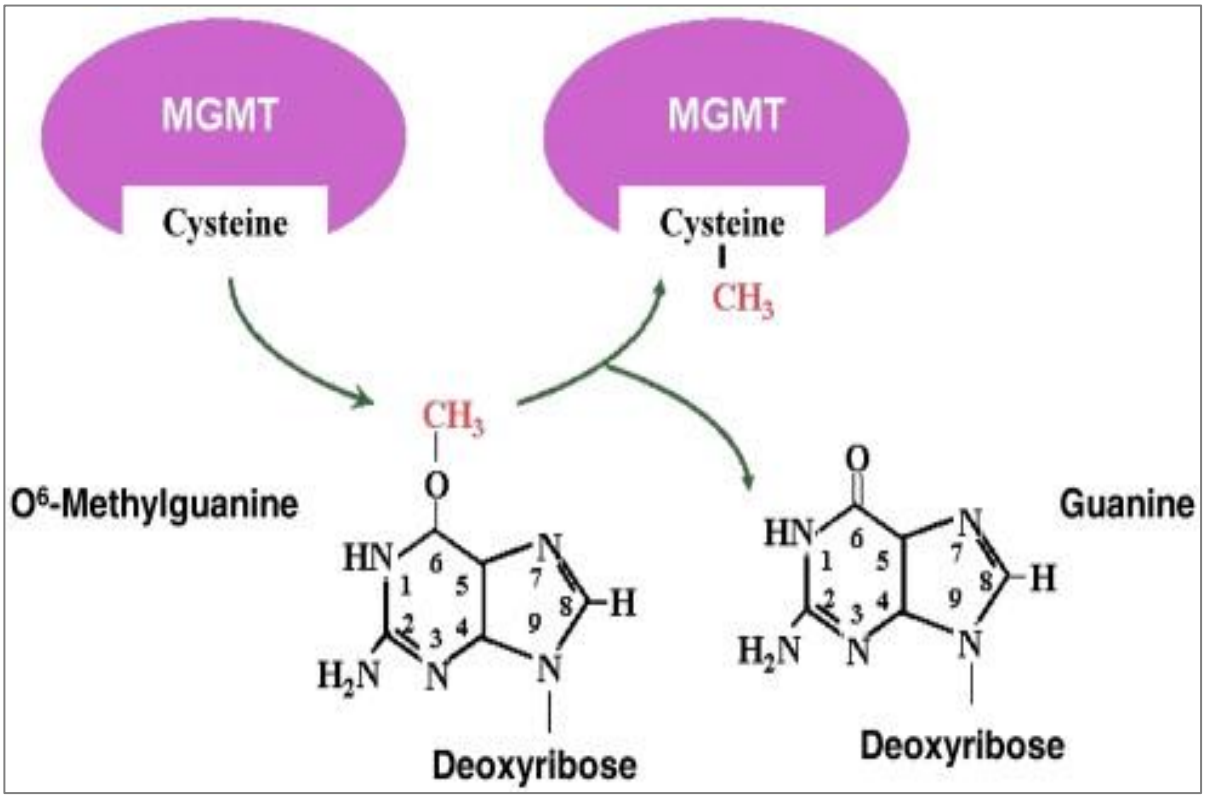

The CH3- group at the O6 position of guanine (O^6-Methylguanine) pairs with thymine rather than cytosine. MGMT repairs this damage and protects the DNA by transferring the CH3-group to a cysteine residue in the protein (Silber *et al.,* 2012).

This enzyme accepts the CH3- group from the lesion in a stoichiometric reaction of 1:1 and undergoes ubiquitination and proteasome-mediated degradation. Thus, when the active MGMT enzyme accepts the CH3- it gets degraded and not regenerated i.e. undergoes suicidal reaction (Rasimas *et al.,* 2004; Kaina *et al.,* 2010). Also the MGMT catalyses the stoichiometric transfer of a variety of alkyl substituents from the O6 position of guanine to an active-site cysteine and prevents incorrect base pairing caused by these adducts (Rasimas *et al.,* 2004).

Although the alkylating agents are important drugs in cancer chemotherapy, their effectiveness is strongly influenced by MGMT DNA repair protein. For example, in both methylating and chloroethylating agents, the MGMT can eliminate the initial O^6 -alkylguanine damage in DNA, and thus preventing toxicity to cells (Verbeek *et al.,* 2008). So, while the removal of adducts by MGMT is beneficial for normal cells, it allows development of resistance to DNA damage in cancer cells (Kaina *et al.,* 2010).

1.1.2 - Base Excision repair (BER)

Base damage, single strand breaks (SSBs), O^6-methylguanine, 8-oxoguanine, uracil, thymine glycol, and apurinic/apyrimidinic (AP) sites are common lesions subject to repair by BER (David *et al.,* 2007; Dianov and Parsons 2007). The majority of these non-bulky lesions are repaired by four proteins found in BER pathway. These include, a DNA glycosylase, an AP endonuclease or AP DNA lyase, a DNA polymerase, and a DNA ligase (reviewed in Robertson *et al.,* 2009). These proteins are able to remove a single or a small subset of chemically altered damaged base and replace it with the correct bases. The BER of DNA damage by glycosylase and AP endonuclease is illustrated in Figure 1.2.

Here the specific damaged bases are recognised by glycosylases, excised and both long patch and short patch BER is initiated. This enzyme cleaves then effectively removes damaged bases and thus, creates an AP site. The DNA backbone is cleaved by DNA AP endonuclease (Robertson *et al.,* 2009). The cleavage by one of these enzymes generates a DNA SSB. In short patch BER pathway, the Polymerase

β (Pol β) removes the 5'-terminal deoxyribophosphate (dRP) and adds one nucleotide into the single nucleotide gap. Then, XRCC1-Lig III complex seals the DNA end. Although, the decision to proceed via the long patch or short patch BER mechanism is poorly understood (Robertson *et al.,* 2009) Dianov (2011) proposes that if the 5'- sugar phosphate is resistant to cleavage by Pol β, then the long patch BER pathway is initiated where, the Pol δ/ε adds 2-8 more nucleotides into the repair gap, generating a flap structure that is removed by flap structure-specific endonuclease 1 (FEN-1) in a proliferating cell nuclear antigen (PCNA) dependent manner. Ligase I then seals the remaining DNA ends.

Figure 1.2 - Model for BER pathways.

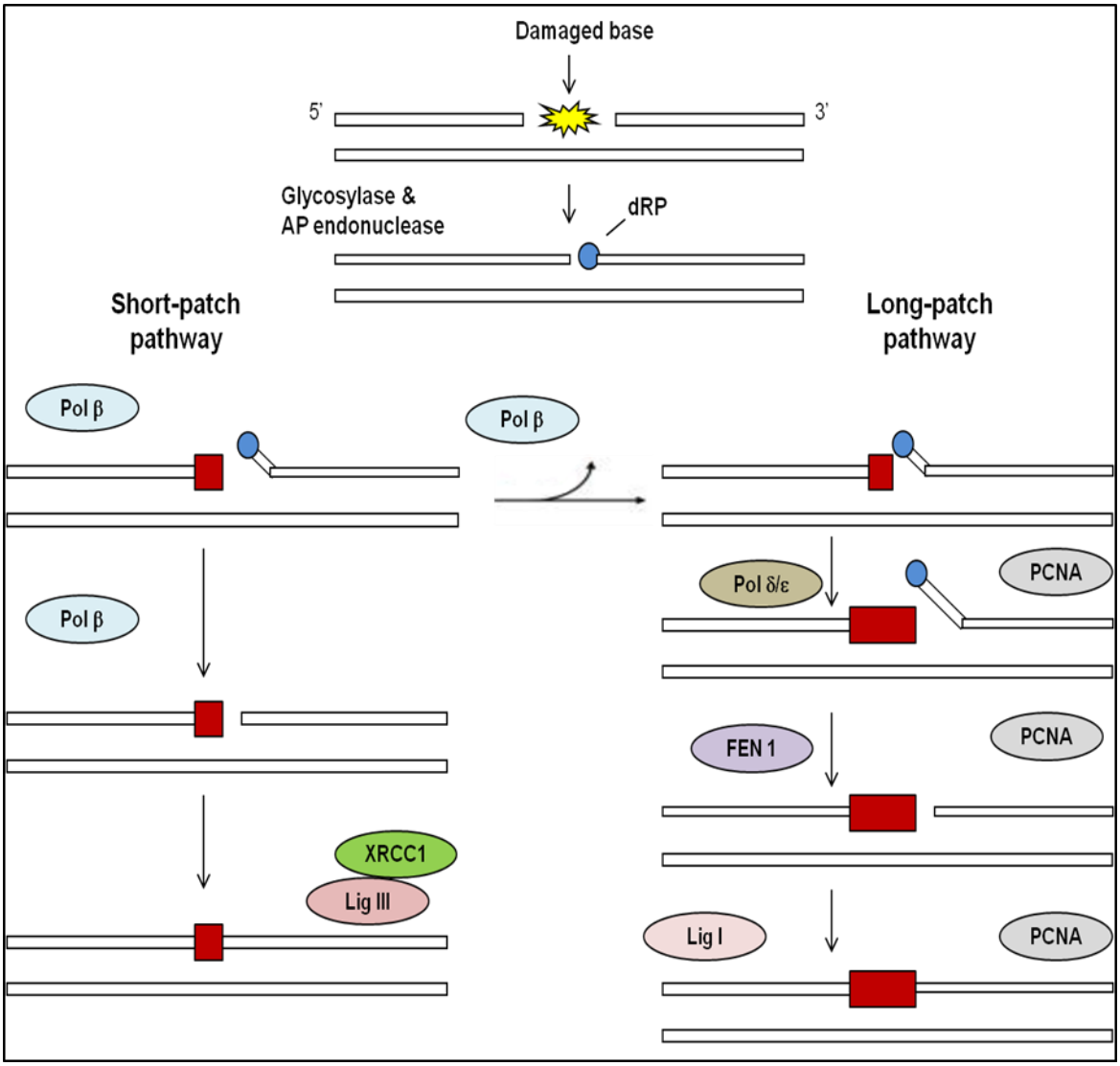

The glycosylase and AP endonuclease first excise the damaged base then incise the arising abasic site, respectively generating a DNA SSB with a 5'- sugar phosphate (blue circle). The repair is completed via short or long patch pathways. Red blocks indicate the incoming nucleotide(s), the size of the blocks represent the number of nucleotides added by the DNA polymerases (adapted from Dianov 2011).

1.1.3 - Nucleotide excision repair (NER)

NER is a highly versatile and sophisticated DNA damage removal pathway that counteracts the deleterious effects of a multitude of DNA lesions, including the major types of damage induced by environmental sources (de Laat *et al.,* 1999). The most relevant lesions repaired by NER are the UV induced cyclobutane pyrimidine dimers (CPDs) and (6-4) photoproducts (6-4PPs) (Wood 1997; de Laat *et al.,* 1999).

There are two sub-pathways of mammalian NER. 1) Global genome nucleotide excision repair (GG-NER) which repairs DNA lesions throughout the genome. 2) Transcription-coupled nucleotide excision repair (TC-NER) which is confined to repair of DNA lesions in transcribed strands (Fousteri and Mullenders 2008). The XPC-RAD23B and UV-DDB complexes recognise and bind to DNA damage-mediated helix distortion and initiate GG-NER while the TC-NER is triggered by blockage of elongating RNA polymerase II complex (RNAPIIo) and interactions of CSB and XPG proteins (the XPG having more stable interaction) with the RNA pol. Then, the CSF recruits HMGN1, XAB2 and TFIIS to enable cleavage of protruding 3'mRNA by RNAPIIo for resumption of transcription upon lesion removal (Fousteri and Mullenders 2008). Once the lesion has been recognised, all subsequent steps leading to assembly of functional NER complex, requires the same NER core factors in GG-NER and TC-NER. The UV-DDB and XPC-RAD23 recruit the basal transcription factor TFIIH. The TFIIH complex, which has two DNA helicase activities (XPB and XPD) unwinds the DNA duplex in the immediate vicinity of the base damage, and generates a bubble in DNA. Then the ERRCC1-XPF and XPG DNA endonucleases cut the damaged strand at 3' and 5' sides of the damage. This incision generates an oligonucleotide fragment (~27-30 nucleotides in length)

containing the damaged bases. This fragment is excised and the 27-34 nucleotide gap is repaired by DNA polymerases δ or ε as well as the PCNA and replication factor C (RFC). The damaged DNA is then sealed by DNA ligase I or ligase III. This process of DNA damage recognition and removal by NER pathway is summarised in Figure 1.3.

Figure 1.3 - Model for NER pathway.

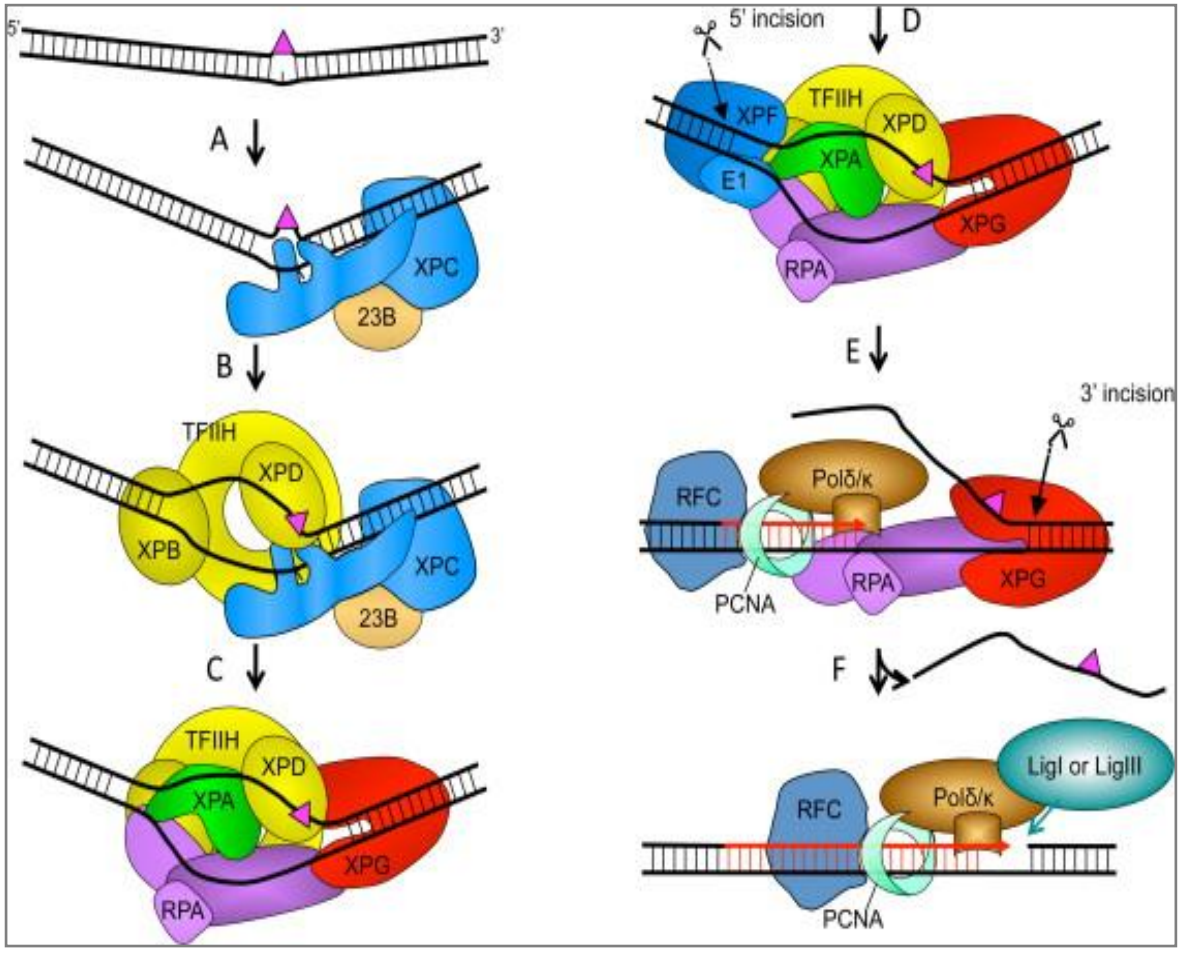

XPC-R23 complex recognises the bulky lesion and binds to the undamaged strand of DNA (A), TFIIH is recruited to the site (B), the lesion is verified by XPD leading to formation of the pre-incision complex through interaction with XPD resulting in the recruitment of XPA, RPA and XPG (C), the XPF is recruited to the pre incision complex through interaction with XPA leading to DNA incision 5' (D), which produces a free 3'-OH group available for initiation of repair synthesis by the replication machinery, and in turn triggers 3' incision by XPG (E). DNA ligase III or ligase I seals the nick to complete the process (F) (Fagbemi *et al.,* 2011)

Deficiency in TC-NER is associated with mutations in the CSA and CSB genes that give rise to a rare disease Cockayne syndrome (CS) (Fousteri and Mullenders 2008).

1.1.4 - Mismatch repair (MMR)

MMR system is employed to detect and repair base-base mismatches and insertion-deletion loops that escape their exonucleolytic proofreading activity during DNA replication (Jiricny 2006). Once the error is detected the mistake is excised, and the gaps are filled in with correct sequences.

Mismatch recognition in human cells is predominantly mediated by MutS homologue (MSH), heterodimer proteins containing MSH2 and MSH6 subunits. The MSH2 heterodimerises with MSH6 or MSH3 to form MutSα or MutSβ respectively, both of which are ATPases that play a critical role in mismatch recognition and initiation of repair (Li 2008). The MSH heterodimer subunits undergo an ATP-dependent conformational change, which recruits the MLH heterodimer containing MLH1/PMS2 subunits. The MSH/MLH complex is translocated towards the strand cut (such as a gap between Okazaki fragments) and eventually encounters proliferating cellular nuclear antigen (PCNA). PCNA interacts with MSH2 and MLH1 and is thought to play roles in the initiation and DNA re-synthesis steps of MMR. It has been proposed that PCNA may help localise MutSα and MutSβ to mispairs in newly replicated DNA.

While PCNA is essential for 3'- directed MMR the EXO1 is essential in both 3'-and 5'-directed MMR. For 5' directed MMR the excision is straight forward by the 5' to 3 exonuclease activity of EXO1. For 3'-directed MMR, the endonuclease function of

PMS2 is activated by presence of the 3’ nick, and stimulated by RFC, PCNA and ATP to introduce a second nick 5’ to the mismatch. The replication factor C (RFC) dependent endonuclease activity plays a critical role in 3′ nick-directed MMR involving EXO1 (Li 2008).

MSH2-MSH6 preferentially recognises base-base mismatches and insertion-deletion loops of 1-2 nucleotides while MSH2-MSH3 has preferences for larger insertion-deletion loops. DNA polymerse fills the gap by synthesis of new DNA and DNA ligase seals the ligation. A model for MMR is illustrated in Figure 1.4.

Figure 1.4 - Human MMR.

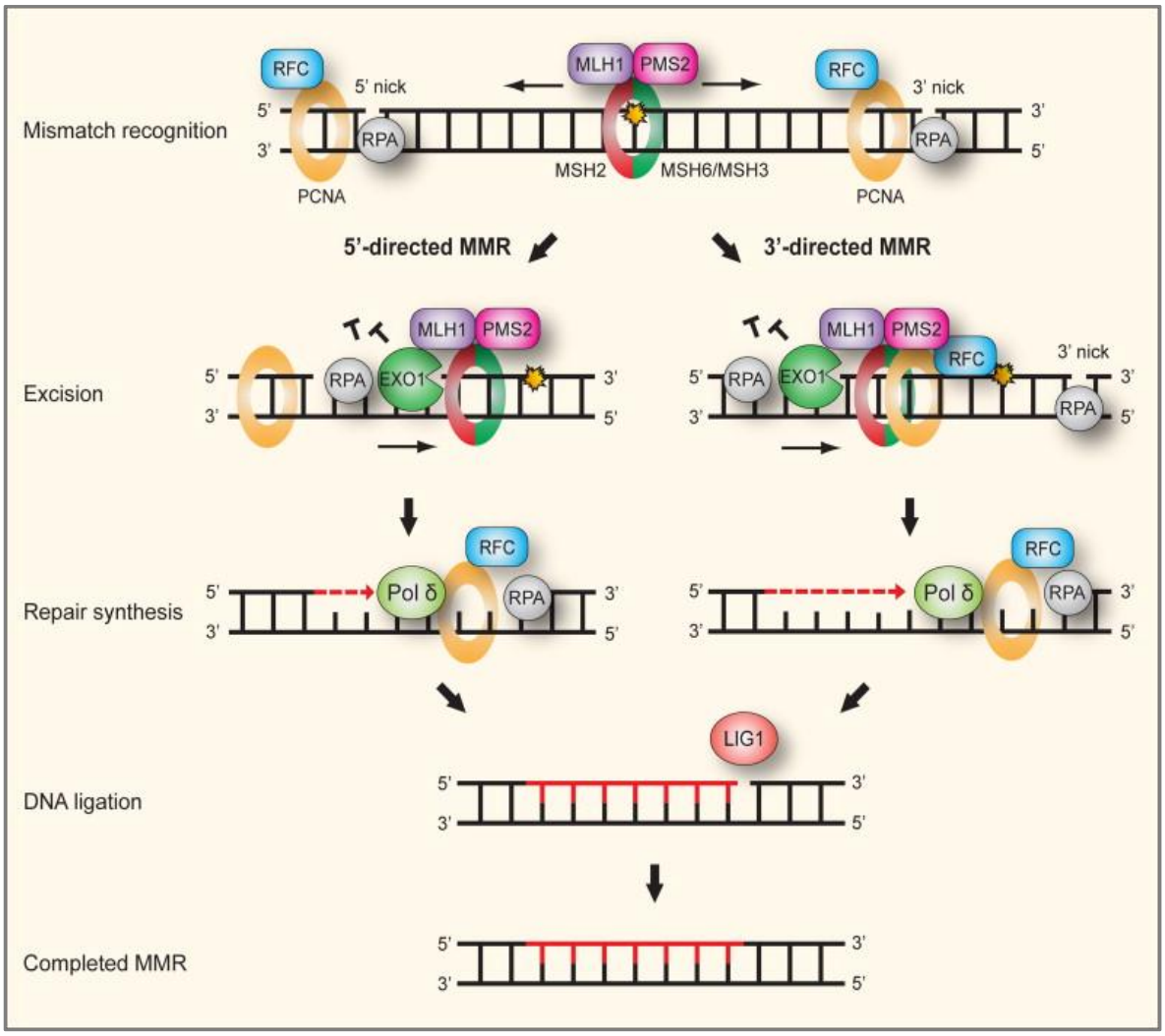

The MSH2-MSH6 or MSH2-MSH3 heterodimeric ATPase complex recognises and binds to the mismatch and recruits the MLH1-PMS2 complex. The PCNA clamp recruits MMR proteins to the replication fork while the clamp loader RFC loads PCNA. RPA binds to single stranded DNA during the excision and facilitates the DNA repair synthesis by Polδ. Finally Lig 1 ligates remaining nicks after synthesis is performed (Jeppesen *et al.,* 2011).

Mutations in MMR genes (hMLH1 and hmSH2) may cause hereditary non-polyposis colorectal cancer (HNPCC) and familial non-HNPCC which is associated with microsatellite Instability (Jiricny and Nystrom-Lahti 2000; Jiricny and Marra 2003; Boland and Goel 2010).

1.2 - DNA Strand breaks

DNA DSBs occur when the sugar backbones of both strands are broken close enough to disrupt the Watson-Crick base pairing, resulting in the liberation of two DNA ends (Bassing and Alt 2004). DSBs can be generated by; exposure to IR, certain classes of anticancer chemotherapeutic drugs such as alkylating agents, as a consequence of normal cellular oxidative metabolism, the action of recombinase activating gene (RAG)-mediated VDJ recombination during the process of immunoglobulin production (Ramsden *et al.,* 2010). In addition, the DSBs are formed from combination of two independently induced single strand breaks that occur within about 10 base pairs of each other (Chadwick 1994). Also the DSB formation is a conserved step in the initiation of meiotic recombination (Richardson *et al.,* 2004).

Although, the DSB is considered the most difficult lesion to repair eukaryotic cells have evolved specialised and redundant systems to detect and repair chromosomal DSBs within the context of normal G1/S, intra-S, and G2/M checkpoints (Bassing and Alt 2004).

Some of the well-known agents that cause DSBs and different types of DSB repair pathways (with main focus on NHEJ repair pathway) will be described next.

1.2.1 - DSBs initiated by Oxidative Damage

When a high-energy radiation strikes molecules in its path, electrons may be displaced from atoms within the molecule. Thus, result in loss of one or more electrons and conversion of electrically neutral molecules to one that carry electrical charge. This is known as an ionising radiation event. Unlike some chemical agents, whose damaging potential are strongly dependent on diffusion processes and thus may be affected by sub-cellular structures, the IR is typically highly penetrating and the ionisation events are complete within a few microseconds at the site of the molecule which it anticipates to damage. The energy deposited in cells depends on the level of dose range which the cell is exposed to over a length of its decay tract. Thus the measure of energy transfer as an ionising particle to any material is referred to as Linear Energy Transfer (LET) which is usually expressed in units of kilo-electron volts per micrometre (keV/μ) (Leonard *et al.,* 2004).

The radiation may be in the form of an atomic particle such as alpha (α) and beta (β) particles or in the form of an energy wave such as X and gamma (γ) rays. The γ-rays penetrate a higher energy radiation compared to other forms of radiation. The radiation absorbance dose, i.e. the amount of energy that IR deposits in a unit of mass of matter such as human tissue, is expressed in a unit called gray (Gy), where 1 gray is equal to 1 joule per kilogram or miligray which is one thousandth of a Gy.

The oxidative damage may be induced as a consequence of normal metabolism, inflammation and IR. The oxidative damage induced by normal metabolism is not as harmful to the cell as the IR induced damage since the previous occur at relatively isolated positions along the DNA molecule, whereas, the IR deposits the energy

unevenly and tend to create clusters of radicals around the DNA leading to multiple independent lesions within a localised region of DNA. As reviewed by Ulsh (2010), the randomly deposited energy by IR produces clustered DNA damage, also known as locally multiple damaged sites (LMDS), which is essentially several regions of DNA damage within a short DNA segment. The LMDS was initially introduced by Ward (1985). Some of these lesions are the abasic sites (separation of a base from the sugar, leaving behind an unpaired base), base alterations (additional bonds between atoms or new chemical groups attach to the base) or single (a strand break in the phosphodiester backbone) and DSBs in the DNA. Also, two or more DNA lesions of the same or different nature may be produced in close proximity to each other on opposite DNA strands (also known as bi-stranded lesions), generally within one-two helical turns of the DNA molecules (Hada and Georgakilas 2008).

Ionising radiation can also impair or damage DNA when alpha particles, beta particles or x-rays create ions which physically break one or both of the sugar phosphate backbones or break the base pairs of the DNA.

Since, water is the largest component in the cell the charged molecules converted from neutral atom interacts mostly with the water molecule (a process known as radiolysis) and generates intermediates called reactive oxygen species (ROS). The ROS create free radicals (a highly unstable, reactive molecule that poses an unpaired electron) such as, hydrogen peroxide (H_2O_2), hydroxyl radical ($OH^{\cdot}$) and superoxide radical ($O^{-}_{2}{}^{\cdot}$), which damages the DNA. Thus, the removal of electrons by species such as the free radicals, a process called oxidation, is one of the main causes of mutations in DNA.

The superoxide anion, arising either through metabolic processes or following oxygen “activation” by physical irradiation, is considered the “primary” ROS, and can further interact with other molecules to generate “secondary” ROS, either directly or prevalently through enzyme or metal-catalysed processes (Valko *et al.,* 2007).

For example, when cells *in vivo* are under stress, an excess of superoxide release free contaminated iron molecules. The released Fe2+ then participate in the Fenton reaction (Fe2+ +H2O2→Fe3+ + •OH+OH−), generating highly reactive hydroxyl free radical ($OH^{\cdot}$) which can easily break the DNA chemical bonds (Valko *et al.,* 2007).

According to Leonard *et al.,* (2004), the H_2O_2 is not a free radical and does not react directly with biomolecules, however, it is biologically significant as it interacts with superoxide in the presence of transition metals, such as iron and copper and leads to formation of highly reactive and most deleterious ROS and $OH^{\cdot}$ through the Haber-Weiss reaction. The superoxide radical also participates in the Haber–Weiss reaction (O2•− +H2O2→O2 + •OH+OH−) which combines a Fenton reaction and the reduction of Fe3+ by superoxide yielding Fe2+ and oxygen (Fe3++O2•−→Fe2+ +O2) (Valko *et al.,* 2007).

Certain viruses such as the human papilloma virus (HPV), Epstein-Barr virus (EBV), hepatitis B virus (HBV), human T-lymphotropic virus type 1 (HTLV-1) integrate their genome in DNA. According to Williams *et al.,* (2011), the integration of the HPV genome in DNA can lead to inflammation which may then result in production of ROS and progression of cervical cancer. In primary liver carcinoma, which is associated

with hepatitis B virus infection, G.C + T.A transversions are the predominant p53 genome mutation (Cheng *et al.,* 1992).

Also the cells of the immune system produce both the superoxide anion and nitric oxide during the oxidative burst triggered during inflammatory processes. Under these conditions, nitric oxide and the superoxide anion may react together to produce significant amounts of a much more oxidatively active molecule, peroxynitrite anion (ONOO−), which is a potent oxidising agent that can cause DNA fragmentation and lipid oxidation (reviewed in Valko *et al.,* 2007).

Oxidation can also produce oxidised bases in the DNA for example the guanine analogue 8-hydroxyguanine (oh'Gua)' formed in human cellular DNA as a by-product of normal metabolic processes is an abundant base modification in mammalian DNA whose levels increase with oxidative stress (Cheng *et al.,* 1992). When Cheng *et al.,* (1992), inserted oh'Gua in *E.coli* cells they have detected misreading of guanine which give a mutation frequency of 0.7% and the twenty two of the 23 mutations were G + T substitutes.

Another endogenously occurring damage to DNA is some of the reactive products derived from the reactive nitrogen species (RNS), such as the nitrogen dioxide radical (NO_2) and peroxynitrite ($ONOO^-$) (Wiseman and Halliwell 1996). The ROS and RNS can damage both the nucleus and mitochondrial DNA. The damage induced by these compounds may be due to formation of DNA adducts that may impair base pairing or block DNA replication and DNA transcription. Also in some cases the DNA bases may be lost or DNA SSBs may occur as a result of ROS and RNS DNA damage (reviewed in Jackson and Bartek 2009).

1.2.2 - DSBs initiation in B and T cell development

During the early B and T cell development, the variable regions of the immunoglobulin (Ig) and the T cell receptor (TCR) which directly binds to the antigen is assembled together with a mechanism known as V(D)J recombination process. This process begins when the recombination activating genes RAG1 and RAG2 makes a single strand nicks between the V (variable), D (diverse) and J (joining) gene segments and the adjacent recombination signal sequences (RSSs) (Bassing *et al.,* 2002). The nick made by RAG protein between the RSS and its adjoining DNA generates a 3 hydroxyl (OH) end on the coding segment. The newly formed OH group on the coding DNA is copied to the phosphate group in the opposite strand, forming a DNA hairpin on the coding end and leaving blunt DSB on the signal end through the direct trans-esterification (Brandt and Roth 2004).

1.3 - DSB repair mechanisms

In eukaryotes there are three enzymatically distinct mechanisms that can recognise and repair DSB with different fidelity; homologous recombination (HR), non-homologous end joining (NHEJ) and single strand annealing (SSA). The repair of DSBs is likely not straightforward because DNA lesions caused by IR may not always be ideal substrates for repair by HR mechanisms that are normally employed during replication restart (Willers *et al.,* 2004).

1.3.1 - Non-Homologous End Joining (NHEJ) Pathway

Through the use of genetic and biochemical studies the scientists have identified several key proteins in NHEJ pathway. The most extensively studied NHEJ repair proteins are the DNA-dependent protein kinase DNA-PK which, includes the Ku70/Ku80 heterodimer (Ku) and the DNA dependent protein kinase catalytic subunit (DNA-PKcs), Artemis, X-ray cross complementing 4 (XRCC4), XRCC4 like factor (XLF) and DNA ligase IV (Wood *et al.,* 2001).

The NHEJ is essentially the canonical DSB repair pathway. This pathway functions primarily in the early phases of the cell cycle and directly re-ligates the DNA broken ends without requirement of homology between the broken ends (Rothkamm *et al.,* 2003). As the DSBs leave the two broken ends of the DNA with additional, deleted or damaged nucleotides, the prerequisite for the ligation of the two end of the DNA is first the removal of these nucleotides. Also, the ligation reaction creates small sequence mutations around the break so the re-joining of the two DNA ends that may be mutated can result in errors. Thus, the NHEJ is error-prone due to the lack of re-joining of the original ends of the DNA (Mladenov and Iliakis 2011).

The DSBs created via the V(D)J recombination are also repaired in a single joint by the NHEJ DNA repair machinery (Market and Papavasiliou 2003). The DSB repair proteins (DNA-PKcs, Ku70, Ku80, XRCC4, Ligase IV, and Artemis) are all involved in V(D)J recombination (Mansilla-Soto and Cortes 2003). The Figure 1.5 will first briefly outline the role of the key genes found in NHEJ repair pathway. Then each of these key genes (with main focus on Artemis gene) will be described in more detail.

Figure 1.5 - Main steps involved in NHEJ.

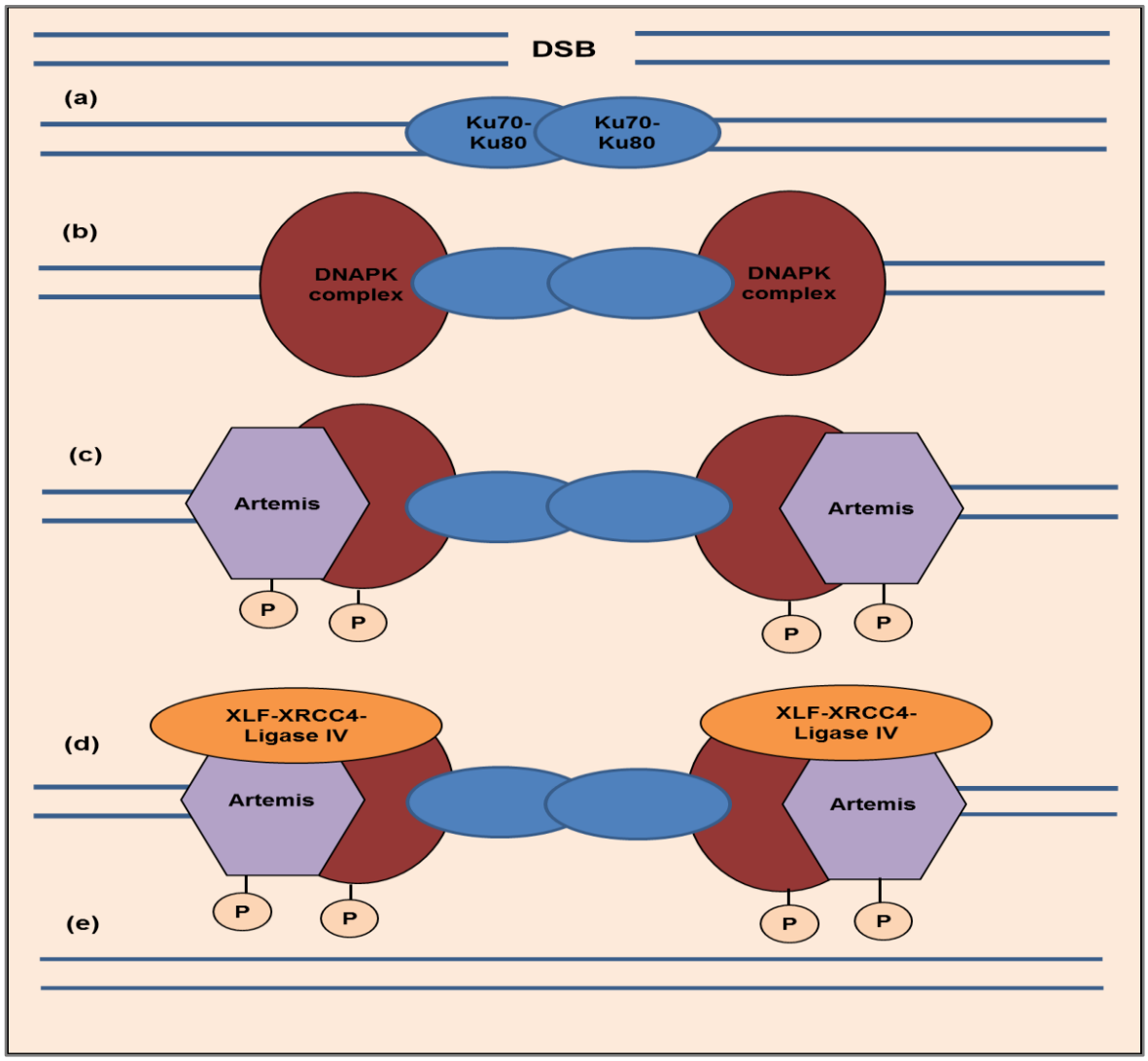

DSB is recognised by the Ku heterodimer (a), DNA-PKcs is recruited to the break by Ku heterodimer and DNPK complex is formed, (b) DNA-PKcs recruits Artemis (c), DNA ends are processed by a complex consisting of XLF, XRCC4, DNA ligase IV, and Artemis (d) DNA-repair factors dissociate and the DSB is repaired (d) (adapted from Misteli and Soutoglou 2009).

Briefly, three main steps are involved in NHEJ repair of DSBs; end binding, bridging and end processing and ligation. The DSB recognition and binding step requires the binding of Ku heterodimer to DNA ends and recruitment of the DNA-PKcs to the break site (West *et al.,* 1998) which, bridges the broken DNA ends. Also due to the fact that the DNA ends at the break are rarely compatible the DNA-PKcs

recruits the Artemis protein which acquires endonucleolytic activity and digests 5' and 3' DNA overhangs. Following, compatible DNA ends are re-ligated by a protein complex containing DNA ligase IV which is stabilised and stimulated by XRCC4 and Cernunos-XLF (Burma *et al.,* 2006).

1.3.1.1 - Ku Heterodimer

The Ku heterodimer is a DNA-binding protein which comprises of two tightly-associated subunits of ~70kD and 83 kD (Ku70 and Ku80, respectively; Ku80 is sometimes referred to as Ku86) (Smith and Jackson 1999). Although, the two subunits of heterodimer have weak primary sequence homology they are very similar in structure as each subunit includes three domains: an N-terminal α/β globular domain with the Rossmann fold, a centrally located DNA binding β barrel domain, which is central to the interactions with DNA, and the extended α-helical arm near the C terminus (Jones *et al.,* 2001).

Ku may act solely as a sensor of DNA damage, binding to ends of a DSB and signalling events that indirectly affect DSB repair (e.g. cell cycle regulation) through induction of DNA-PK activity or it may play a more direct role, including protection of ends from degradation, bridging of DNA ends prior to joining, or recruitment of other proteins that repair DSBs (Ramsden and Gellert 1998). According to Shin *et al.,* (2004), the broken ends of the DNA with either blunt or fidelity ligation are promoted by the Ku70/Ku80 heterodimer. Briefly the Figure 1.6 summarises the role of Ku70/Ku80 heterodimer in the repair of NHEJ repair of DSB.

Figure 1.6 - Binding and bridging of DNA ends through Ku heterodimers.

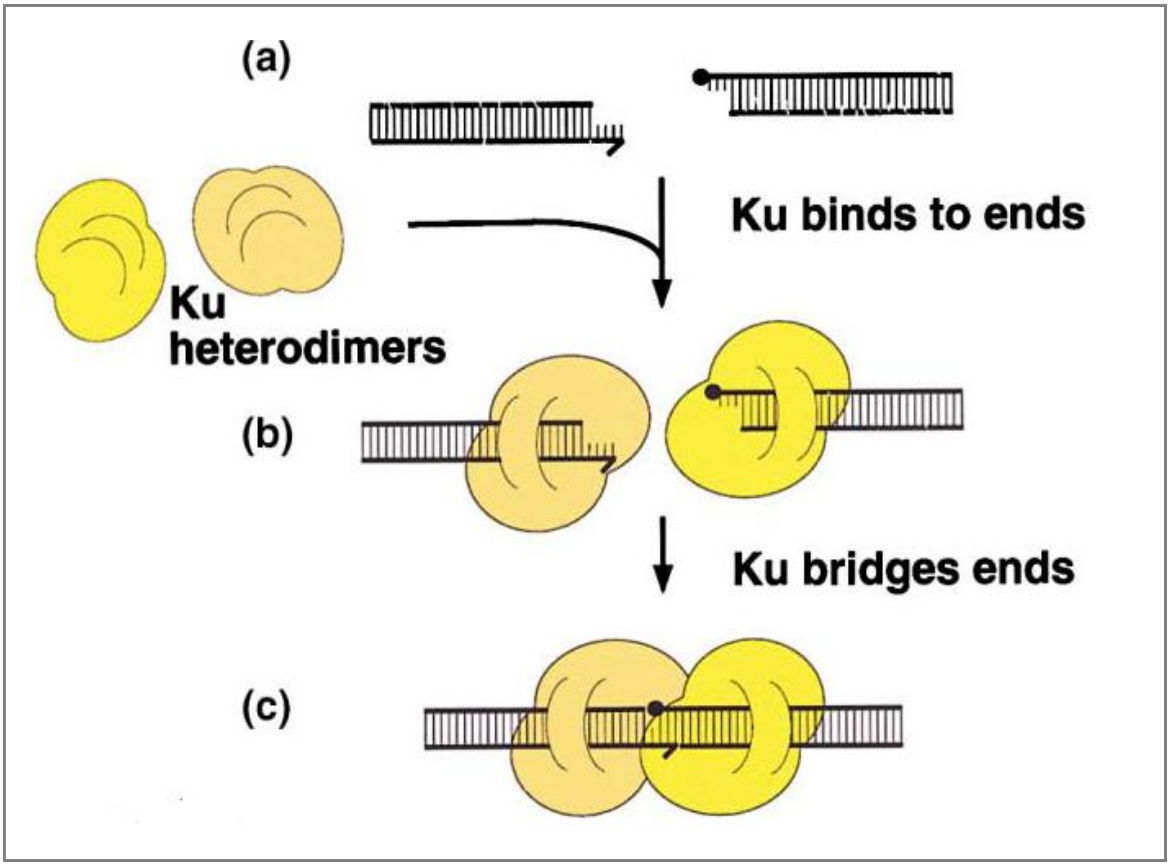

The broken DNA molecule is missing a base and is blocked by a non-ligatable moiety (black circle) on the right-hand side (a) Ku heterodimer binds to both ends at the break (b) and interacts with each other to form a bridge between the each ends of the DNA (c) (adapted from Jones *et al.,* 2001).

If the broken ends are compatible, ligation would be rapid and efficient. However, if the ends are not a competent substrate for ligation (e.g. hairpins from V (D) J cleavage, non-complementary overhangs, etc.), one or both of the Ku heterodimers could translocate internally, continuing to stabilise the intermolecular association of the ends (i.e. form a bridge between the two ends) and permit processing to occur until a substrate that is competent for ligation is produced (Ramsden and Gellert 1998).

1.3.1.2 - DNA-Dependent Protein Kinase (DNA-PK)

The DNA-PK complex, which includes Ku70/80 heterodimer and DNA-PKcs, is a key player in NHEJ pathway of DSB repair (reviewed in Burma *et al.,* 2006). The DNA–PK components are also important in a variety of other processes, including the modulation of chromatin structure and telomere maintenance (Smith and Jackson 1999). The DNA-PKcs is a large catalytic subunit (~460-kDa in size) and is one of the members of the phosphatidylinositol-3-kinase-like (PIKK) family of serine/threonine protein kinases. Other members include Ataxia Telangiectasia-Mutated (ATM), Ataxia and Rad3 related (ATR), mammalian target of rapamycin (mTOR), suppressor of morphogenesis in genitalia (SMG-1) and transformation/transcription domain-associated protein (TRRAP) (Leuther *et al.,* 1999; Lempiainen and Halazonetis 2009).

A study by Chan *et al.,* (2002) has shown that phosphorylated DNA-PKcs plays important role in the repair of DNA DSBs, by virtue of its localisation at the site of damage. Once the DNA DSB is recognised by the Ku heterodimer the DNA-PKcs are recruited to the site of the DNA damage. Upon binding to DNA ends, DNA-PKcs becomes active and exhibits serine/threonine kinase activity and is phosphorylated (Lee and Kim 2002). It then functions as a scaffold and bridges the broken DNA ends in a synaptic complex containing two DNA-PKcs molecules (DeFazio *et al.,* 2002). DNA-PKcs provides binding sites for other NHEJ proteins such as nuclease Artemis (Ma *et al.,* 2002), required for the trimming of the DNA ends or XRCC4/DNA ligase IV complex involved in the re-joining step of NHEJ (O'Driscoll and Jeggo 2002).

1.3.1.3 - Artemis

The Artemis is one of the most recently identified NHEJ repair protein located on chromosome 10p13 and has a predicted molecular weight of 77.6kDa (Moshous *et al.,* 2000). This protein belongs to metallo-β-lactamase superfamily and is composed of three identifiable regions; the β-Lactamase homologous region (aa 1-155), the associated β-CASP domain (aa 156-385), and the COOH-terminal region (aa 386-692) (Poinsignon *et al.,* 2004). When Poinsignon *et al.,* (2004), investigated the role of β- Lactamase and β- CASP domains with regard to V(D)J recombination and DNA repair after IR, they have found that the DNA repair during V(D)J recombination and after IR are quantitatively different, as different regions of the Artemis are required for the DSB repair. The β-CASP region for example, participates within the β-Lactamase region in forming the catalytic site of Artemis (Poinsignon *et al.,* 2004). The COOH-terminal region of the Artemis may be required for DNA repair after IR (Poinsignon *et al.,* 2004). The metallo β-lactamase region shows homology to yeast PSO2 and murine SN1. The conserved homology of β-lactamase region and the catalytic activity of β-CASP are crucial for the functioning of the Artemis protein. The C terminal consists of eight Serine-glutamine (SQ)/ threonine-glutamine (TQ) domains required for ATM, ATR, and DNA-PKcs proteins carry out phosphorylation of Artemis (Poinsignon *et al.,* 2004).

The Artemis protein has shown to have exonuclease and endonuclease activities when in the presence of DNA-PKcs and ATP. Mutations in Artemis protein encoded DNA Cross Link Repair 1C Gene (DCLRE1C) gene in 29 SCID patients has been reported by (Pannicke *et al.,* 2010). In total, 13 different mutated DCLRE1C alleles

were detected and the most mutations (59%) were gross deletions of exons 1-3 or exons 1-4.

The DNA-PKcs auto-phosphorylation at the T2609–T2647 cluster, in the presence of Ku and target DNA, is required for Artemis mediated endonuclease activity. Also the DNA-PK autophosphorylation regulates Artemis access to DNA ends (Ma *et al.,* 2005). The Artemis:DNA-PKcs complex gains DNA endonuclease activity that specifically targets and cleaves single-stranded to double-stranded DNA junctions (including 50 or 30 overhangs, hairpins, flaps, bubbles, loops and gaps) (Ma *et al.,* 2005). After the trimming of excess or damaged DNA, the Artemis:DNA-PKcs complex may de-bind and permit the ligase complex, XRCC4:DNA ligase IV, which completes the joining of the two DNA strands.

The Artemis:DNAPKcs complex also has hairpin-opening activity. Although, Artemis alone has 5’ to 3’ single-strand-specific exonuclease activity, upon complex formation with and phosphorylation by DNA-PKcs gains endoncleolytic activity which is critical for the hairpin-opening step V(D)J recombination and for the 5’ and 3’ overhang processing in NHEJ (Ma *et al.,* 2002). As explained earlier, during V(D)J recombination, the RAG proteins create DNA hairpins at the V, D, or J coding ends, and Artemis is essential to open these hairpins prior to binding.

The DNA-PKcs and Artemis are only detectable in vertebrates (reviewed in Ma *et al.,* 2002) suggesting the absence of hairpin activity in eukaryotes. Different hairpin sequences are opened by the native DNA-PKcs and full-length Artemis in variable ways and with varying efficiency. The sequence dependent variation in the efficiency

and even the position of hairpin opening by Artemis:DNA-PKcs is important from the standpoint of immunologic diversity (Lu *et al.,* 2007). The way which the Artemis:DNAPKcs complex processes the two ends of the DNA and gets the DNA ready to repair the DSB is demonstrated in more detail in Figure 1.7.

Figure 1.7- DNA-PK and Artemis mediated DNA end processing.

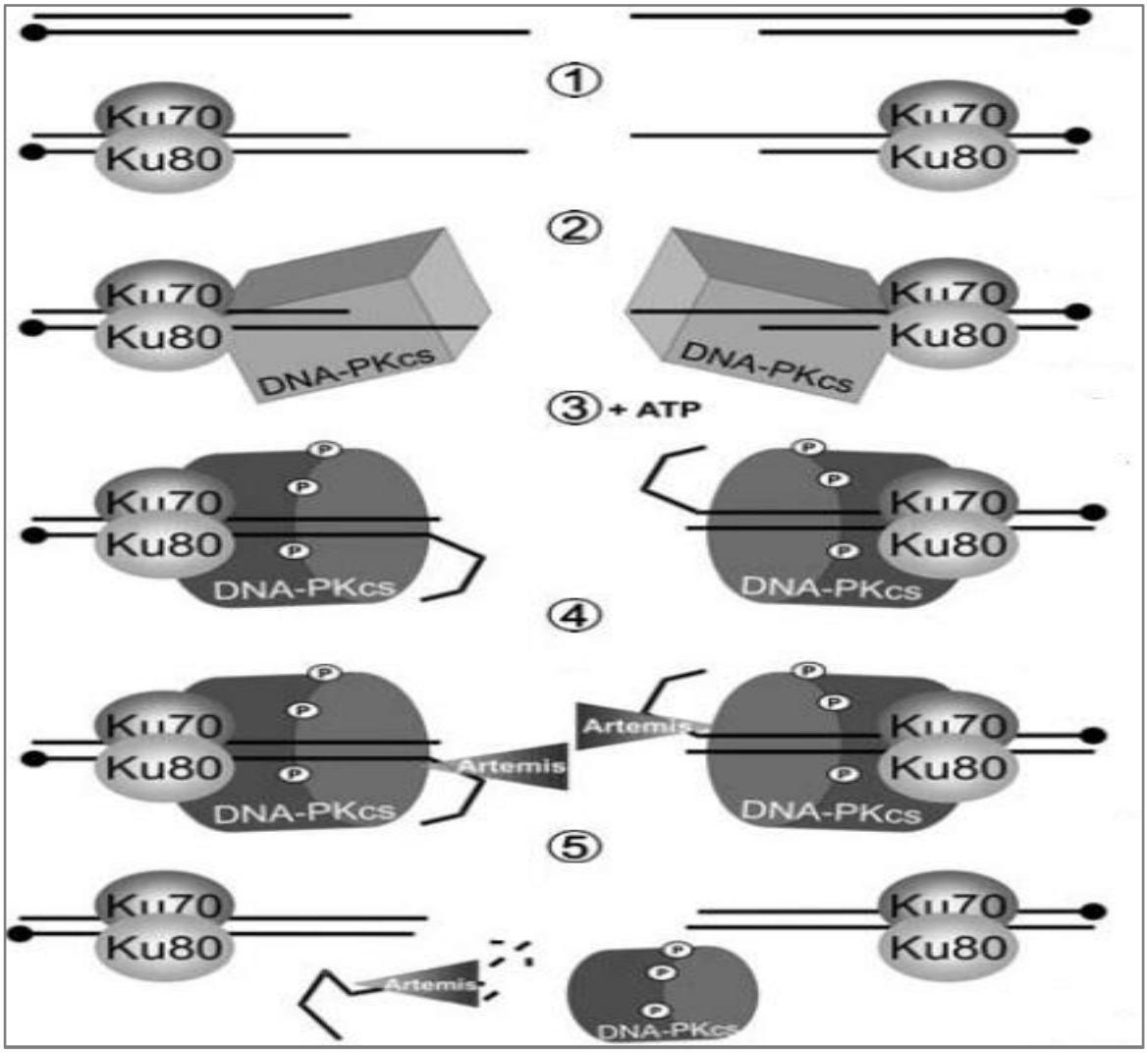

Two SSBs resolve into a DSB with long overhangs (1). The Ku70/80 heterodimer binds the DNA end to confer protection and recruit DNA-PKcs (2). When bound to a DNA end, DNA-PK autophosphorylates and undergoes a conformational change that alters the orientation of the DNA such that (4) Artemis can now recognise the ssDNA–dsDNA junction of the overhang, make an intra-strand incision and cleave the fragment via its exonuclease activity (5). With reduced affinity for the now blunt DNA, autophosphorylated DNA-PKcs eventually dissociates leaving Ku-bound DNA ends ready for further processing by NHEJ factors (adapted from Goodarzi *et al.,* 2006).

1.3.1.4 - XRCC4, XLF and DNA Ligase IV complex

The XRCC4 promoter consists of an N-terminal head domain which constitutes β-sandwich and a long helical C-terminal stalk which constitutes α-helixes. The head domain and the stalk are held together by van der Waals contacts and form a helix turn helix (HTH) structure which faces the major groove and interacts with the DNA backbone (Junop *et al.,* 2000).

The XRCC4-like factor (XLF, also known as Cernunnos) has structural similarity to XRCC4 and could be required for XRCC4-Ligase IV complex recruitment to DNA ends or could help the XRCC4-Ligase IV complex to bridge with other NHEJ components such as Ku and DNA-PKcs (Ahnesorg *et al.,* 2006).

The DNA ligase IV is a nuclear enzyme that joins the breaks in the phosphodiester backbone of DNA. Although, the DNA ligase IV carries out the ligation step, it requires the binding of XRCC4 to do so. The XRCC4 functions as a regulatory element to stabilise DNA ligase IV, to stimulate ligase activity, and to direct the ligase to the site of DNA breaks via its recognition helix and DNA-binding capacity.

A complex of XRCC4, XLF and DNA Ligase IV performs the final ligation step in NHEJ. According to Li *et al.,* (2008), the possible modes of interaction between XRCC4, XLF and Ligase IV are formed by; linker region between Ligase IV BRCA1 COOH-terminal domain (BRCT) binding to XRCC4's coiled-coil, the folded XLF/Cernunnos contact of XRCC4 via the head domains, the C termini of XLF molecules unfold and bind to Ligase IV in a similar way to XRCC4, the XLF and XRCC4 form a heterodimer and bind to Ligase IV in the composite coiled-coil region.

When Chen *et al.,* (2000) have co-expressed human DNA ligase IV and XRCC4 in insect cells and purified an active complex of these proteins to near homogeneity they have found that the DNA ligase IV-XRCC4 associates with both Ku and the catalytic subunit (DNA-PKcs) of DNA-PK at the ends of DNA molecules to allow the DNA ligase IV-XRCC4 complex to bind specifically to DNA ends and acts as an alignment factor, holding together the short complementary single-strand ends of linear duplex DNA molecules. However, Ku and DNA-PKcs have markedly different effects on DNA end joining by DNA ligase IV-XRCC4. Ku inhibits intermolecular DNA joining, whereas DNA-PKcs stimulates intermolecular DNA joining even in the presence of Ku (Chen *et al.,* 2000).

When Ahnesorg *et al.,* (2006), has reintroduced wild-type XLF into NHEJ-deficient 2BN cells derived from a radiosensitive and immune-deficient patients lacking XLF due to an inactivating frameshift mutation their radiosensitivity and NHEJ defects were corrected. Thus, the XLF constitutes a novel core component of the mammalian NHEJ apparatus.

Another protein implicated in mammalian NHEJ is the DNA polymerases of the Pol X family that are thought to mediate strand-filling steps in the pathway (Ma *et al.,* 2005).

1.3.2 - Homologous Recombination (HR) Pathway

The HR repairs double-strand DNA breaks, single-strand DNA gaps and interstrand cross links with high fidelity (Krejci *et al.,* 2012). The HR occurs during S and G2 phases and repairs the DNA DSBs using homologous chromosomal or sister chromatid DNA as a template for synthesis of new error-free DNA (Shin *et al.,* 2004). During this process a Holliday junction is created whereby lost genetic information from the undamaged sister chromatid (mitosis) or homologous chromosome (meiosis) is used to restore the original information lost at the site of the break (Helleday 2003; Wyman *et al.,* 2004).

This process is conserved from bacteria to man and recent observations suggest that mitotic HR is essential for faithful replication in vertebrate cells (Helleday 2003). Different HR mechanisms exist in different organisms and at different biological circumstances (Jackson 2002).

The initial step in HR is thought to be a 5' to 3' exonuclease re-sectioning of the DNA end to produce a 3' ssDNA overhang (Helleday 2003). The ensuing 3' ssDNA tails are then bound by Rad51 in a process that is influenced by a range of other proteins including replication protein A (RPA), Rad52p and Rad54p (Jackson 2002). A central player in HR is the strand exchange protein, called Rad51 in eukaryotic cells (RecA in *E coli*). During synapsis (homolog search and DNA invasion are collectively called synapses) the Rad51 facilitates the formation of a physical connection between the invading DNA substrate and homologous duplex DNA template, leading to the generation of heteroduplex DNA (D loop). The D-loop intermediates are where the 3'-end of the invading strand primes DNA synthesis off the template duplex DNA

(Li and Heyer 2008). The 3' terminus of the damaged DNA is then extended by a DNA polymerase that copies information from the undamaged partner, and the ends are ligated by DNA ligase I. Finally, after migration, the DNA crossover, i.e. the holiday junctions are resolved by cleavage and ligation to yield two intact DNA molecules. A model of HR repair of DSBs which occur in eukaryotes is illustrated in Figure 1.8.

Figure 1.8 - Main steps involved in HR.

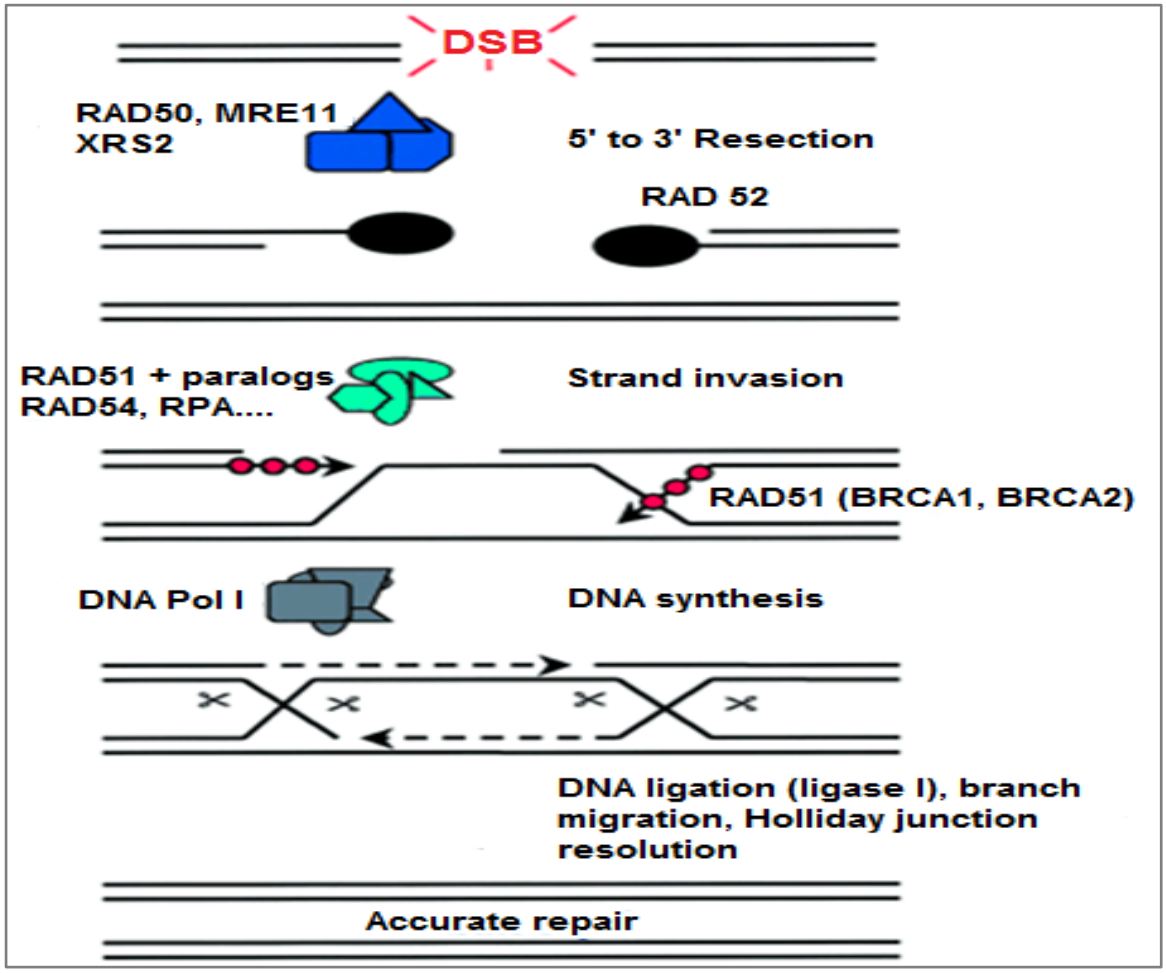

HR initiates with processing of DNA DSB in the 5'→3' direction by the MRE11-Rad50-NBS1 complex to form 3' overhangs. RAD52 binds to ssDNA-RPA and recruits RAD51 to form a nucleoprotein filament that searches for homologous DNA molecule. RAD51-bound DNA exchanges DNA strand with the undamaged, homologous DNA molecule, resulting in formation of recombination intermediate heteroduplex DNA (Holiday Junction). Holiday junctions are resolved by structure-specific endonucleases and branch migration, restoring the original lost genetic information (adapted from Jackson 2002).

Following resolution and separation of the two sister chromatids by the action of resolvase enzymes, DNA replication is completed and genomic integrity at the site of the DSB is maintained (Ip *et al.,* 2008).

According to Saintigny et al., (2002), patients with Werner syndrome (WS), an uncommon autosomal recessive disease with features of premature aging and genetic instability, is defective in HR pathway. A physiological role for the WRN RecQ helicase protein in RAD51-dependent HR and a link between defective recombination resolution and limited cell division potential, DNA damage hypersensitivity, and genetic instability in human somatic cells was detected in a study reported by (Saintigny *et al.,* 2002). Also the BRCA 1 defect in breast cancer patients may lead to defective processing of DSBs via HR in these patients.

1.3.3 - Single-Strand Annealing (SSA)

SSA is a process that is initiated when a DSB is introduced between two repetitive sequences oriented in the same direction. Four steps have been suggested for the repair of DSBs by SSA (Figure 4): (i) an end resection step which is needed for the formation of long 3'-ssDNA, (ii) annealing step in which the two repetitive sequences are annealed together forming a flap structure, (iii) a second resection step in which the flap structures (formed by the regions between the repeats) are resected and finally, (iv) the DNA ends are ligated. An example of direct SSB repair is illustrated in Figure 1.9.

Figure 1.9 - SSA model for repair of a two-ended DNA DSB.

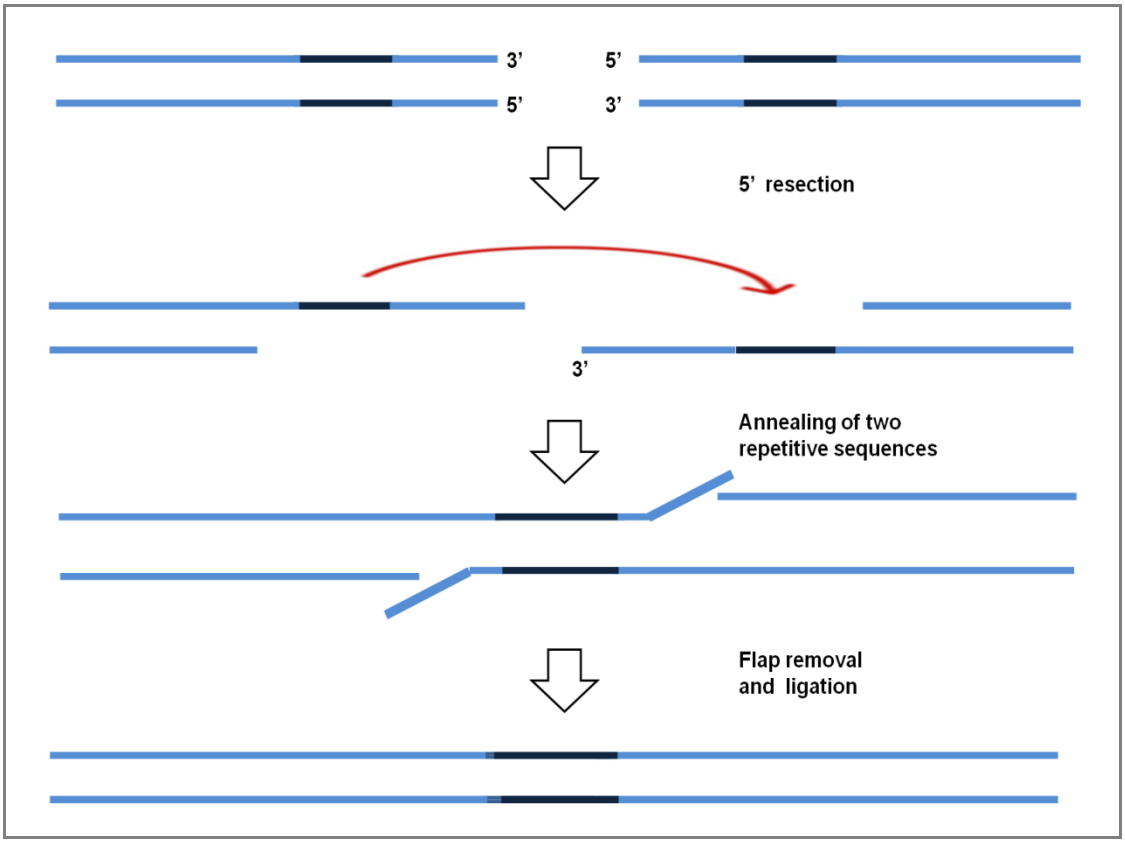

After DNA DSBs are introduced the DNA ends are resected 5'→3' direction and 3' overhangs containing complementary repeat sequences (dark blue regions) are generated. The complementary ends are paired. The non-complementary ends are removed by FEN-1 like nuclease. DSBs are ligated (adapted from Helleday *et al.,* 2007).

This chapter to this point has focused more on different types of DNA damaging agents that cause DSBs, the DNA repair mechanisms that recognise and repair different DNA damages (with particular emphasis being around the DNA DSBs). However, as the overall aim of this research is to detect the cause of radiosensitivity in 84BR and 175BR patients, the next step of our discussion will be largely based on a discussion for different types of diseases associated with defective DSB repair mechanisms (especially those diseases that are associated with defective NHEJ repair pathway).

Also, since the patient 84BR under study is considered over responder or over reactor to radiotherapy, the effects of radiotherapy on this patient will be discussed in more detail. Then, a discussion on a small group of patients found in population that are classified as over responders to radiotherapy will put an end to this chapter.

1.4 - Radiosensitivity and human syndromes

There are number of human genetic disorders which are characterised by defective DSB response to IR. Animal models reveal that defects in any component of NHEJ pathway can lead to hypersensitivity to IR, genome instability, immunodeficiency and cancer (Bassing and Alt 2004). In humans, defects in the specific genetic components of NHEJ also result in predisposition to cancer (lymphoma and leukaemia) or to extreme radiosensitivity. For example, defects in ligase IV (Riballo *et al.,* 1999) deficiency in Artemis expression (Musio *et al.,* 2005) or a mutation in the DNA-PKcs gene are associated with extreme clinical and cellular radiosensitivity and increased cancer incidence (Abbaszadeh *et al.,* 2010). Diseases that exhibit radiosensitivity are listed in Table 1.3.

Table 1.3 - Radiosensitivity associated disorders.

Syndrome	Defect	References
Ataxia telangiectasia (A-T)	ATM	(Chun and Gatti 2004)
Radiosensitive Severe Combined Immunodeficiency (RS-SCID)	Artemis DNA-PKcs	(Kobayashi *et al.,* 2003; van der Burg *et al.,* 2009)
Ligase IV syndrome	LIG4	(Chistiakov *et al.,* 2009)
Nijmegen Breakage Syndrome (NBS)	NBS1	(Bakhshi *et al.,* 2003)
Breast / ovarian cancer	BRCA1	(Gatti 2001)
Blooms syndrome	BLM	Ellis *et al.,* 1995
DNA-PKcs syndrome	DNA-PKcs	(van der Burg *et al.,* 2009; Abbaszadeh *et al.,* 2010)

1.4.1 - RS-SCID

Defects leading to a reduction in functional Artemis endonuclease activity at the cellular level manifest extreme radiosensitivity. In human subjects, Artemis deficiency results in radiation sensitive severe combined immunodeficiency (RS-SCID). This disorder was originally identified in Athabscan speaking Americans who display high level of SCID (Murphy *et al.,* 1980), hence the name SCID-A. SCID-A is characterised clinically by extreme radiosensitivity and by a complete absence of T and B cells due to a failure of the receptor recombination stage of V(D)J recombination (Dvorak and Cowan 2010).

Nicolas et al.,1998 showed that a number of radiosensitive $T^{-}B^{-}NK^{+}$ SCID patients without mutations in the *RAG* genes and without any mutations in any of the five key NHEJ repair genes (DNA-PKcs, Ku70, Ku80, XRCC4, XLF, Ligase IV). Then the *Artemis* gene was identified by (Moshous *et al.,* 2000) was involved in the pathogenesis of RS-SCID. Also a study by Noordzij *et al.,* (2003) confirms that the deletions and missense mutations in the *Artemis* gene can cause RS-SCID with defective coding joint formation and lead to an early and complete B-cell differentiation block. Artemis deficiency also causes mild telomere dysfunction phenotype and show significantly elevated IR induced telomeric fusions (Yasaei and Slijepcevic 2010).

The increase radiosensitivity of RS-SCID to gamma rays is not restricted to the cells of the immune system, but is also a characteristic of fibroblasts. An example is an. This patient with T-B severe combined immunodeficiency, whose cells have defects closely resembling those of NHEJ-defective rodent cells showed dramatic

radiosensitivity, decreased DSB re-joining, and reduced fidelity in signal and coding joint formation during V(D)J recombination. Also the patient was defective neither in the known factors involved in NHEJ in mammals (Ku70, Ku80, DNA-dependent protein kinase catalytic subunit, XRCC4, DNA ligase IV, or Artemis) nor in the Mre11-Rad50-Nbs1 complex. Then a research by a French group with Turkish-Italian-German collaborators analysed five new patients and identified the XLF protein which happen to be mutated in 2BN which was responsible for radiosensitivity as reintroduction of wild type XLF rescued radiosensitivity in these patients (Dai *et al.,* 2003; Ahnesorg *et al.,* 2006). Van der Burg et al., (2009) also reports the first human patient with the radiosensitive T-B severe combined immunodeficiency with a DNA-PKcs missense mutation.

Attempts to correct the deficiency in *Artemis* gene in cells by transduction with lentiviral gene expression vectors containing the *Artemis* cDNA has led to over-expression of *Artemis* in a number of mammalian cell types (Multhaup *et al.,* 2010). However, over-expression has also resulted in a loss of cell viability, associated with increased DNA damage and elevated apoptosis as a result of abnormal activity of the Artemis endonuclease inducing DNA breaks (Multhaup *et al.,* 2010). While such findings have significant implications for the role of gene therapy approaches for the treatment of SCID, it also reveals a potentially novel mechanism which may explain radiosensitivity in human cell types.

1.4.2 - Ataxia Telangiectasia (A-T)

A-T is a human autosomal recessive disorder characterised by progressive cerebral degeneration, immunodeficiency, lack of balance (Ataxia), dilated blood vessels of the eye (ocular Telangiectasia) and skin, radiosensitivity, predisposition to lymphoreticular and other malignancies, and cell cycle checkpoint defects (Lavin and Shiloh 1997). A-T is caused by a mutation in ATM gene which is central to cell cycle checkpoint responses such as intracellular signalling; DNA-damage induced cell cycle checkpoints and DNA DSB repair.

Patients with A-T either lack the ATM protein or ATM kinase activity or have mutations in ATM gene. Thus, a defect in a single ATM gene could cause a diverse problem such as ataxia, cancer susceptibility, radiosensitivity, characteristic translocations and immunodeficiency. Also, ATM-deficient cells show enhanced sensitivity and greatly reduced responses to genotoxic agents that generate DNA DSBs, such as IR and radiomimetic chemicals (Rotman and Shiloh 1999).

Xu and Baltimore (1996), examined the ability of ATM deficient (ATM -/-) mice cells (which they have created in their laboratory) to arrest cell cycle at G1 following gamma irradiation and UV irradiation. According to their results the ATM deficient cells exhibited an intermediate defect in cell cycle arrest following higher dosage (>5 Gy) of radiation. This characteristic support the idea that ATM is responsible for signalling the P53 mediated cell-cycle arrest that follows IR. ATM is also required for

efficient G1 to S phase transition during the cell cycle progression (Xu and Baltimore 1996).

A-T cells exhibit defective induction of all checkpoints in response to DSBs. The abnormal responses of A-T cells to IR include increased chromosomal breaks and radioresistant DNA synthesis, impaired p53-dependent arrest in G1 and other cell cycle checkpoint defects (reviewed in Delia *et al.,* 2000).

Other defects in the cellular responses of A-T cells to IR might also contribute to their radiosensitivity, such as defective induction of NF-kB (Rotman and Shiloh 1999). Inhibition of NF-kB activation was shown to enhance IR-induced cell death of normal cells and introduction of a truncated IkB-a corrected the hypersensitivity to IR and streptonigrin of A-T cells (reviewed in Rotman and Shiloh 1999).

A study by Sandoval et al., (1999) investigated the mutational spectrum of the ATM gene in a cohort of sixty six unrelated A-T patients living in Germany. They have identified 46 different ATM mutations among which were the amino acid deletion, amino acid substitutions, frameshift deletions, frameshift insertions, nonsense, missense and splicing mutations and 26 sequence polymorphisms and variants scattered throughout the gene. The majority of the mutations were truncating, confirming that the absence of full length ATM protein is the most common molecular basis of A-T. Cultured cells from A-T patients are also hypersensitive to IR and show defective activation of radiation-induced cell cycle checkpoints; including retarded p53 stabilisation (reviewed in Sandoval *et al.,* 1999). The radiation sensitivity of A-T

cells generally is assumed to result from an inability to delay the cell cycle to allow sufficient time to repair DNA damage (Meyn 1995).

The ATM protein activates several cellular functions such as the p53, cell cycle checkpoints and apoptosis in response to DNA damage. The defect in ATM gene in A-T patients leads to suppression of these pathways and the A-T phenotypes described above.

So to recap, the mutation of the ATM gene regulating cell cycle control and DSB repair is associated with clinical and cellular radiosensitivity in A-T.

1.4.3 - Nijmegen Breakage syndrome (NBS)

The NBS is a rare autosomal recessive syndrome of chromosomal instability. Some of the characteristic features of the NBS are microcephaly at birth, combined immunodeficiency and predisposition to malignancies and cellular hypersensitivity to IR (Chrzanowska *et al.,* 2012).

The first reported NBS case was described in 1979 in a Dutch boy with microcephaly, stunted growth, mental retardation, café-au-lait spots and immunodeficiency. Then in 1981, his brother was reported to have same clinical symptoms by researchers at the University of Nijmegen in Netherlands hence the name, Nijmegen breakage syndrome which was named by the Dutch group (Weemaes *et al.,* 1981).

Although, the clinical features of the NBS and AT are different the NBS shares a number of cellular features with A-T notably, a specific sensitivity to IR, characteristic chromosomal rearrangements in cultured and a predisposition to malignancies, particularly lymphoid cancers.

The gene mutated in NBS was cloned in 1998. This gene termed the NBS1 gene encodes a protein called Nibrin which is a member of the hRad50/hMre11 protein complex involved in DNA DSB processing in HR (Varon *et al.,* 1998). Nibrin together with Mre11 and Rad50 is part of a trimeric complex (M/R/N complex) that is conserved between yeast and mammals (Demuth and Digweed 2007).

Although, there is controversy in literature the deficient G1- to S-phase and G2 to mitosis transitions have been reported for NBS cells (Demuth and Digweed 2007). The NBS1 is involved in signal transduction for cell-cycle checkpoints as a substrate of ATM kinase and, when this mechanism is defective, induces impaired G2 checkpoint control and also allows continued DNA synthesis in the presence of DSBs, so-called radio- resistant DNA synthesis (RDS) (reviewed in Tauchi *et al.,* 2002).

1.4.4 - Bloom's Syndrome (BS)

BS as reviewed in German (1995) and Ellis *et al.,* (1995) is a rare autosomal recessive disorder characterised phenotypically by retarded growth, hypersensitivity to IR, sun sensitivity, immunodeficiency and predisposition to a wide variety of cancers at an early age. The gene mutated in Bloom's syndrome, *BLM*, encodes a member of the RecQ family of DExH box-containing DNA helicases (Ellis *et al.,* 1995). Some genes in the DExH family e.g. PB, XPD, and ERCCG genes are found in DNA repair and mutations where such genes are found in XP and Cockayne syndrome patients.

The BS gene product, BLM, is a 159 kDa DNA helicase enzyme belonging to the RecQ family (Turley *et al.,* 2001). It was found that BS cells are much more sensitive to the irradiation than control cells at the end of S and at G_2 phases. The rate of induction of chromosome breaks is significantly increased and that of chromatid breaks and exchanges is also increased, though to a lesser degree (Aurias *et al.,* 1985).

1.5 - Over responders to radiotherapy

Radiotherapy is an important modality of treatment for a wide variety of histologically distinct cancers. Most cancer patients receive radiotherapy alone or in combination with other forms of therapy. Approximately 20% of patients experience side effects or normal tissue toxicity during radiotherapy, which can include mild erythema to ulceration and haemorrhage and occasionally neuropathy and paralysis. Also a few individuals manifest disproportionately severe normal tissue toxicity (NTT) to IR and such patients are often referred to as radiotherapy (RT) “over-reactors”. Such individuals respond so extremely to RT that NTT can be life-threatening. The Table 1.4 summarises normal tissue toxicity for skin. However standardised scales of NTT for all tissue and organ types have been developed (Cox *et al.,* 1995).

Table 1.4 - NTT (Skin) following radiotherapy.

RTOG Scale	**Normal tissue toxicity**
0	No side effects.
1	Faint, dull erythema, dry superficial desquamation.
2	Tender erythema, moist deep desquamation, oedema.
3	Extensive moist desquamation, increased oedema.
4	Ulceration, haemorrhage, tissue necrosis.
5	**Death (over-reactors).**

There is considerable inter-patient heterogeneity in the development of NTT as a consequence of RT which has been recognised for over half a century (e.g., Holthusen 1936). During clinical RT, normal tissue tolerance levels are appreciated and severe sequel is avoided in the majority of patients.

The NTT scoring system was developed by the Radiotherapy Oncology Group (RTOG) (e.g. Cox *et al.,* 1995) and the Late Effects Normal Tissue Task Force Subjective, Objective, Management and Analytic (LENT/SOMA) provided standardised scales of NTT for all tissue types (Pavy *et al.,* 1995).

In addition many studies have examined the development of NTT in breast cancer patients following RT and have demonstrated the occurrence of NTT such as telangiectasia, fibrosis, oedema, atrophy, ulceration and neuropathy, at a predictable rate. For example, slight fibrosis in approximately 15% of patients; moderate in 5% and severe in 5% of patients (e.g. Fehlauer *et al.,* 2003; Hoeller *et al.,* 2003).

A classical example of an over-reactor disease is A-T in which inherited mutations in the ATM gene controlling cell cycle control and DNA DSB repair is associated with extreme clinical and cellular radiosensitivity (Lavin and Shiloh, 1997). Moreover, Abbaszadeh *et al*., (2010) have recently demonstrated a unique mutation in DSB repair gene *DNA*-PKcs which resulted in clinical and cellular radiosensitivity in a patient whom died as a consequence of RT-induced NTT.

As demonstrated in the previous section the core cause of radiosensitivity in these individuals is due to some form of defect in the repair of DNA DSBs or signalling pathways that are involved in the repair of DNA damage.

1.5.1 - 84BR and 175BR Patients: Over-responders to radiotherapy

Briefly, some of the clinical data known from the literature for the two cell lines under study are as follows:

1. The patient cell line 84BR is an adult female with breast cancer who had extreme reaction to radiotherapy.
2. The patient cell line 175BR is an adult male with multiple primary tumours of independent histological origin but no evidence of over-reaction to radiotherapy.

A skin biopsy from the patient 84BR who have had adverse reactions at radiotherapy was provided to Dr Arlett (MRC Genome Damage and Stability Centre, Sussex University) by Professor N.M. Bleehan (MRC Clinical Oncology and Radiotherapeutics Unit, Cambridge). The patient from which the 84BR cells were derived can be categorised at a RTOG class three patient with severe oedema, swelling and persistent fibrosis. Cell strains developed from this patient biopsy had a reduced competence for RPLD (repair of potentially lethal damage) which is a form of a measure used to detect the level of cell survival to genotoxic agents such as IR.

In a study by Arlett *et al.,*1989 the RPLD assay was used to measure the effect of potentially lethal damage of IR on the survival of five fibroblast cell strains (84BR and 83BR (both from radiosensitive breast cancer patients) A-T patient CS (patient with Cockayne's syndrome) and 1BR.3 (DNA repair normal individual). Their results revealed that the 84BR was not only sensitive to IR but also lacked in RPLD while the rest of the cell strains under study were only slightly sensitive than the normal individuals and showed little capacity for RPLD. Another study by Alsbeih (1996)

looked at the recovery ratios (RR) of the three hypersensitive cell lines (84BR, GM739 and 180BR) to radiation and detected a significantly higher RR for those cell lines compared to the controls.

Thus, some of the studies conducted on 84BR cell line confirm the hypersensitivity of 84BR cell line to IR at cellular level and a defect in the ability of the cells to repair the DNA damage.

An established cell line for 175BR patient was also provided by Dr Arlett but originally was isolated from a non-affected skin biopsy by Professor Bruce Ponder (Cambridge Research Institute, Cambridge, UK). A brief history of this patient can be observed in a family pedigree illustrated in Figure 1.10. As can be seen from the pedigree the most of the family members of the 175BR patient exhibit a multiple number of tumours independently, some of which are the brain tumour, breast cancer, bowel and pancreas cancer while the 175BR patient is the only member that exhibits multiple tumours. The patient 174BR, the brother of 175BR, also exhibits multiple primary tumours. It is also very unfortunate that majority of his family members who have had cancer have died.

Figure 1.10 - Cancer Prone Kindred.

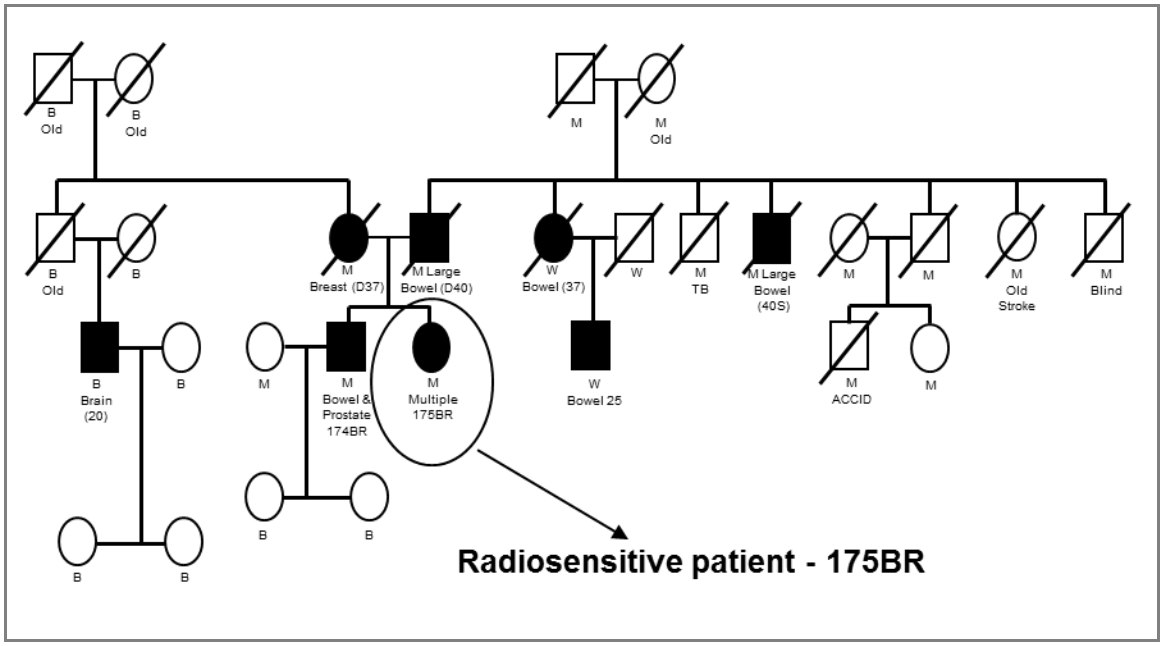

From the literature we know that the cytotoxic chemotherapy and radiotherapy exerts its anticancer effect by inducing DNA damage e.g. DNA strand breaks and DNA crosslinks. Also the efficacy of DNA repair mechanisms in cells will be important in governing the response to anticancer therapy. Therefore, the aim of this project will be briefed in the next page.

1.6 - Project Aim

The aim of this project is twofold; first to determine if the 84BR and 175BR exhibit cellular radiosensitivity. Thus, once the radiosensitivity in the two patients are identified the next aim of the research will be to determine if the radiosensitivity in these patients is associated with failure to effectively repair the DNA DSBs.

Chapter 2 - Clonogenic assays

2.1 - Introduction

In order to determine the cellular radiosensitivity of 84BR and 175BR fibroblast cell lines, clonogenic assays were first conducted with IR to establish sensitivity. Then clonogenic assays with nitrogen mustard (HN2) were carried out, to determine the defective DNA repair pathway (NHEJ or HR) responsible for the potential cellular radiosensitivity in 84BR and 175BR patient fibroblast cells.

Clonogenic assays are a reliable method for the determination of inherent cellular sensitivity to a variety of DNA damaging agents. Briefly, a cell that is not reproductively dead and has retained the capacity to divide after exposure to IR or other cytotoxic agents has the potential to form a clone or colony, and it is said to be clonogenic (Munshi *et al.,* 2005). The clonogenic cell survival assay, first described in 1950s for the study of radiation effects on reproductive survival of cells, is still a widely used experimental approach to test the effects of radiation, drugs or genes on the growth and proliferative characteristics of cells *in vitro* (Munshi *et al.,* 2005; Guda *et al.,* 2007). This assay is also known as colony forming assay (CFA) and it can be performed on monolayer cultures as well as cells growing in semi-solid soft agar media. The monolayer CFA measures effects of drug or radiation toxicity on anchorage-dependent cell growth while soft-agar CFA measures anchorage-independent growth (Yung 1989).

In this chapter the clonogenic assays were used to identify differences in the response to genotoxic agents such as IR and HN2. In clonogenic assays the cell

survival is demonstrated with a cell survival curve, which defines the relationship between the doses of the agent used to produce an insult and the fraction of cells retained to reproduce. From the survival curve the D_{10} (dose of radiation required to reduce colony survival to 10%) is determined, which is used as a quantitative index of a given cell types response to the lethal action of the radiation or drug exposure.

There are many published papers where scientists have conducted the clonogenic assays on various cell types, a few of which are summarised below;

A previous study by Abbazsedeh *et al.,* (2010), demonstrates the use of clonogenic assay for the determination of hypersensitivity of XP14BR patient with Xeroderma Pigmentosum (XP) to IR. In a study by Arlett and Cole 1989 the clonogenic cell survival assays are also used to determine the hypersensitivity of A-T patients to IR. In this study the D_0 (mean lethal radiation dose), for five normal, (1BR.3, 1BR.2, 48BR, GM730 and 54BR), based on seventy-four survival curves, was at 1.457±0.018 Gy, while the D_0 based on fifteen survival curves for five A-T heterozygotes (ATHM4BI, ATHM1SF, ATHF4BI, ATH96TO and ATHM7BI) was at 1.280±0.037 Gy. Thus, the results show a slightly more radiosensitivity to IR in A-T patients compare to their five counterparts. A larger study, by Paterson *et al.,* (1979) on 143 strains, consisting of twenty one supposedly normal and hundred twenty two cancer patients (such as patients with Hodgkin's disease, Lymphoma, malignant melanoma and breast cancer) was conducted where a total of 407 survival curves were generated. Their study also demonstrates hypersensitivity in those patients to IR with clonogenic assays.

Although, clonogenic assay is a widely used technique, in some circumstances, the clonogenic assays may be misleading particularly when using primary (non-immortalised) cells. Here cells may be very viable and able to divide very efficiently and may not form colonies very well. Under these circumstances it may be useful to use some sort of proliferative assay rather than a clonogenic assay. Also primary cells are subject to, after a number of population doublings, replicative senescence. Here cells are metabolically viable but unable to undergo cell division and thus are non-clonogenic. For example, the cell survival assays such as the MTT assay 3-(4,5-dimethylthylthiazol-2-yl)-2,5-dithenyltetrazolium bromide might be useful.

The MTT, a yellow coloured tetrazolium-based compound (2,5-dithenyltetrazolium bromide), is taken up by live cells and reduced to blue-purple formazan crystals by mitochondrial enzyme succinate dehydrogenase (Yung 1989) (Yung 1989) and (Price and McMillan, 1990). Once the live cells take up this dye the absorbance of the MTT solution is read at 540nm to quantify the number of live cells that survive the exposure to a cell damaging agent.

In a study by Price and McMillan (1990) the MTT assay was used as an alternative to clonogenic assay to measure the response of cultures of primary human tumours (HX142 cell line derived from patients with neuroblastoma and MGHU1 and RT112 from patients with bladder cancer) to IR. Briefly, in this study, the cells were irradiated with ^{60}Cobalt source then the MTT was added to the cells. Depending on the individual cell requirement the cell culture was incubated for 3-5 hours. The MTT solution was then removed and DMSO was added to dissolve the formazan crystals. The cell viability was then quantified by measuring the absorbance of the resultant

solution. Although, their results showed a reproducible measure of survival with MTT compared to clonogenic assays the usefulness of MTT assay in determining the radiosensitivity in primary human tumour cultures was limited as it required a several optimisation conditions for each cell lines.

Another example is the sulforhodamine B (SRB) assay which was developed by Skehan and colleagues in 1990 to measure drug induced cytotoxicity and cell proliferation for large-scale drug screening applications (Voigt 2005). Briefly, cells grown in a 96 well plate are incubated in sulforhodamine B dye to allow this dye to bind to protein basic amino acids. Then the protein-bound to the dye is fixed in trichloroacetic acid and dissolved in Tris base solution. The cellular protein is then measured by reading the OD values at 510nm. So in principle the more live cells there is the more protein is made and the higher is the binding of SRB dye to the cells. This method is more efficient and highly cost effective as large number of samples can be tested within a few days, and requires only simple equipment and inexpensive reagents (Vichai and Kirtikara 2006).

Although, the clonogenic assay is over 50 years old, it is still the gold standard technique for measuring cellular radiosensitivity (Eastham *et al.,* 2001). Hence, the use of this technique to detect the radiosensitivity in 84BR and 175BR cancer patients was very crucial to my research. Arlett *et al.,* (1989) reports that the clinically radiosensitive 84BR patient is also sensitive to gamma radiation at cellular level. Thus, the clonogenic assays were performed with gamma radiation to confirm the clinical radiosensitivity at cellular level in 84BR and to detect radiosensitivity also at cellular level in 175BR patient cell line. Once the cellular radiosensitivity is detected,

the clonogenic assays with HN2 will be conducted to determine the defective pathway that may be responsible for the radiosensitivity seen at cellular level.

2.2 - Materials and Method

2.2.1 - Cell Lines

Human fibroblasts (84BR, 175BR, 1BR.3, NB1) and NB1-tert human dermal fibroblast cell lines were used in this study. The 84BR diploid fibroblast cell line was derived from a non-affected skin biopsy of radiosensitive breast cancer patient (Arlett *et al*., 1989). The 175BR cell line was derived from a non-affected skin biopsy of an individual with multiple tumours of independent histological origin and was a kind gift from Professor Bruce Ponder. The NB1 normal diploid fibroblast cell line is described in Bridger and Kill (2004) and the 1.BR3 diploid fibroblast cell line was derived from a normal individual (Arlett *et al.,* 1988). The NB1-tert cell line was established during this research, by transfecting the NB1 cell line with human telomerase reverse transcriptase (hTERT) in Brunel institute for cancer genetics and pharmacogenomics.

2.2.2 - Cell Culture

Cells were routinely cultured in complete medium consisting of Dulbecco's Modified Eagle Medium (DMEM). (PAA Laboratories Ltd, Yeovil, Somerset, UK), supplemented with 10% (V/V) foetal calf serum (PAA Laboratories Ltd), 2mM L-glutamine and 100 U mL^{-1} penicillin and streptomycin (PAA Laboratories Ltd). Cells were grown as monolayers in sterile Petri dishes (P100) or tissue culture flasks (75 cm^2) (Nalgen Nunc International, Life Technologies Ltd, Paisley Scotland) at 37°C in a humidified atmosphere with 5% CO_2 in a class 2 Heraeus 6000 incubator (Heraeus Holding GmbH, Hanau, Germany).

2.2.3 - Sub-culturing

Cells were routinely sub-cultured ($2x10^5$ cells/ dish) when they reached approximately 80% confluence. Medium was aspirated, and cells washed with 10ml of versene (phosphate buffered saline and 2mM EDTA), after which 1-2ml of 10% (v/v) trypsin (0.25% trypsin with Ethylene-diamine-tetra-acetic-acid (EDTA) was added. Immediately after, the cells were transferred to 50ml centrifuge tubes (Nunc), recovered by Heraeus Megafuge 1.0 centrifugation (DJB Labcare Ltd, Buckinghamshire, England) at 1200rpm and then subjected to a five-fold dilution before seeding into fresh 75 cm^2 cell culture flasks or P100 Petri dishes. Culture media refreshed every 3-4 days and sub-cultured as they became 80% confluent.

2.2.4 - Cell Count

The 80% confluent cells were trypsinised and re-suspended in 10ml complete growth medium in a 15ml centrifuge tube. Approximately, 10µl of this cell suspension was applied to a Neubauer haemocytometer (Weber Scientific International Ltd., Teddington, Middlesex, UK) and five 4 x 4 squares were counted using x10 objective of an Olympus CK2 inverted microscope (Olympus Europa GmbH, Hamburg, Germany). The total cell count established using the formula $A = n \times r \times 10^4$, where A is total cell number, n is the mean of cell count, and r is the total re-suspension volume.

2.2.5 - Irradiation of cells

Cells were irradiated in suspension in DMEM with 0, 2, 4, 6 and 8Gy gamma radiation from a higher activity ^{60}Cobalt source (Puridec Irradiation Technologies, Ltd, Oxford) at a distance of 25cm from the source at a dose rate of 1.4-1.5Gy min^{-1}. An appropriate number of cells were plated into each of five 10cm dishes containing 10ml DMEM to allow the growth colonies in each dish.

2.2.6 - Feeder Layers

Before commencing the clonogenic cell survival assay, cultures of feeder layer were established. The feeder layer provides extracellular matrix and certain nutrients for the growth of primary fibroblasts. To establish feeder layer, the cells, not greater than 80% confluence, were recovered by trypsinisation, diluted in approximately 10ml complete medium and counted. Cells were diluted to approximately 10^5 cells per ml and subjected to 30Gy gamma irradiation, on a ^{60}Co source, which is a dose rate of approximately 2.5Gy per minute. Following irradiation, 2 x 10^6 cells were cryo-preserved in liquid nitrogen in 1ml complete medium containing 20% FCS and 10% DMSO. One day prior to nitrogen mustard and IR cell survival analysis, appropriate feeder cells were recovered from liquid nitrogen and diluted to 10^4 cells/ml of complete medium. Feeder cells (10^5 per dish) were added to each of twenty five 10cm plastic Petri dishes and these were incubated overnight.

2.2.7 - Clonogenic Cell Survival Assay with Gamma Radiation

Clonogenic assays following exposure to gamma radiation were conducted as described previously (Arlett *et al.,* 2006). In brief, approximately 2.5 x 10^5 cells were seeded in 75cm^2 tissue culture flasks and incubated overnight. Cells at 80% confluency were trypsinised, suspended in 10ml media and counted to determine the number of cells per ml. The cell suspension was serially diluted to concentrations of 1000, 2000, 3000, 5000 and 8000 cells/ml at a final volume of 5ml. Cells in suspension were irradiated with 0, 2, 4, 6 and 8 Gy of gamma radiation. One ml aliquots of each cell dilution were transferred into 90mm dishes (5 replicates) containing 10^5 autologous feeder cells in 10ml DMEM. Feeder cells were produced by exposure to 30Gy gamma irradiation as described earlier. Cultures were incubated for three weeks at 37°C. After three weeks of incubation, colonies that had grown were fixed with 70% methanol and stained with 0.5% methylene blue (Sigma Aldrich, UK) diluted in distilled water. The colonies were counted and the survival of cells was expressed as a percentage of survival of untreated control cells.

2.2.8 - Clonogenic cell survival assay with HN2

Clonogenic assays following exposure of cells to HN2 was conducted as described by (Clingen *et al.,* 2007). In brief, approximately 1 x 10^5 cells were seeded in five 75cm^2 tissue culture flasks and incubated overnight. Analytical grade HN2 (Sigma Aldrich, UK) was dissolved in serum free medium (SFM) immediately before use. Overnight cultures, at about 80% confluency, were washed once with versene and then treated with 5ml of 2, 4, 6 and 8 µM HN2 for 1 h at 37°C. Treated cells were harvested with trypsin, and serially diluted to concentrations of 1000, 2000, 3000, 5000 and 8000 cells/ml at final volume of 5ml. One ml aliquots of each cell dilution

were seeded into 90mm dishes (5 replicates) containing 10^5 autologous feeder cells. Cultures were incubated for three weeks at 37°C. Microscopic examination revealed colony formation after three weeks, which were fixed with 70% industrial methylated spirit (IMS) and stained with 1% methylene blue. The stained colonies were counted and the percentage plating efficiency (PE) was calculated using the following equation: PE % = colonies counted / total number of cells plated X 100.

2.3 - Results

2.3.1 - Clonogenic cell survival assays - Radiation

The response of 84BR and 175BR diploid fibroblast cell lines to increasing dose of gamma radiation is shown in Figure 2.1 and is compared with the response from the repair normal human diploid fibroblast cell lines, NB1 and 1BR.3. It can be seen that for all cell lines the exposure to increasing doses of gamma radiation causes a proportionate decrease in clonogenic cell survival. However, in 84BR and 175BR cell lines there is an abnormal reduction in colony survival when compared to the NB1 and 1.BR3 normal fibroblast cell lines. Comparison of the D_{10} values as illustrated in Table 2.1 show that the D_{10} values for the repair normal fibroblasts is 5 Gy for the NB1 cells and 5.7 Gy for the 1BR.3 cells. Therefore, the NB1 cells are 1.47 fold more radioresistant than the 84BR and the 175BR cells while the 1BR.3 cells are 1.68 fold more radioresistant than the 84BR and 175BR cell lines. These observations confirm those of Arlett *et al*., (1989) and demonstrate the inherent cellular radiosensitivity of the 84BR and 175BR fibroblast cell lines. A Student's unpaired T-test, comparing the D_{10} values of the 84BR and 175BR cell lines with the normal fibroblasts, demonstrated that the cells were significantly more sensitive to gamma radiation ($P < 0.05$).

Figure 2.1- Sensitivity of 84BR and 175BR to IR Compare to Control Cell Lines.

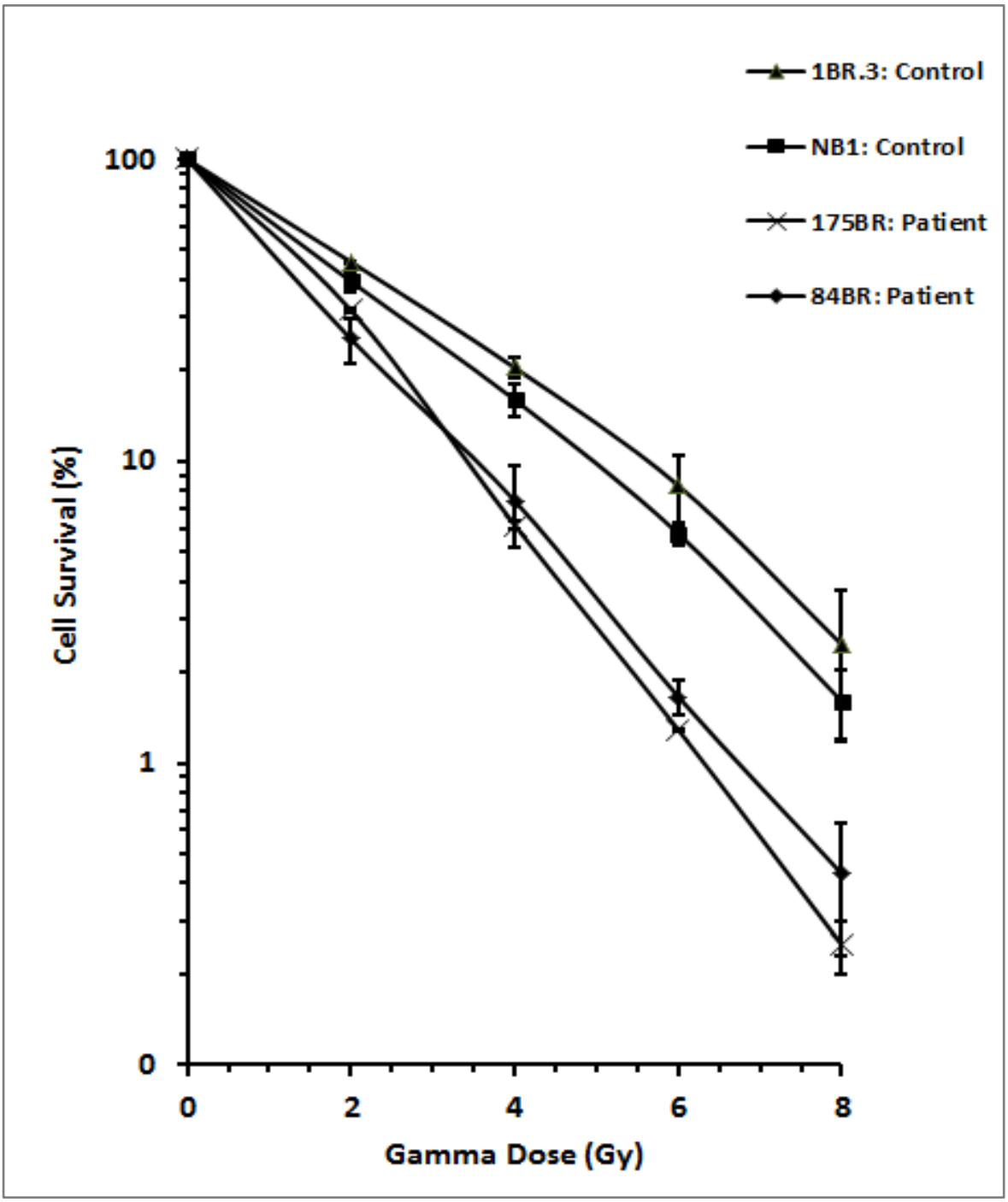

Here the clonogenic cell survival of 84BR and 175BR in comparison to the repair normal fibroblast 1BR.3 and NB1 following exposure to increasing doses of gamma radiation is illustrated. Data are derived from at least five independent experiments and error bars represent standard error of the mean survival following exposure to 2, 4, 6, and 8 Gy gamma radiation. The P value is < 0.05.

Table 2. 1 - The Dose of radiation required to reduce cell survival in a clonogenic assay to 10% (D_{10}) in patient and control cells.

D_{10} Values			
175BR	84BR	NB1	1BR.3
3.50	3.60	5.13	6.00

To summarise, the exposure of cells to IR has induced DSBs in DNA. Due to the defect in the repair pathways the DSBs remained unrepaired. Thereby, the inability of the patient cells to repair the DNA damage resulted in more sensitivity to IR than the normal cells. Thus, the radiosensitivity seen at cellular level confirms the clinical radiosensitivity seen in 84BR.

To determine the defective repair pathway that may be responsible for the cellular radiosensitivity seen here, the clonogenic assays were conducted with HN2.

2.3.2 - Clonogenic cell survival assays - HN2

DNA DSB can be repaired by one of two mutually exclusive repair pathways as described in Chapter 1. In order to determine if the radiosensitivity of the 84BR and 175BR cell lines was associated with a defect in either the NHEJ or HR repair pathway, clonogenic assays were performed in which the sensitivity to HN2 was determined as shown in Figure 2.2.

Figure 2.2 - Sensitivity of 84BR and 175BR to HN2 Compare to Control Cell Lines.

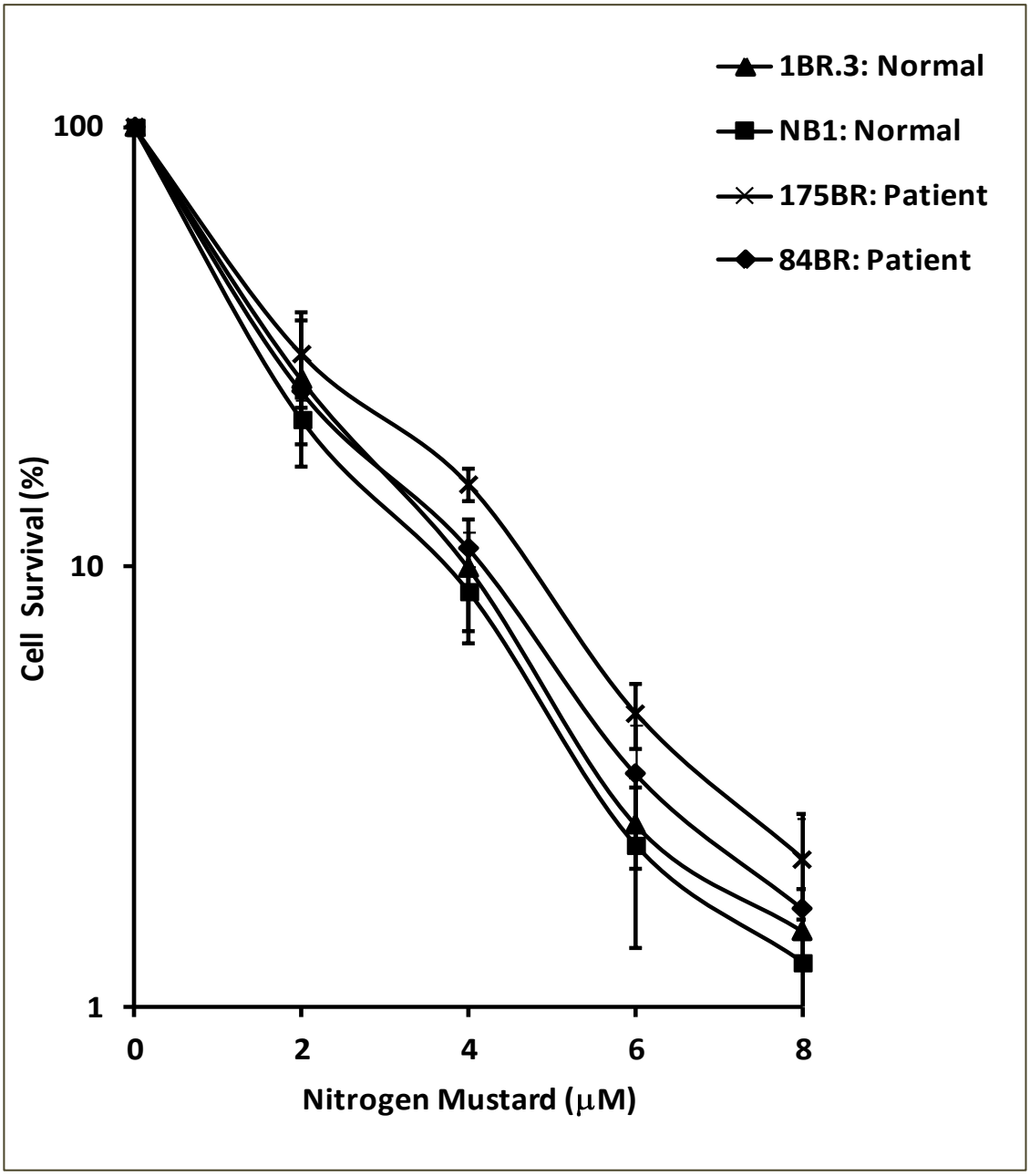

Here the cell survival to HN2 exposure is illustrated. The patient cells having survived the nitrogen mustard suggests a defect in NHEJ repair and efficient repair via HR pathway. The error bars represent the SEM of at least five independent experiments. The P value is 0.18.

The Figure 2.2 shows the response of HN2 on 84BR and 175BR together with the repair normal NB1 and 1BR.3 cells. It can be observed that for all cell lines as the concentration of HN2 increases there is a decrease in clonogenic cell survival. However, all cell lines display a similar sensitivity profile in response to HN2 exposure indicating that the radiosensitivity of 84BR and 175BR cell lines is not due to a defect in HR repair pathway and more likely to be a defect in one or more components of NHEJ repair pathway. This agent primarily exerts its cytotoxicity by the introduction of DNA interstrand crosslinks (ICL) which compromise both strands of the DNA. Such adducts are particularly challenging for the cell to repair which occurs via a two-step process. Here the ICL is 'unhooked' from one strand via the action of the nucleotide excision repair-associated endonuclease ERCC1-XPF protein complex. This in turn creates a substrate for repair of the strand break by HR. Using a Student's unpaired T-test to compare the half maximal inhibitory concentration (IC_{50}) values of the 84BR and 175BR cell lines with the normal fibroblasts it was demonstrated that there were no significant differences in IC_{50} values indicating similar responses to HN2 ($P = 0.18$). This observation indicates that the radiosensitivity of the 84BR and 175BR cell lines is not due to a defect in HR repair pathway and more likely to be a defect in one or more components of the NHEJ repair pathway.

2.4 - Discussion

The clonogenic cell survival of the radiosensitive patients, 84BR (patient with breast cancer) and 175BR (patient with multiple tumours) to IR and HN2 was measured against normal human fibroblasts 1BR.3 and NB1. The use of clonogenic cell survival assay, being the gold standard technique for measuring cellular radiosensitivity for many years (Eastham *et al.,* 2001), had twofold purpose in my research: First, the clonogenic assays were conducted with IR to confirm 1) the clinical radiosensitivity of the 84BR patient cell line at cellular level, 2) to detect the radiosensitivity of 175BR at cellular level. Then, the clonogenic assays were conducted with the HN2, to determine the defective pathway that may be responsible for the cellular sensitivity to IR seen in these patients.

On the basis of the cell survival curves the 84BR and 175BR patient cells seem to be more sensitive to gamma radiation when compared to controls. Thus, the findings confirm the observations made by Arlett *et al*., (1989) and demonstrate the inherent cellular radiosensitivity of the 84BR and 175BR fibroblast cell lines. The findings further confirm that the 84BR patient is not only clinically sensitive to IR but is also sensitive to IR at cellular level.

IR causes DSBs in DNA. The DSBs in eukaryotic cells is repaired via HR or NHEJ repair pathways. The NHEJ repair pathway is the principal mechanism of repair of IR induced DSBs in eukaryotic cells and can occur in non-dividing cells. In HR repair pathway the genetic information lost after DSBs in DNA is borrowed from the sister chromatid so the repair of the lost genetic information is achieved in an error free manner.

To find out which pathway might be defective in the patient cell lines which, lead to sensitivity of these cells to IR, clonogenic assays were conducted with HN2. This DNA damaging agent exerts it is effect by simply introducing ICRs in DNA. The ICRs are repaired via interaction between the NER and HR DNA repair pathway. Here the ICL is unhooked by the action of the site specific endonuclease XPF-ERCC1. This unhooking then provides a substrate for the action of the HR pathway. Thus cells defective in HR are likely highly sensitive to cross linking agents such as HN2 (Clingen *et al.,* 2007). As illustrated in cell survival curves generated after the treatment of cells with HN2 the patient cells are repair normal compare to the controls. The normal sensitivity of patient cells to HN2 suggests that the HR DNA repair pathway may be functioning normal and it is more likely that the defect is in the NHEJ repair pathway. The NHEJ repair pathway repairs the DNA strand breaks in an error prone manner in all phases of the cell cycle but with preference to the G1 and early S phase. It is well known that defects in any key genes found in NHEJ repair pathway results in radiosensitivity (Scott and Pandita 2006). Since, patient cells under study display cellular radiosensitivity to gamma radiation the radiosensitivity seen in these cells may be due to a defect in the NHEJ repair pathway which leads us to further investigate this defect using various other functional and molecular techniques.

Chapter 3 - DNA DSB Assay (γ-H2AX detection)

3.1 - Introduction

In Chapter 2 the clonogenic assays conducted with two patient cell lines revealed a cellular hypersensitivity of about two fold when compared to repair normal diploid fibroblasts. These observations also confirmed that the clinical radiosensitivity of 84BR patient was evident at cellular level. In addition the cellular hypersensitivity of the 175BR cell line may be associated with the increased cancer incidence observed in the patient. Moreover, the clonogenic assay conducted with HN2 demonstrated a normal HR DSB repair. Thus, the cellular radiosensitivity observed in 84BR and 175BR fibroblast cells was likely associated with abnormal NHEJ.

To determine if the cellular radiosensitivity observed in two patient cell lines was associated with a defect in DNA DSB repair, a phosphorylated H2AX (γ-H2AX) assay was performed following the exposure of cells to 2Gy of gamma radiation from a ^{60}Cobalt source.

DNA DSBs occur when both strands are broken close enough to disrupt the Watson-Crick base pairing, resulting in the liberation of two DNA ends (Bassing and Alt 2004). They arise from exogenous agents such as, IR and certain chemotherapeutic drugs, or endogenously generated from ROS and from chromosomal stress (Scott and Pandita 2006). The DSB is probably the most deleterious of the many types of DNA damage that exist within the cell and are potentially lethal if not repaired (Scott and Pandita 2006).

Histones are among the most evolutionary conserved proteins in eukaryotes. They can be classified into five groups, namely the four core histones H2A, H2B, H3, and H4 and the linker histone H1. There are two copies of the four core histones, so in total the eight histones come together to form a histone octamer, which binds and wraps about 1.7 turns of DNA, which is about 146 base pairs of DNA. In addition to this the H1 protein wraps another 20 base pairs, resulting in two full turns around the octamer (Annunziato 2008). This method of packaging allows close to two meters, negatively charged molecules of DNA to exist in relatively small 3D space (Bilsland and Downs 2005). Despite this enormous degree of compaction, the DNA must still be rapidly accessible to permit its interaction with protein machineries that regulate the functions of replication, repair and recombination (Ridgway *et al.,* 2002).

Figure 3.1 - Chromatin structure and histone-modifying enzymes.

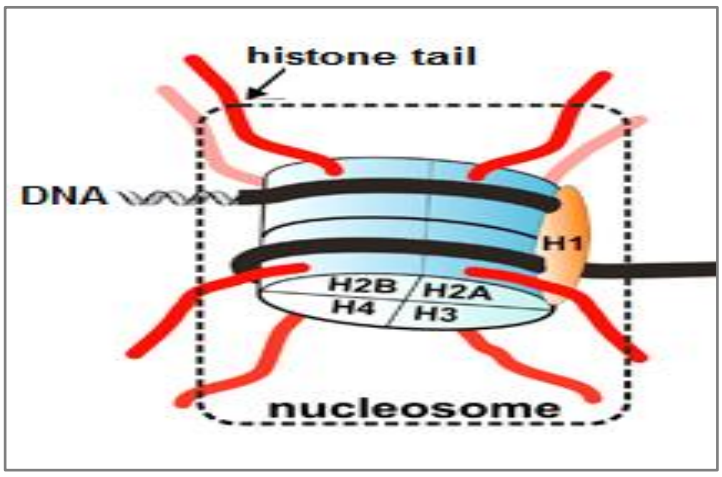

Base pairs of DNA wrapped around a histone octamer consisting of two copies of each of the core histones H2A, H2B, H3, and H4. Linker histone H1 is positioned on top of the nucleosome core particles stabilising higher order chromatin structure (adapted from Fullgrabe *et al.,* 2010).

There are a number of histone H2A variants, two of which are the H2AX and H2AZ proteins that are highly conserved as unique H2A species from *S.cerevisiae* to humans (Redon *et al.,* 2002). The H2AX represents between 2-25% of the total cellular H2A, whereas the H2AZ appears to account for 10% (Redon *et al.,* 2002). The H2A variants contain a sequence (SQ) motif conserved at its carboxy terminus which is somehow evolutionary from *Drosophila* to *S.cerevisiae* (Bilsland and Downs 2005). It is the phosphorylation of this SQ motif in H2AX immediately after the DSBs in the DNA, which is measured to determine the level of DSBs in cells. As one of the early studies by (Rogakou *et al.,* 1999) provides evidence that the cells of the normal human fibroblast IMR90 and the human breast cancer line MCF7 both respond to DNA DSBs caused by IR with the formation of discrete foci containing gamma H2AX. Rogakou *et al.,* (1998) also demonstrated that, after DNA DSBs the H2AX is phosphorylated on the residue serine 139 in the unique carboxy-terminal tail.

Therefore, within minutes after DNA DSBs, the H2AX is phosphorylated and the DNA repair proteins are accumulated in large nuclear domains known as foci at the sites of DNA DSBs (Bilsland and Downs 2005). These foci, also known as the DNA repair centres, contain hundreds to several thousand phosphorylated H2AX molecules per DNA DSB (Rakiman et al., 2008; Bilsland and Downs 2005).

The γ-H2AX phosphorylation is carried out by the PIKK family of protein kinases such as; ATM, ATR (ATM- and Rad3-related or the yeast homologous Mec1 and Tel1) and DNA-PKcs. The formation of γ-H2AX redundantly requires the Met1 and Tel1 kinases in fission yeast strains (Nakamura *et al.,* 2004). Although, previous studies have suggested that the ATM is required for the induction of foci at DSBs, and ATR

is involved in the recognition of stalled replication forks when Friesner *et al.,* (2005) investigated the ATM and ATR dependency of the formation of γ-H2AX in M-phase *Arabidopsis* plant cells exposed to IR they have also found that at least a 10% of the IR induced γ-H2AX foci require functional ATR.

One possible role of the γ-H2AX foci formation at the sites of DNA DSBs could be to serve in recruiting proteins that are involved in re-joining DNA ends such as MRE11 or RAD50 to those sites, either directly, through binding to the γ-H2AX COOH terminus, or indirectly, through an altered regional chromatin structure (Rogakou *et al.,* 1999). Paull *et al.,* (2000), investigated the co-localisation of γ-H2AX and repair factors at sites of laser induced DSBs in MCF7 human breast tumour cell lines and found that the repair factors Rad50 and Rad51 and the tumour suppressor gene (BRCA1) co-localises with phosphorylated H2AX foci at the site of DSBs immediately after the DNA damage. The BRCA1 recruitment to the sites of γ-H2AX phosphorylation happens several hours before the Rad50 and Rad51 co-localises.

3.1.1 - Techniques employed for the measurement of DNA DSBs

Over the years many techniques have been employed to determine the level of DNA DSBs induced by DNA damaging agents such as IR. Few of which will be outlined here.

- The γ-H2AX assay is used to measure the phosphorylated H2AX as an indicative measure for DNA DSBs. The idea in this assay is that, after the exposure of cells with IR, the DSBs are introduced and, where there is DSBs there is accumulation of γ-H2AX at it is site as demonstrated by some of the studies mentioned above. Then the cells are immunofluorescently labelled with antibodies specific to the

phosphorylated H2AX, which binds to the phosphorylated H2AX and fluoresces as discrete spots of foci under the fluorescent microscopy. Also from the literature it is known that the number of foci approximate the number of expected DNA DSBs in the ratio of one γ-H2AX to one DSB in DNA. So by scoring the number of foci as (<5 foci = DSB repair normal and >5foci = DSB repair defective) the DSB repair defect can be established. As the cells are able to repair the DSBs, the number of phosphorylated H2AX will drop, in another term are de-phosphorylated, and in the repair defective cells the level of H2AX phosphorylation will persist.

The phosphorylated H2AX used as a marker for the measurement of DNA DSBs, can be visualised through the use of imagestream imaging flow cytometry. This procedure was recently employed by our group (Bourton *et al.,* 2012), to detect the differences in the induction and repair of DNA DSBs in XP14BRneo17 cell line from XP patient defective in DNA-PKcs, AT5BIVA cell line from A-T patient defective in *ATM* gene, and MRC5-SV1 SV40 immortalised lung fibroblasts derived from repair normal cells. Here cells were exposed to 2Gy of IR to induce DSBs then cells were immunofluorescently labelled with antibodies specific for phosphorylated H2AX. Through the analysis of frequency and distribution of γ-H2AX foci in a minimum of 20,000 cells, our group was able to show a DNA DSBs defect in both the XP and AT patients.

Figure 3.2 - Imagestream analysis of Gamma-H2AX foci in human cells.

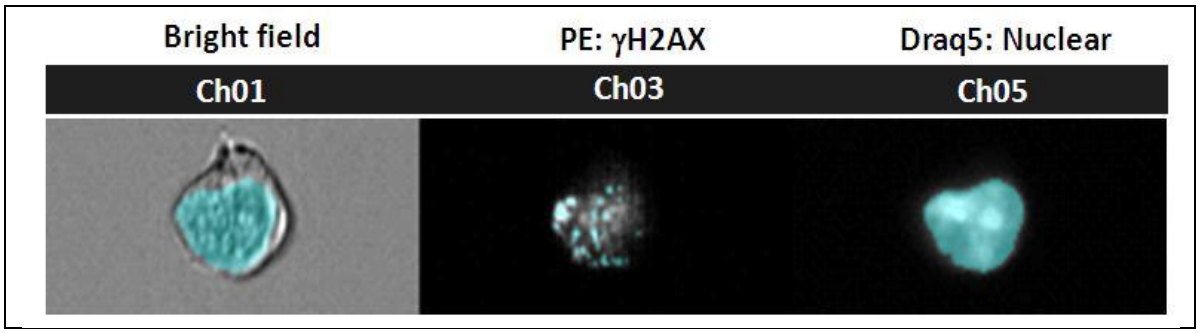

Multispectral imaging in cells at 30 minutes after exposure to 2Gy gamma radiation is illustrated here. Chanel 1: Brightfield image; Chanel 3: Brightfield image with Draq 5 nuclear merge; Chanel 5: Nuclear staining by Draq 5.

- The comet assay also known as the single-cell gel electrophoresis (SCGE) is a simple, rapid, cheap, versatile and sensitive method for detecting a wide variety of DNA damage including single and double strand breaks (Collins 2004), DNA interstrand crosslinks, and base damages that appear as endonuclease sensitive sites in individual cells (Olive and Durand 2005). A unique property of the comet assay is its ability to detect cellular heterogeneity (nuclei containing mixture of damaged and undamaged strand breaks) which is crucial when predicting tumour response to specific treatment (Olive *et al.,* 1998; Olive and Banath 2006). Different types of comet assays exist where each type vary on the bases of pH of the buffer used in lysis buffer at the lysis step. So if the lysis buffer is alkali (pH>13) the alkali sites (ALS) are detected as SSB and if neutral (non-denaturing at pH <13) then DSBs are mainly detected. However, briefly in this assay, the cells are exposed to DNA damaging agents such as IR, then approximately 2µl sample is suspended in 0.5% low melting agarose and sandwiched between a layer of 0.6% normal melting agarose and top layer of 0.5% low melting agarose on fully frosted slides. After the solidification of 0.6% agarose layer, the slides are lysed for approximately an hour in pre-chilled lysing solution or longer up to 24

hours depending on the types of DNA damage being analysed. Then the slides are placed in electrophoresis buffer for 20 minutes at RT, to allow for DNA unwinding and then electrophoresed at 20V 300mA. The electric current pulls the charged DNA from the nucleus so that relaxed and broken DNA fragments also known as comets migrate further from the nucleus than intact DNA. The comets formed during electrophoresis are then neutralised using the neutralisation buffer, and stained with ethidium bromide to be imaged under the fluoresce microscopy. According to Mozaffarieh *et al.,* (2008), the cells containing damaged DNA have the appearance of comet with bright head and tail. In contrast, undamaged DNA appears as an intact nucleus with no tail Figure 3.3.

Figure 3.3 - Fluorescence microscopy visualisation of comet assay.

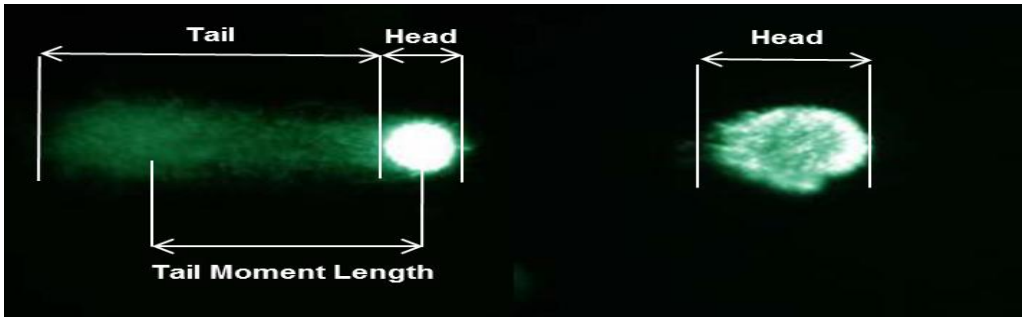

The comet created by electrophoresis has an astronomical body, with head consisting of intact DNA and a tail containing damaged and broken pieces of DNA. Intact nucleus with no tail represents undamaged DNA (adapted from Hastak *et al.,* 2008).

Pulsed field gel electrophoresis (PFGE) analysis the DNA DSBs caused by IR, through the separation of broken DNA from extremely large chromosome (Gunderson and Chu 1991). Briefly, in this assay the irradiated cells are embedded in agarose plugs and lysed to release DNA without any mechanical damage to it before subjecting to an electrophoretic condition. During electrophoresis DNA above 30-50 kb migrates with the same mobility as single large diffused bands. The DNA is

then forced to change direction during electrophoresis to allow different sized fragments within this diffuse band begin to separate from each other. With each reorientation of the electric field relative to the gel, smaller sized DNA will begin moving in the new direction than the larger DNA. Thus the larger DNA lags behind, providing a separation from the smaller DNA.

Figure 3.4 - A model for PFGE.

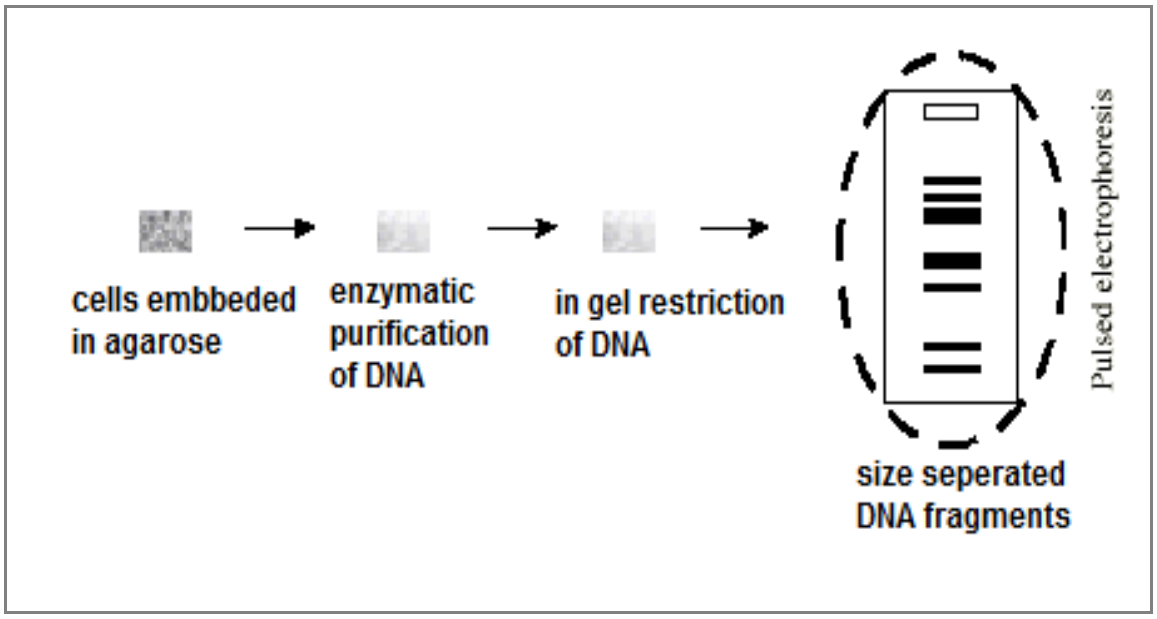

Whole cells are embedded in agarose and DNA is enzymatically purified and restricted by rare cutting enzymes in situ. The agarose plug is then inserted into a well in an agarose gel and the restricted fragments are separated by an electric current which pulses from different angles (O'Sullivan 2000).

The use of H2AX, comet or PFGF assays for the detection of DSB defects in radiosensitive patients with various human diseases is known for many years. One example is the use of H2AX assay by Abbaszadeh *et al.,* (2010), which revealed an altered cellular response to IR as a DSB repair defect in XP14BR cell lines in a 14 year old XP patient. Other human diseases with evidence for altered cellular response to DNA damage where one of these techniques have been employed to

detect DSB defect are the Bloom's syndrome (Nocentini 1995) and Nijmegen Breakage Syndrome (Girard *et al.,* 2000).

Kühne *et al.,* (2004), employed immunoflurosence detection of γ-H2AX nuclear foci and pulsed gel electrophoresis assay in AT1BR cell lines, deficient in ATM, from a patient with A-T, to analyse the time course for DSB repair between days 1 and 14 after 2Gy of X-ray exposure. According to their findings the AT1BR cells exhibited a substantial fraction of unrepaired DSBs many days after irradiation and contribute to radiosensitivity in ATM deficient cells.

Girard *et al.,* (2000), used untransformed skin fibroblasts 87RD102 derived from NBS patients displaying radiosensitivity and cell cycle checkpoint defect and 347BR derived from a patient with a diagnosis of common variable immunodeficiency. The aim of their research was to find out if the radiosensitivity of the NBS cells was the result of a repair defect in these cells or if it can be attributed to impaired checkpoint arrest. Using the PAGE assay, they have found a modest but reproducible defect in DNA DSB re-joining in 347BR and 87RD102 cells after exposure to IR.

The ability of radiosensitive patient cells (84BR and 175BR) to repair the DSBs induced by IR was measured in this study using the γ-H2AX assay as described in materials and method section.

3.2 - Materials & Method

The detection of phosphorylated H2AX as an indicative measure for the repair of DNA DSBs after the exposure of cells to gamma radiation as described by Abbaszadeh *et al.,* (2010), will be outlined here in detail.

3.2.1 - Irradiation of cells

Cells were grown as monolayers on 13 mm diameter circular coverslips (Sigma) and exposed to 2Gy of gamma radiation from a ^{60}Cobalt source.

3.2.2 - Fixing of cells

Cells were washed for three times in 5ml PBS and fixed in a 50:50 acetone and methanol mixture for 8 minutes at 4ºC, at specific time points (30 minutes, 3, 5 and 24 hours). Control cells were not exposed to γ-radiation. After fixing, cells were washed twice with ice-cold PBS.

3.2.3 - Permeabilisation and Blocking

On each coverslip 0.5 ml Permeabilising buffer (0.5% TritonX100) (Sigma) in PBS was added for 5 minutes, after which the buffer was aspirated then blocking buffer (0.2% skimmed milk, 0.1% Triton X-100 in PBS) was applied. Then the cells were incubated in a humidified box at 4ºC overnight. The next day, the blocking buffer was removed from the cells with three washes of PBS.

3.2.4 - Immunostaning with Anti-γH2AX Antibody

Cells were incubated with 25µl (per coverslip) of anti γ-H2AX phosphoserine[139] (Clone JW301) mouse monoclonal antibody (Millipore Ltd., Watford, UK) diluted 1/10,000 in blocking buffer, for an hour at room temperature. After incubation the cells were washed with PBS three times with 15 minutes incubation at each wash. Cells were then incubated with 200µl/well of secondary antibody Alexa Fluro® 488 goat anti-mouse IgG (Invitrogen Ltd., Paisley, Scotland, UK) diluted 1:1000 in blocking buffer, for 1 hour at room temperature in dark. Antibodies were then washed off with PBS and cell nuclei were counterstained with 2µg/ml of Propidium iodide in PBS for 3 minutes and de-stained with distilled water for 20 minutes.

3.2.5 - Mounting Slides

Cells were washed, and mounted in mowoil mountant containing 1µg/ml 4'6-diamidino-2 phenylindole (DAPI) (Sigma Aldrich Ltd). The excess mounting medium and air bubbles were removed before sealing the edges of the coverslip with clear nail polish. Slides were stored at -20ºC until the analysis.

3.2.6 - Cell Scoring and Imaging

Analysis was performed by counting the number of foci in a minimum of 200 nuclei of each cell line at each time point (un-irradiated and 30 minutes,3, 5 and 24 hours post exposure) using a Zeiss Axioscope fluorescence microscope with a 100X magnification objective. Untreated cells typically exhibited 0-2 foci per/cell. Also images of each cell lines were captured by using the fluorescence microscopy equipped with Photonic Science Cooled charge-coupled device (CCD) camera (West Germany) with integration times of between 0.5-10 seconds depending on the brightness of staining.

3.3 - Results

3.3.1 - γ -H2AX foci assay: DNA DSB repair

Exposure of radiosensitive cell lines to 2Gy of gamma radiation induced DSBs in two radiosensitive patient cell lines (84BR and 175BR) and in two repair normal individuals (NB1 and 1BR.3), which resulted in accumulation of phosphorylated H2AX proteins at the sites of DSBs. Following the cell exposure to gamma radiation the cells were fixed, permeabilised and stained with primary and secondary antibodies. Then the induction and repair of DNA DSBs in radiosensitive cell lines and in normal individuals was determined by counting the number of γ-H2AX foci in the nuclei of untreated cells and those exposed to 2Gy gamma radiation at 30 minutes, 3, 5 and 24 hours post irradiation.

The induction and repair of DNA DSB in all cell lines was determined by counting the number of γ-H2AX foci in the nuclei of untreated cells and those exposed to 2 Gy gamma radiation at 30 minutes, 3, 5 and 24 hours post-irradiation. The data displayed in Figure 3 show that in the untreated cells there are more residual γ-H2AX foci in the radiosensitive 84BR and 175BR cell lines (5.12 and 4.32 foci per nucleus respectively), compared to the repair normal NB1 and 1BR.3 cells (0.81 and 1.02 foci per nucleus). At 30 minutes post-irradiation there is a dramatic induction of foci in all cells consistent with the induction of DNA DSB. In the NB1 and 1BR.3 cells the number of foci return to near normal levels at 5 and 24 hrs. In the 84BR and 175BR cells however, there is a significant (Student's unpaired T-test) retention of foci at 5 and 24 hours when compared to the NB1 and 1BR.3 cells.

Figure 3.5 - DSB repair measured by formation and disappearance of γ-H2AX foci in radiosensitive cells and controls.

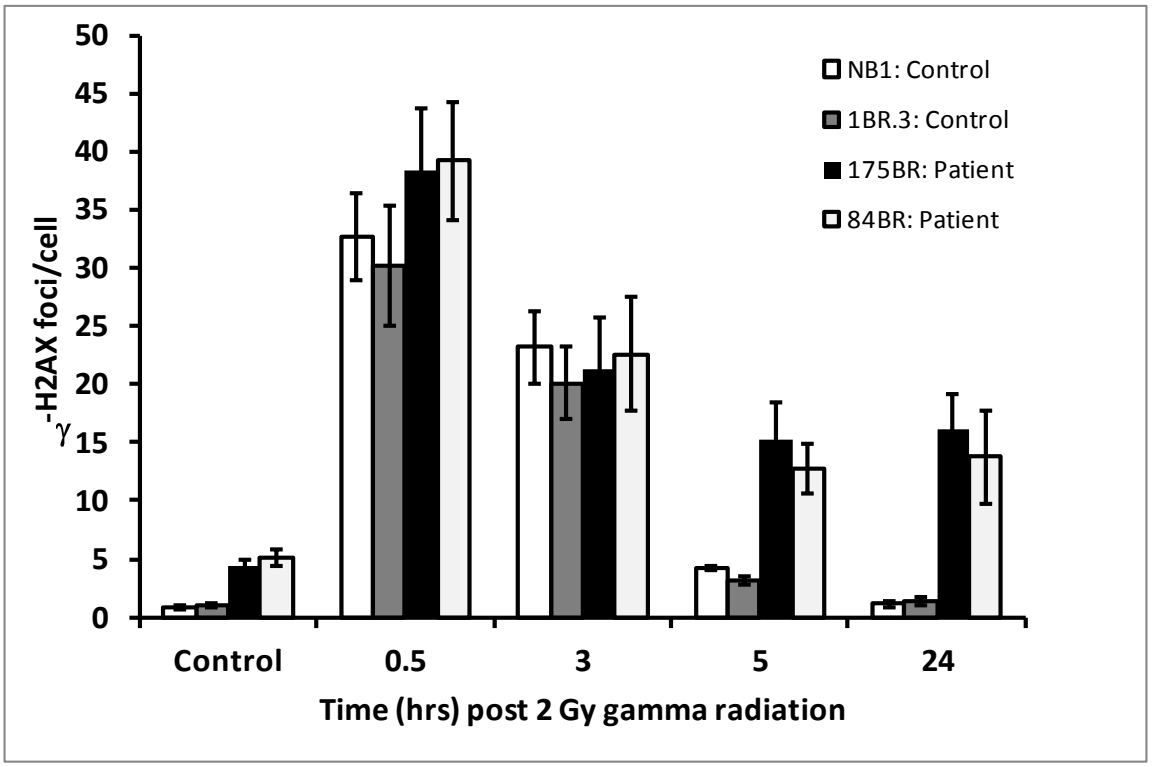

The induction and repair of DNA DSBs in the radiosensitive 84BR and 175BR fibroblasts in comparison to the repair normal 1BR.3 and NB1 fibroblast cells. Cells were exposed to 2Gy gamma radiation and the induction and repair of DNA DSB was measured by the appearance and removal of γ-H2AX foci in the nuclei of un-irradiated and irradiated cells. Data are derived from three independent experiments, the error bars represent standard error of the mean and the P value is < 0.05.

Since the γ-H2AX level after five and twenty four hours post irradiation remained significantly higher in 84BR and 175BR patient cells a reduced repair in DNA DSBs in these cells is clearly visible. However, in the repair normal NB1 and 1BR.3 cells the γ-H2AX returned to near normal levels after five and twenty four hours post irradiation thus, indicating an efficient level of repair of DNA DSBs.

As illustrated in Table 3. 1 the efficient repair of γ-radiation-induced by DSBs is determined by de-phosphorylation of foci (clearing of γ-H2AX foci) in 84BR and 175BR patient cells and NB1 with IBR.3 cell lines from normal individuals in five independently conducted experiments.

Table 3. 1 - The γ-H2AX foci formation following 2Gy of gamma irradiation in irradiated patient and control cells.

Number of γ-H2AX per nuclei				
Time Points (hr)	175BR	84BR	NB1	1BR.3
Untreated	4.2	5.12	0.81	1.02
0.5	37	39	33	30
3	22	24	24	20
5	17	15	5	4
24	17	15	0.81	0.81

So, to conclude, the visualisation of γ-H2AX formation confirms the clonogenic radiosensitivity seen in patient cells and is likely to be associated with a defect in DSB repair.

3.4 - Discussion

The clonogenic assay conducted with IR revealed cellular radiosensitivity in 84BR and 175BR patient cells. The IR causes DSBs in DNA which can be repaired via NHEJ or HR repair pathways. Then, the clonogenic assays were conducted with HN2 to detect the defective DNA DSB repair pathway that may be responsible for the cellular radiosensitivity seen in patient cells. This alkylating agent induces cross links in DNA, which is repaired primarily by HR repair pathway. The ability of patient cells to repair the cross links induced by HN2 suggested a normal HR but a possible defect in the NHEJ repair pathway. Then a gamma H2AX assay was conducted to find out if the cellular radiosensitivity in both patients is due to a defect in the ability of cells to repair the DSBs induced by IR.

The γ-H2AX assay is a widely accepted technique for the detection and estimation of DSBs induced by DNA damaging agents such as IR. The γ-H2AX assay being the most simple and sensitive assay was chosen in our research for the detection of DSB repair defect in radiosensitive patient cells.

The H2AX, one of the variants of H2A histone proteins, along with other core histone proteins (H2B, H3, and H4) and linker histone (H1) protein compacts two meter long DNA in a 3D space. The H2AX constitutes a carboxyl tail which is a highly conserved sequence comprising of an SQ motif. Immediately after DSBs are induced this 139 residue is phosphorylated (γ-H2AX) and DNA repair proteins are recruited to the DSB sites where a group of H2AX at each site of DSBs are known as foci.

Immunofluorescence assay was conducted, where specific antibodies were raised against γ-H2AX, to detect the γ-H2AX foci formation in the patient cells. At least 200 foci, each foci containing hundreds to thousands of γ-H2AX, were viewed and images were taken with the florescence microscopy. The number of γ-H2AX foci were counted and plotted against various time points, post exposure to IR. The rate of disappearance of γ-H2AX has been shown to be associated with a greater ability to survive following treatment with clinically relevant doses of (2Gy) of IR (Olive and Banath 2006; Abbaszadeh *et al.,* 2010).

The γ-H2AX induction was approximately the same in both the patient cells and the repair normal cells after 30 minutes exposure to IR (15 and 14 foci per nucleus). Then after 24 hour post irradiation, the level of γ-H2AX foci was reduced to 5 and 4 foci per nucleus in 84BR and 175BR cell lines. Thus, indicating a normal DSB repair in the controls and DSB repair defect in patient cells. The evidence provided from this data strongly dictates a defective NHEJ repair pathway in patient cells.

Here we have demonstrated that the enhanced radiosensitivity in these cell lines was associated with a failure to effectively repair DNA DSB following radiation exposure as measured in a γ-H2AX foci retention assay.

Since γ-H2AX foci loss monitors all repair events, that is, NHEJ and HR (Beucher *et al.,* 2009) we sought alternative techniques, which would more specifically measure the key genes in NHEJ repair pathway. So, to determine the defective component of the NHEJ pathway an investigation of expression levels of key NHEJ genes was conducted using the technique of quantitative real time PCR (qRT-PCR).

Chapter 4 - Quantification of NHEJ genes in radiosensitive cells by qRT-PCR

4.1 - Introduction

The existence of a potential NHEJ repair defect in cells derived from two radiosensitive patients (84BR and 175BR) was shown after observing:

1. Cellular radiosensitivity in a clonogenic assay.
2. A normal response to the crosslinking agent (nitrogen mustard), as an indicative measure to normal functioning of HR pathway.
3. Abnormal repair of DNA DSB measured by γ-H2AX retention.

Taken together, these data suggest the DSB repair defect found in cells is most likely due to aberrant or abnormal NHEJ repair causing the cellular and clinical radiosensitivity described.

Subsequently, to reveal the possible defect in NHEJ repair pathway the expression of the key NHEJ genes was examined using the qRT-PCR. The principal genes whose proteins function in this pathway and their locations on different chromosomes are shown in Table 4. 1

Table 4. 1 - NHEJ repair genes and their locations on different chromosomes.

Chromosome location	NHEJ repair genes	Protein function in NHEJ
2q35	Ku80	Binds to DNA ends and recruits DNA-PKcs to the break site.
22q13.12	Ku70	Binds to DNA ends and recruits DNA-PKcs to the break site.
8q11	DNA-PKcs	Recruits Artemis.
10p13	Artemis	Endonuclease trimming of un-compatible DNA ends.
5q13	XRCC4	Promotes gap filling and reseals DSBs.
13q33	Ligase IV	Re-ligates compatible DNA ends.
2q35	XLF /Cernunnos gene	Involved in the ligation step.

As briefly covered in the Chapter 1, defects in any components of NHEJ pathway can lead to hypersensitivity to IR, genome instability, immunodeficiency and cancer (Bassing and Alt 2004). In humans, defects in the specific genetic components of NHEJ also result in predisposition to cancer (lymphoma and leukaemia) or to extreme radiosensitivity. For example, defects in ligase IV (Riballo *et al.,* 1999) deficiency in artemis expression (Musio *et al.,* 2005) or a mutation in DNA-PKcs gene (van der Burg *et al.,* 2009; Abbaszadeh *et al.,* 2010) are associated with extreme clinical and cellular radiosensitivity and increased cancer incidence.

Vis-à-vis published evidence we have employed the qRT-PCR method to determine if abnormal gene expression of any key genes found in the NHEJ repair pathway is responsible for the cellular hypersensitivity seen in 175BR and 84BR cell lines.

The quantitative or real time PCR is not a new discovery but more of a new development by Higuchi *et al.,* (1992), from the traditional PCR assay first discovered

by Kary B. Mullis in 1983. To this date the real time PCR has been the gold standard for gene expression analysis but, other techniques may also be used to examine genetic defects in cells which may lead to abnormal DNA repair processes (D'Haene *et al.,* 2010). These include conventional karyotyping, fluorescent in situ hybridisation (FISH) analysis, microarray-based copy number screening, multiplex ligation-dependent probe amplification (MLPA). However, real time PCR distinguishes itself from other methods in terms of accuracy, sensitivity, and fast results. Because of this, the technology has established itself as the golden standard for medium throughput gene expression analysis (Derveaux *et al.,* 2010). Some of the basic steps involved in real time PCR method for the detection of gene expression are summarised in Figure 4.1.

Figure 4.1 - Steps in nucleic acid quantification by real time PCR.

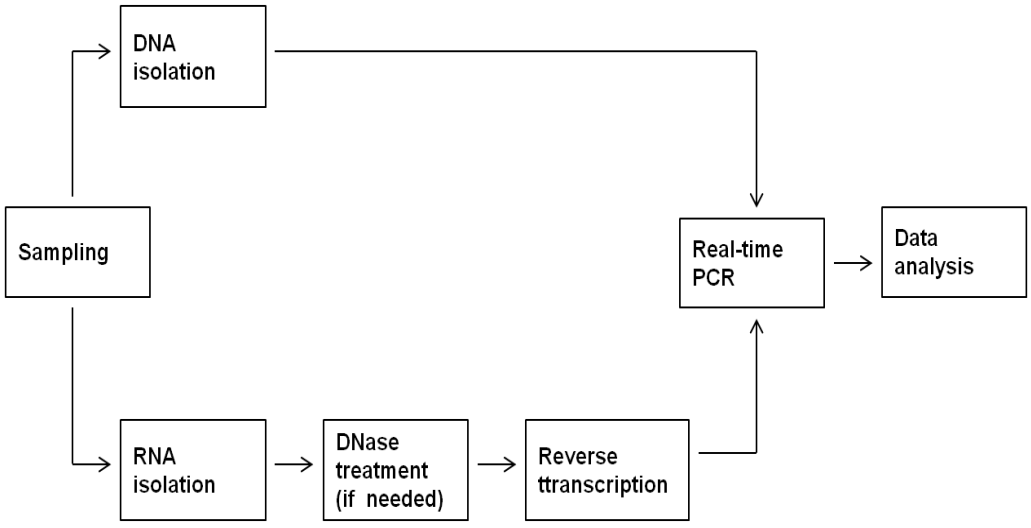

Here the processing of a sample using real time PCR as a detection method is illustrated (adapted from Stahlberg *et al.,* 2005).

The real time PCR detects the amplicon as the reaction is happening and the data is gathered at the exponential phase of the PCR reaction. The data is then manifested on a amplification plot or a melting curve.

The amplification plot is a graphical representation of gene expression. As the fluorescent signal reporter increases to a detectable level the gene expression is captured and displayed on this plot. A threshold on this plot is the point at which a reaction reaches a fluorescent intensity above background. A cycle threshold (Ct) is the cycle at which the sample reaches the threshold. Several mathematical methods make use of the Ct value to calculate the gene expression level. One recently developed mathematical model is the delta-delta comparative Ct method of relative quantification, written in short as $2^{-[\Delta Ct\ Sample\ -\ \Delta Ct\ Control]}$ or $2^{-\Delta\Delta Ct}$ (Pfaffl 2001). The $2^{-\Delta\Delta Ct}$ was employed in this research to detect the expression of NHEJ repair genes in 84BR and 175BR patient cells.

The dissociation or melting curve provides a graphical representation of the PCR products. A single peak on this graph usually suggests a single size product and a presence of a peak in the negative control sample usually indicates a primer dimer.

Although, the literature search reveals no specific study on the use of qRT-PCR for the detection of NHEJ repair genes in radiosensitive cells the two papers that prompted the use of qRT-PCR assay to detect the possible defect in NHEJ repair genes were;

1. The study by Mohrin et al., (2010), which makes use of the qRT-PCR assay for NHEJ repair gene expression analysis in quiescent hematopoietic stem cells

(HSPCs) from adult mouse cells. Their findings reveal that the HSPCs are intrinsically more resistant to IR exposure than common myeloid progenitors (CMPs) and granulocyte/macrophage progenitors (GMPs). They imply that the long-lived HSPCs are resistant to IR-mediated cell killing, have enhanced NHEJ repair gene expression and a strong induction of p53-mediated DNA damage response (DDR) leading to growth arrest and DNA repair; whereas short-lived MPs are molecularly poised to undergo apoptosis and are predominantly eliminated in response to genotoxic stress.

2. The study by Chiou *et al.,* (2007) uses qRT-PCR to examine the mRNA transcripts of KU70, Ku80, DNA-PK, Artemis, XRCC4, Ligase IV and XLF in paediatric acute lymphoblastic leukaemia (ALL) patients. This study reveals that the mRNA expressions of all NHEJ members in untreated fresh ALL were elevated when compared with (the non-leukemic) thalassemia cases. The overexpressed NHEJ mRNAs were down regulated after therapy i.e. after complete remission and mRNA transcripts of Ku80, DNA-PK, Artemis, XRCC4 and ligase IV were elevated again in relapsed specimens. Therefore, differential mRNA expressions of NHEJ genes were observed between persons of various disease statuses.

Based on the studies outlined here a qRT-PCR assay was designed to detect the expression of the NHEJ repair genes in two radiosensitive patient cell lines compared to the expression of these genes in repair competent normal fibroblasts.

4.2 - Materials & Method

4.2.1 - RNA Extraction

The first critical step prior to commencing qRT-PCR is continual production of high quality intact cellular RNA which requires, the yield of the RNA extract, the RNA integrity, purity, storage and stability to be of high standard. The steps involved in RNA extraction are as follows.

4.2.1.1 - Cell Lysis

Medium from cell cultures of 80% confluence was aspirated. The cells were thoroughly washed by adding 10ml of ice cold PBS to the cells and gently agitating the cells by swirling the Petri dish. The PBS was aspirated; 2ml (as manufacturer's recommendation of 2ml for 10cm dishes) of TRIzol (Sigma Aldrich, Dorset, UK) was added to the adhered cells and incubated for 2-3 minutes at room temperature to detach the cells from the dish. Further cell detachment and homogenisation was achieved by pipetting the cells up and down for several times. The homogenised cells were incubated at room temperature for 5 minutes to completely dissociate the nucleoprotein complex. Then the cells were collected in 1 ml eppendorf tubes and pelleted at 13,000 rpm centrifugation for 1 minute.

4.2.1.2 - Phase Separation

Two hundred µl of chloroform was added to the cell pellet in TRIzol, then the tube was vigorously shaken for 15 seconds and the cells incubated at room temperature for 3 minutes. All work with chloroform performed in fume cupboard (Premier Labserve Limited, County, UK) as the chloroform is a narcotic reagent. The samples

were centrifuged at 13,000 rpm at 4°C for 30 minutes to separate the sample into following phases:

Top colourless aqueous phase	=	RNA
Inter phase	=	DNA
Bottom red organic phase	=	Protein, Lipids

4.2.1.3 - RNA Precipitation

The upper (clear) aqueous layer transferred to a fresh 1ml eppendorf tube (Sarstedt Ltd, Leicester, UK) with a p1000 (1000 ml) Gilson Pipette (Sarstedt) ensuring that the upper layer was not contaminated with the lower two layers. Then 0.5ml of propan-2-ol was added to the decanted aqueous layer, shaken thoroughly for 15 seconds and incubated at room temperature for 10 minutes. Samples centrifuged at 4°C (Sorvall® Legend T, Thermo Scientific) for 20 minutes to precipitate the RNA also to form a gel-like pellet.

4.2.1.4 - RNA Wash and Re-suspension

Following centrifugation the supernatant was discarded and 1ml of 75% ethanol was added to the RNA pellet and briefly vortexed for 10 seconds to wash the pellet. The sample was centrifuged at 4°C, 8,000 rpm, for 5 minutes. The supernatant was removed and the pellet was air dried for 5 minutes at room temperature. The RNA pellet was re-dissolved in 30µl of 1% Diethylpyrocarbonate (DEPC) treated water and incubated at 60°C for 10 minutes to dissolve the pellet in solution.

4.2.2 - RNA Concentration and Purity Detection

Once the RNA was extracted 1µl of RNA was placed in a Nanodrop 2000C (Thermo Scientific, Wilmington, USA) and the RNA concentration and purity was determined. Pure preparation of RNA had $A_{260} - A_{280}$ ratio values in the range of 1.5 to 2. The RNA purity was further determined on 1% agarose gel by approximately running 10µl 1:1 dilution of RNA (200ng RNA suspension in 9µl of DEPC treated water containing 1µl 6X Loading Buffer (30% w/v/ sucrose, 0.35% orange G) on a 1% agarose gel. The RNA purity was then visualised with Ethidium bromide (EtBr) under UV transilluminator (Alpha Innotech Corporation, USA). As the RNA degrades fast at RT, immediately, after RNA quantification, the RNA in solution was stored at -80°C.

4.2.3 - Deoxyribonuclease I, amplification grade treatment of RNA

The quality of the extracted RNA may be influenced by certain factors for example, the DNA or protein during RNA extraction may be carried over into the RNA extract which, may then interfere with the gene amplification. To circumvent this problem, a 20µl reaction mix was prepared in a 1ml RNase free microcentrifuge tube (Sarstedt Ltd), containing 4µg total RNA, 2µl 10X DNAse I (Deoxyribonuclease I) reaction buffer (Sigma Aldrich) 0.5µl (40U/µl) RNase out (Sigma Aldrich) 2µl (1U/µl) DNAse 1, Amp Grade (Sigma Aldrich) and DEPC treated water. The reaction was incubated at RT for 1 hour. After the incubation 25mM (2µl) DNase 1 stop solution (EDTA) at pH 8 was added to the reaction and heated for 15 minutes at 65°C. The RNA sample is now ready for reverse transcription. The sample can be stored at -80°C for future use.

4.2.4 - cDNA Preparation

4.2.4.1 - Annealing of Primers to RNA

In a 1ml nuclease free-microcentrifuge tube (5 µl) 1µg DNase treated total RNA, 1 µl (10mM) dNTP mix (Invitrogen, Paisley, Scotland, UK), 1 µl (250ng) Random primers (Invitrogen) were added and the reaction volume was made to 13ml with 6ml DEPC treated water. The mixture was heated at 65°C in a heating block (Techne, Fisher Scientific, UK) for 5 minutes then incubated on ice for at least 1 minute. Then the content of the tube was collected by brief centrifugation.

4.2.4.2 - Synthesis of First Strand cDNA

To the content above plus 4 µl (5X) first-strand buffer, 1 µl (0.1 M) DTT, 1 µl (40 units) RNaseOUT ™ RNase Inhibitor, 0.5 µl (100 units) SuperScript™ III (all purchased from Invitrogen Ltd) and 0.5 µl DEPC treated water were added to make up a total volume of 20µl reaction. With gentle pipetting the reaction was mixed up and down and incubated at following temperatures (25°C for 5 minutes, 50°C for 50 minutes and 70°C for 15 minutes) inside the gradient PCR (Peltier Thermal Cycler) for 70 minutes. The first DNA strand (cDNA) was stored at -20°C.

4.2.4.3 - Determining the quality of cDNA

In an eppendorf tube 10µl ReddyMix (Thermo Scientific), 2µl (5µM) forward GAPDH primer (Sigma Aldrich), 2µl (5µM) reverse GAPDH primer and 4µl DEPC treated water was added. The reaction was run at following parameters in gradient PCR.

Table 4. 2 - PCR amplification cycles for detection of cDNA quality.

Number of cycles	Temperature (°C)	Time
1	94	5 min
35	94	45 sec
	58	45 sec
	72	45 sec
1	72	10 min

The quality of the cDNA was visualised with EtBr under UV transilluminator and an image of the cDNA run was captured.

4.2.5 - Determining the quality of primers

Before commencing qPCR it was crucial to know if the primers work well, whether there is any primer dimers and if the NHEJ repair genes are being expressed. A PCR reaction made with following reagents answered some of these questions.

- 100ng cDNA from NB1 cell line
- 1µl forward primer (10µM)
- 1µl reverse primer (10µM)
- 16µl 1.5 X ReddyMix

The volume was made to 20µl with DEPC treated water then the PCR mix was amplified at following cycles in the gradient cycler as summarised in Table 4.3.

Table 4. 3 - PCR amplification cycles for detection of primer quality.

Number of cycles	Temperature (°C)	Time
1	95	5 min
34	95	40 sec
	60	40 sec
	72	40 sec
1	72	15 min
1	4	∞

4.2.6 - Determining the quality of PCR products

The amplified PCR products were run on 1% agarose gel. The 1% agarose gel was prepared by dissolving 1g agarose (Fisher BioReagents, New Jersey, USA) in 90ml distilled water and 10ml 10 X TBE (89 mM Tris-HCI pH 7.8, 89 mM borate, 2 mM EDTA) in the microwave until the agarose was translucent in solution. When the solution was hand temperature hot 2µg/ml EtBr was added to the agarose and poured in electrophoresis chamber with a comb already in place. Once the gel had solidified 1X TBE buffer was poured on the gel, the comb was removed and the PCR samples were loaded to the wells. Five µl molecular weight DNA ladder was loaded in another well to accurately size the PCR product. The samples were run at 40V for 50 minutes, and visualised under UV transilluminator. An image of the DNA run was captured with the image acquisition end analysis system.

4.2.7 - Designing Primers for NHEJ repair genes

The Applied Biosystems (AB) ABI Prism prime express version 2.0 was used to design primers for the key NHEJ repair genes. First the primer annealing temperature (PARAMS) was set to 60°C, the GC content of the primer was set to max: 45 or min: 55%, the primer length was set to min 18bp or max: 22bp and the amplicon product size was set to max: 100bp or min: 150bp. Then the icon ‘optimal primers’ was selected to retrieve a list of optimal i.e. the best known primers for the genes under study. From this list the primer that was the most GC rich at the 3’ end of the primer sequence was selected. The FASTA sequence of mRNA of interest was downloaded from National Centre for Biotechnology Information (NCBI) and loaded into the primer express software. The chosen primer pair sequences were then BLASTED in NCBI website to check for specificity of each primer. A list of

primers designed and ordered from Sigma-Aldrich for the qPCR analysis of NHEJ repair genes are listed in Table 4. 4.

Table 4. 4 - Primer sequences used for the amplification of NHEJ genes during qRT-PCR analysis.

Gene	Primer sequence (5' – 3')	Amplicon size (bp)
Ku70	F: CCCCAAAGACAAACCAAGTGG R: AGCGATGGCAGCTCTCTTAGA	121
Ku80	F: AATGACAGTGCCAAAGCCAGC R: CAAGGATATGTCAAAGCCCCC	113
Artemis	F: ACAGGAGACTTCAGATTGGCG R: CACTCCTCCCGACTTGGAATT	145
XRCC4	F: TTTGGATAATCTCCTTCGCCC R: TTCGCACCCGTAGAATCAGTG	103
Ligase 4	F: CTGCACCTTGCGTTTTCCA R: TACCAGATGCCTTCCCCCTAA	115
XLF-cernunnos	F: TTTGGATAATCTCCTTCGCCC R: TCACTTCGCACCCGTAGAATC	107
DNA-PKcs	F: CCAGCTCTCACGCTCTGATATG R: CAAACGCATGCCCAAAGTC	125

The dry oligonucleotides were re-suspended to a 100µM concentration with DEPC treated water following the manufacturer's guideline and stored at -20°C. The glyceraldehyde-3-phosphate dehydrogenase (GAPDH) (F: GAAGGTGAAGGTCGGAGT and R: GAAGATGGTGATGGGATTTC) was used as an internal control in experimental sample to normalise the quantitation of a cDNA target for the differences in the amount of cDNA added to each reaction. The normalisation of target gene expression levels must be performed to compensate intra and inter-kinetic qRT-PCR variations i.e. the sample-to-sample and run-to-run variations (Pfaffl and Hageleit 2001).

4.2.8 - Optimising Primer Concentration

In three separate PCR tubes a PCR reaction was prepared at 10µM primer concentration and the reaction was run under fast real time ABI PRISIM® 7900HT Sequence Detection System (SDS).

Table 4. 5 - PCR reaction conducted at 10µM primer concentration.

100ng *cDNA (µl)	10µM ^forward primer (µl)	10 µM ^reverse primer (µl)	2X SYBR Green (µl)	DEPC treated water (µl)
2	1	1	10	6
2	1	1	10	6
2	1	1	10	6

***cDNA derived from NB1 cell line; ^primer is the GAPDH**

A melting curve was generated where each peak in the curve represented an approximate expression value of the NHEJ repair genes. Also primer dimer formation, if any, was visualised from this graph.

4.2.9 - qRT-PCR

A master mix consisting of 10µM (1µl) forward primer, 10µM (1µl) reverse primer, (except for GAPDH which was used at 5µM) 10µl (2X) SYBR green (Applied Bio-systems) and 7µl DEPC treated water was prepared in a 0.5ml eppendorf tube. In a pre-cooled 96 well plate (Applied Bio-systems) 100ng (1µl) cDNA was pipetted per well. To each well 19µl of master mix was added. The plate was then sealed with optical adhesive cover (Applied Bio-systems), inverted few times and centrifuged at 4°C at 12,000 rpm for few seconds. It was important to keep the 96 well plate on ice whilst preparing the qRT-PCR reaction to minimise the degradation of cDNA. The 96

well plate was placed in ABI prism 7900HT SDS and the reaction was ran under fast real time PCR program.

4.2.10 - qRT-PCR data analysis on SDS.3 Software

The SDS 2.3 software installed on the ABI PRISIM® 7900HT instrument was used to quantitatively run the PCR products. The following parameters; relative quantification (ΔΔCt) and container 96 well plate were selected to create an SDS file with a 96-well plate map. The detectors (DNA-PKcs, GAPDH, XLF, Ligase IV, Artemis, KU70, KU80, XRCC4) once added to the detector tab were assigned to the 96 well plate. The endogenous gene and the target genes were selected. The wells not in use were omitted. Under the instrument tab the thermal profile was edited to the following temperatures and a dissociation stage was added at stage 4. The Table 4.6 summarises the thermal profile set for the qRT-PCR reaction.

Table 4.6 - The thermal profile set for the qRT-PCR reaction.

Stage	Number of cycles	Temperature (ºC)	Time
1	1	50	2 min
2	1	94	10 min
3	35	94	15 sec
		58	1 min
4	1	72	1 min

The volume of the reaction was kept to 20µl. The real time tab was selected. The 96 well plate was loaded to the ABI machine and the PCR reaction began under the fast run option. After the run was complete, which took approximately 45 minutes, the dissociation program was set up.

4.2.11 - Setting up the Dissociation Program

Under a new document file the absolute quantification assay was selected. The template was kept blank and the barcode was left empty. The appropriate detectors were added, then under the instrument tab the thermal profile was set to the following parameters as in Table 4.7.

Table 4.7 - The thermal profile set for the dissociation curve.

Stage	Number of cycles	Temperature (°C)	Time (sec)
1	1	95	15
2	1	60	15
		95	15

Data collected at the end of the run was analysed using the SDS.3 RQ manager software. The results were plotted on separate bar charts to show the level of gene expression in both patient cells.

4.3 - Results

It can be hypothesised from the clonogenic assays and the γ-H2AX DNA DSB assay conducted so far that a defect in NHEJ was responsible and causing the 175BR and 84BR cell lines radiosensitive. To confirm this hypothesis the expression of the key genes (Ku70, Ku80, XLF, XRCC4, DNA-PKcs, Ligase IV and Artemis) found in NHEJ in patient cells were measured using the SYBR Green I based qRT-PCR assay.

In order to accurately detect the expression of the key genes found in NHEJ repair pathway the quality of the RNA and cDNA had to be carefully evaluated. Also the concentration of the primers designed for the detection of NHEJ repair genes had to be optimised.

Firstly, the quality of the RNA extracted with TRIzole reagent was measured by running the RNA samples from all four cell lines (NB1, 1BR.3, 175BR and 84BR) on a 1% agarose gel and an image of all RNA samples was captured on a UV transilluminator. From this image one can tell whether the RNA is degraded or intact or whether there is any DNA contamination.

Figure 4.2 - Total RNA for NB1, 1BR.3, 84BR and 175BR samples.

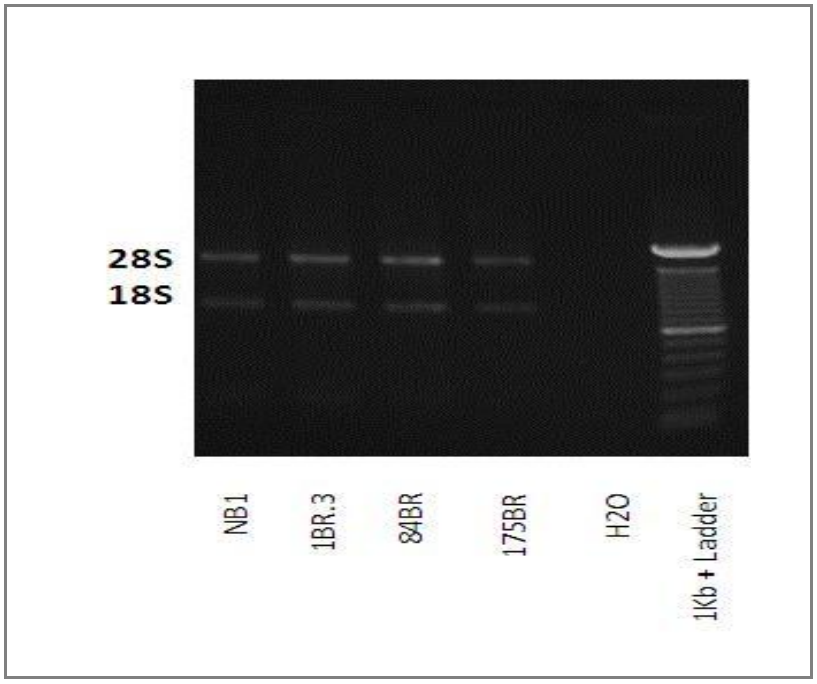

Here the image shows the two species of RNA (28S and 18S rRNA) which suggests that the extracted RNA is completely intact. The absence of the DNA contamination is an indication that a clean RNA preparation was made. Also the 1+Kb DNA ladder and the water control illustrated here provided a good measure for smooth running of the RNA on the agarose gel.

Secondly, the quality of the cDNA prepared for all four cell lines under study was determined. The quality of the cDNA preparations were measured with the use of GAPDH since this gene is widely expressed in all cell types it provides not only a good internal control for the running of the sample but also provides a good indication to whether a good quality cDNA was being made. The cDNA samples ran on 2% agarose gel and the image captured on the UV transilluminator is shown in Figure 4.3.

Figure 4.3 - cDNA samples for GAPDH in patient and control cells.

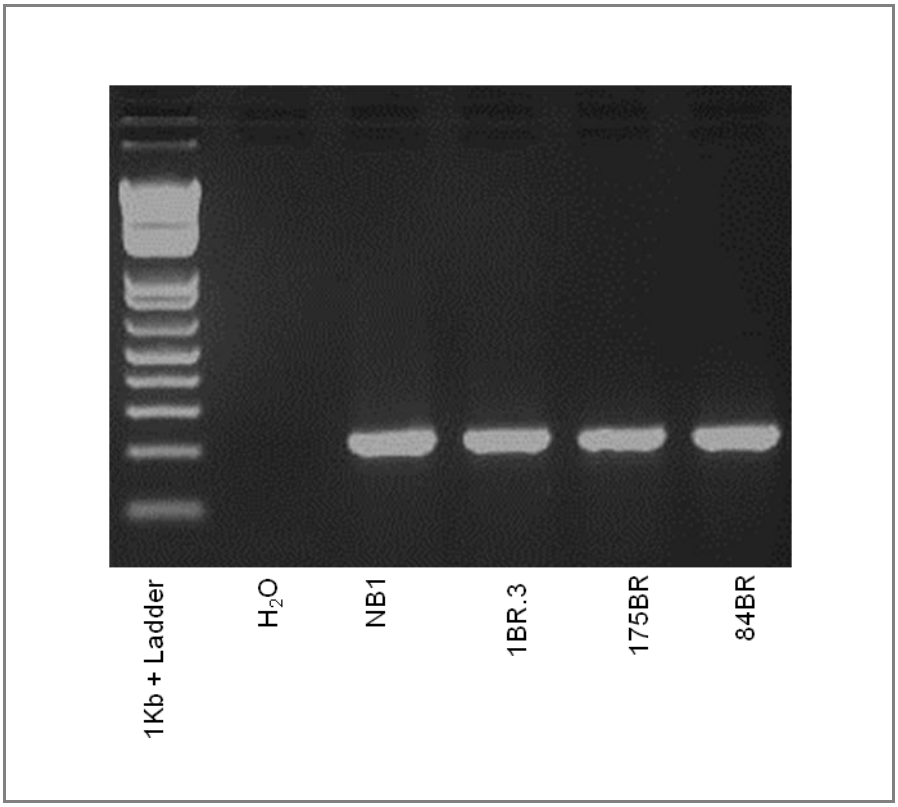

An image of all cDNA samples for GAPDH from four cell lines under study is shown here. The cDNA samples are approximately 100bp's long, which is an indication to a correct length of cDNA required for the detection of the expression of NHEJ repair genes. Also the quality of the cDNA is of good quality as there is no degradation and no contamination in any of the cDNA preps made for the four cell lines.

Thirdly, the primers designed for the NHEJ repair genes were optimised in order to achieve an optimum concentration of primer for the running of the qRT-PCR products. When a gradient PCR was conducted at 10µM primer concentration and a gel image was captured on the UV transilluminator the expression of all NHEJ repair genes was clearly observed.

Figure 4.4 - Primers at 10µM concentration.

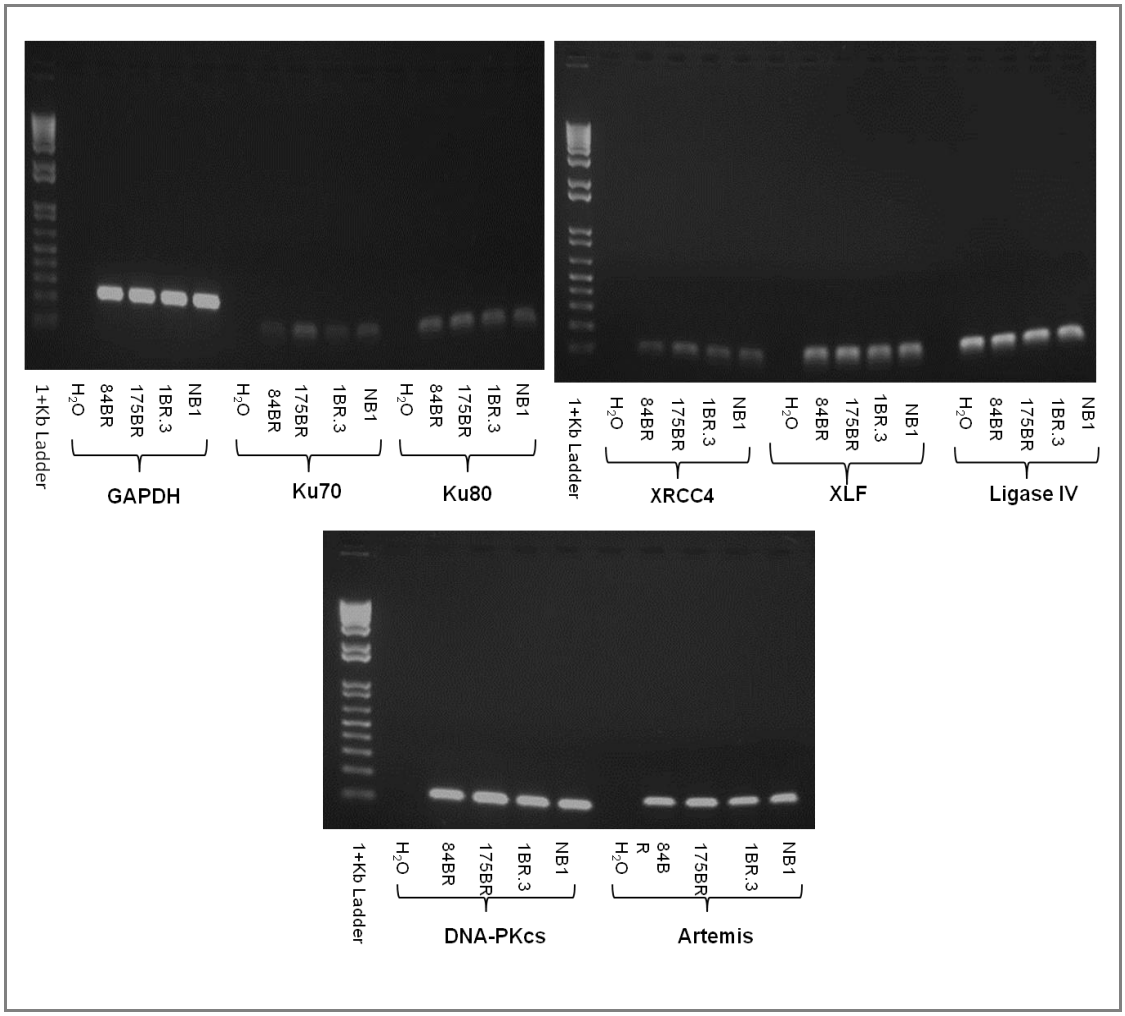

A normal expression of GAPDH, XLF Ligase IV, XRCC4, Ku70, Ku80, DNA-PKcs and Artemis for all four cell lines at10µM concentration is illustrated here.

The image in Figure 4.4 confirms not only that the GAPDH, XLF Ligase IV, XRCC4, Ku70, Ku80, DNA-PKcs and Artemis are being expressed in all four cell lines but also the concentration of primers at 10µM is optimum for the running of the samples as there are no dimer formed at this concentration. Thus the 10µM concentration is optimum for the running of all four samples for the expression of the key genes found in NHEJ repair pathway.

Although, no primer dimer was detected when the gradient PCR was conducted with all primers at 10µM concentration when a qRT-PCR was conducted with all primers again at 10µM concentration a primer dimer was observed with GAPDH.

Figure 4.5 - Melting curve showing the primer dimer with GAPDH at 10µM concentration.

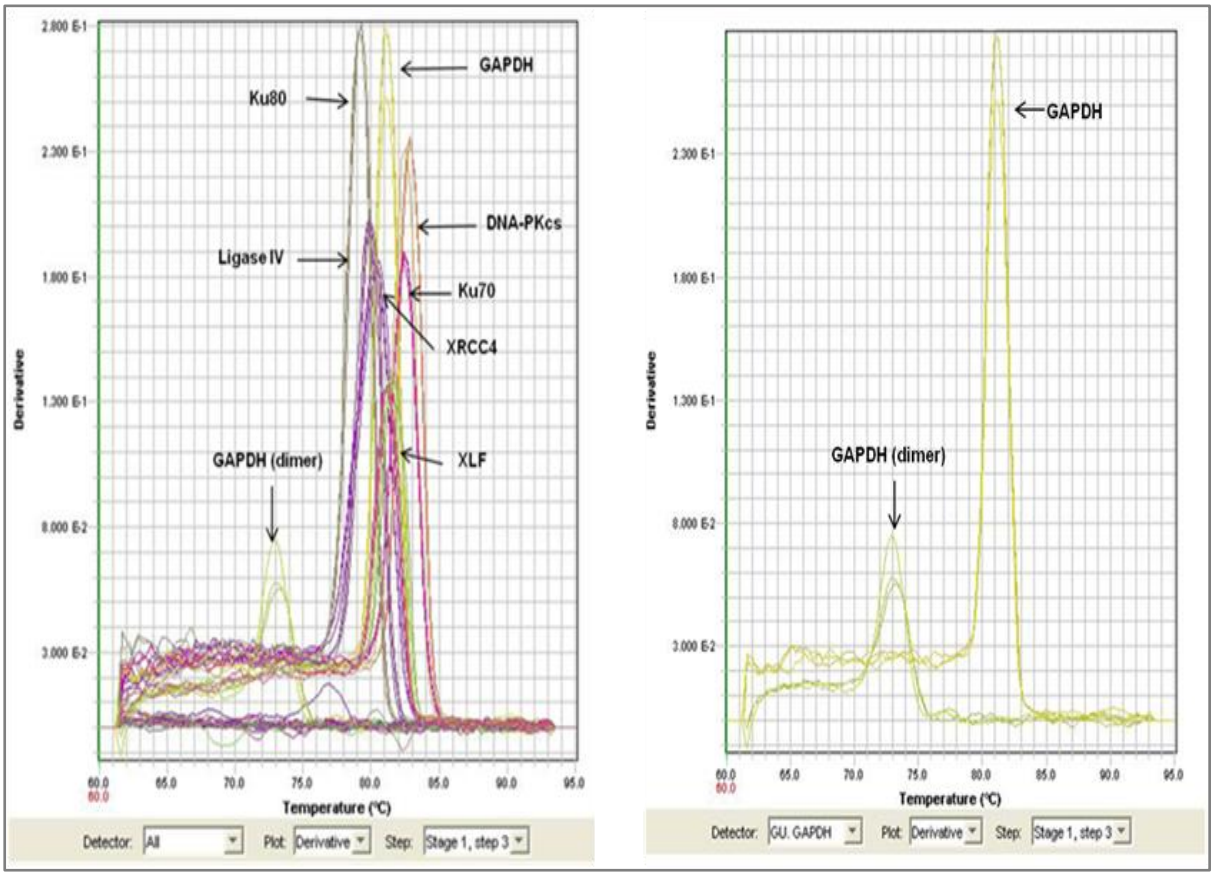

Images on the left and right panel show dimer formation in GAPDH non template control (NTC).

Also when a quantitative PCR reaction was separately prepared and run on a 1% agarose gel, as illustrated in Figure 4.6 the presence of primer formation with GAPDH at 10µM concentration was once again obvious. Thus, further supporting the presence of primer formed with GAPDH in the melting curve.

Figure 4.6 - Primers run at 10µM concentration on 1% agarose gel.

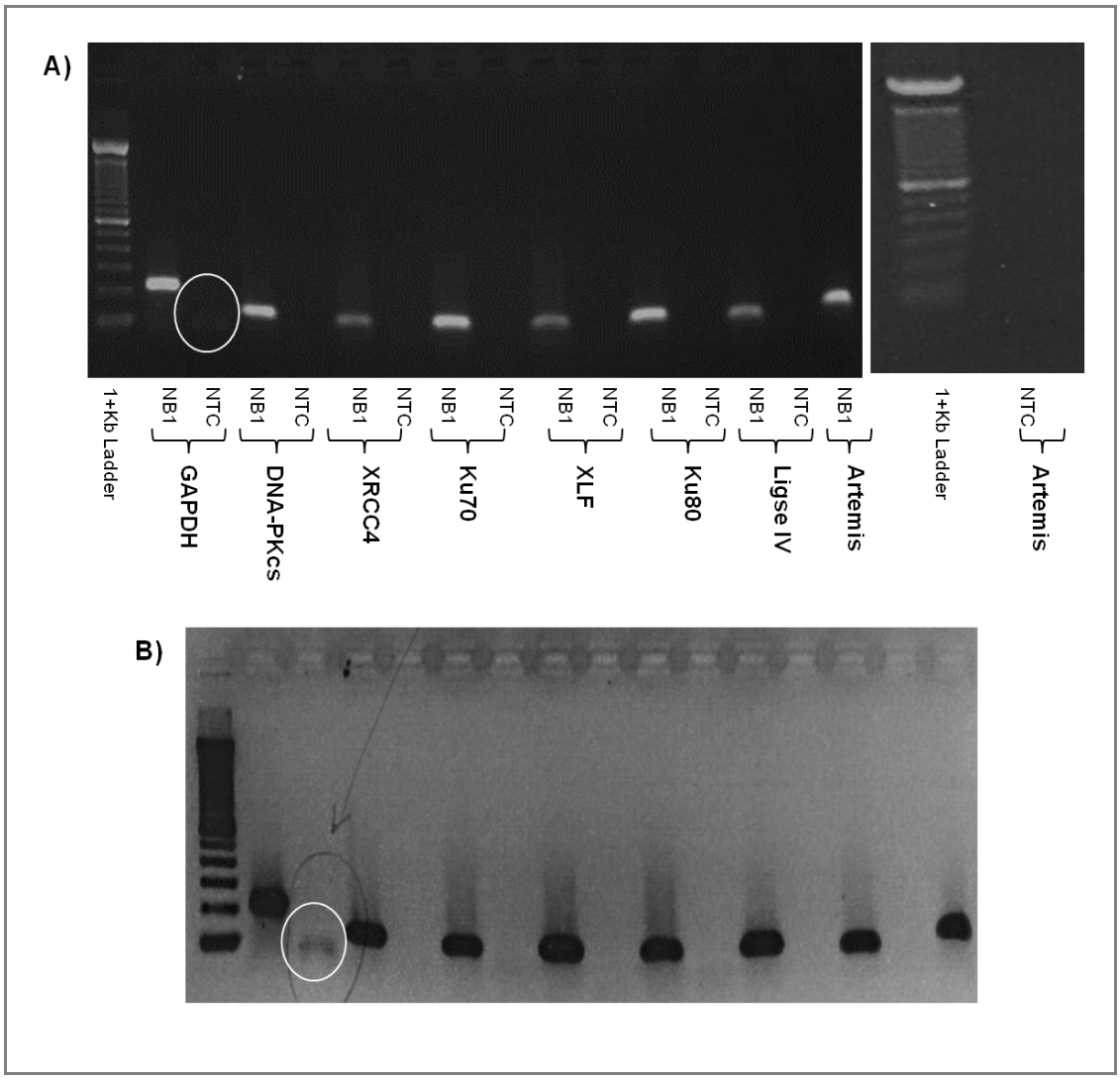

The primer dimer as circled is illustrated in both images A and B. Image A is a replicate of image B.

Therefore, to avoid the dimer formation the GAPDH was used at 5µM concentration whereas the rest of the primers were used at 10µM concentration. The amplification curve shows the effect of the primer concentration on the efficiency of amplification.

Figure 4.7 - GAPDH run at 5µM and remaining primers run at 10µM concentration.

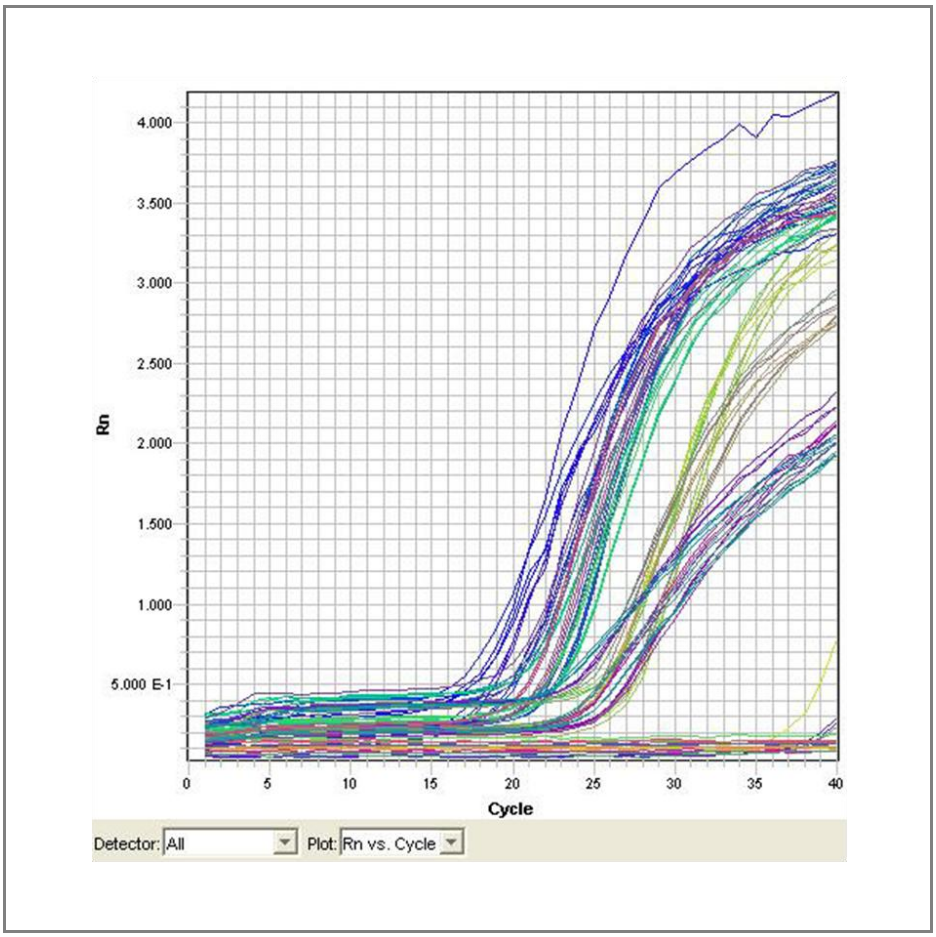

The amplification curve from real-time PCR shows the effect of the primer concentration.

Once the required parameters were optimised, the qRT-PCR assay was conducted with SYBR Green I dye to measure the expression of the NHEJ repair genes. The repair normal NB1 and 1BR.3 fibroblasts were used as internal calibrators for the expression of the NHEJ genes and the levels of gene expression in these cells were represented at 1.0. Also the expressions of the NHEJ genes in the radiosensitive cells (84BR and 175BR) were plotted relative to the repair normal fibroblasts.

Figure 4.8 - NHEJ Gene expression in 84BR radiosensitive fibroblasts.

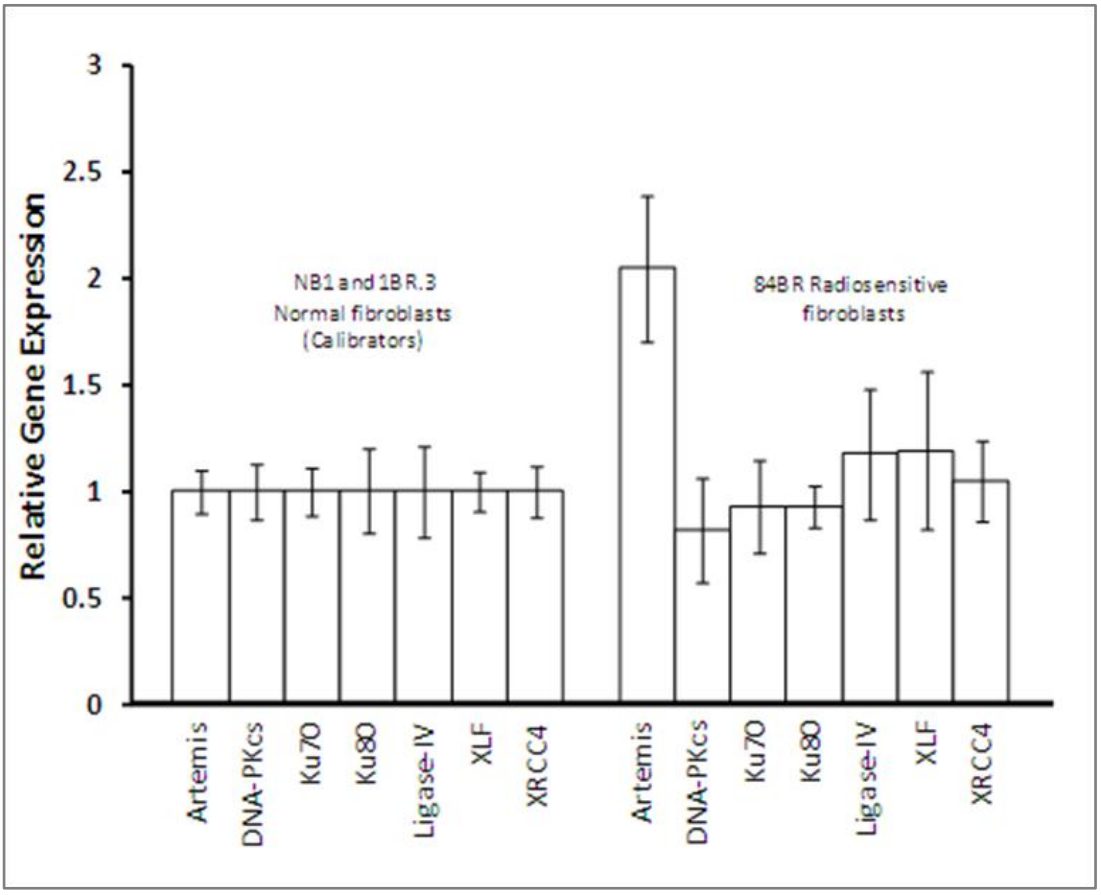

Here the expression of the NHEJ genes in the radiosensitive 84BR fibroblasts in comparison to the repair normal NB1 and 1BR.3. The data are derived from three independent experiments and error bars show standard error of the mean. Gene expression in 84BR cells is expressed in comparison to the normal fibroblasts cells (calibrators) in which levels of expression are regarded as a level 1. The P value is 0.003.

As it is clear in Figure 4.8 there is an approximately 2 fold over-expression of the *Artemis* gene in 84BR fibroblast cells when compared to the repair normal NB1 and 1BR.3 fibroblasts. Comparison of the expression levels of *Artemis* in 84BR cells with the repair normal fibroblast using a Student's unpaired T test also reveals a statistically significant difference in expression levels.

Similarly for the radiosensitive 175BR fibroblasts, it can be seen that there is an approximate 1.7 fold over-expression of the artemis protein when compared to the control cells. Also a Student's unpaired T test reveals a statistically significant difference in expression levels between the 175BR radiosensitive cells and the repair normal control cells.

Figure 4.9 - NHEJ Gene expression in 175BR radiosensitive fibroblasts.

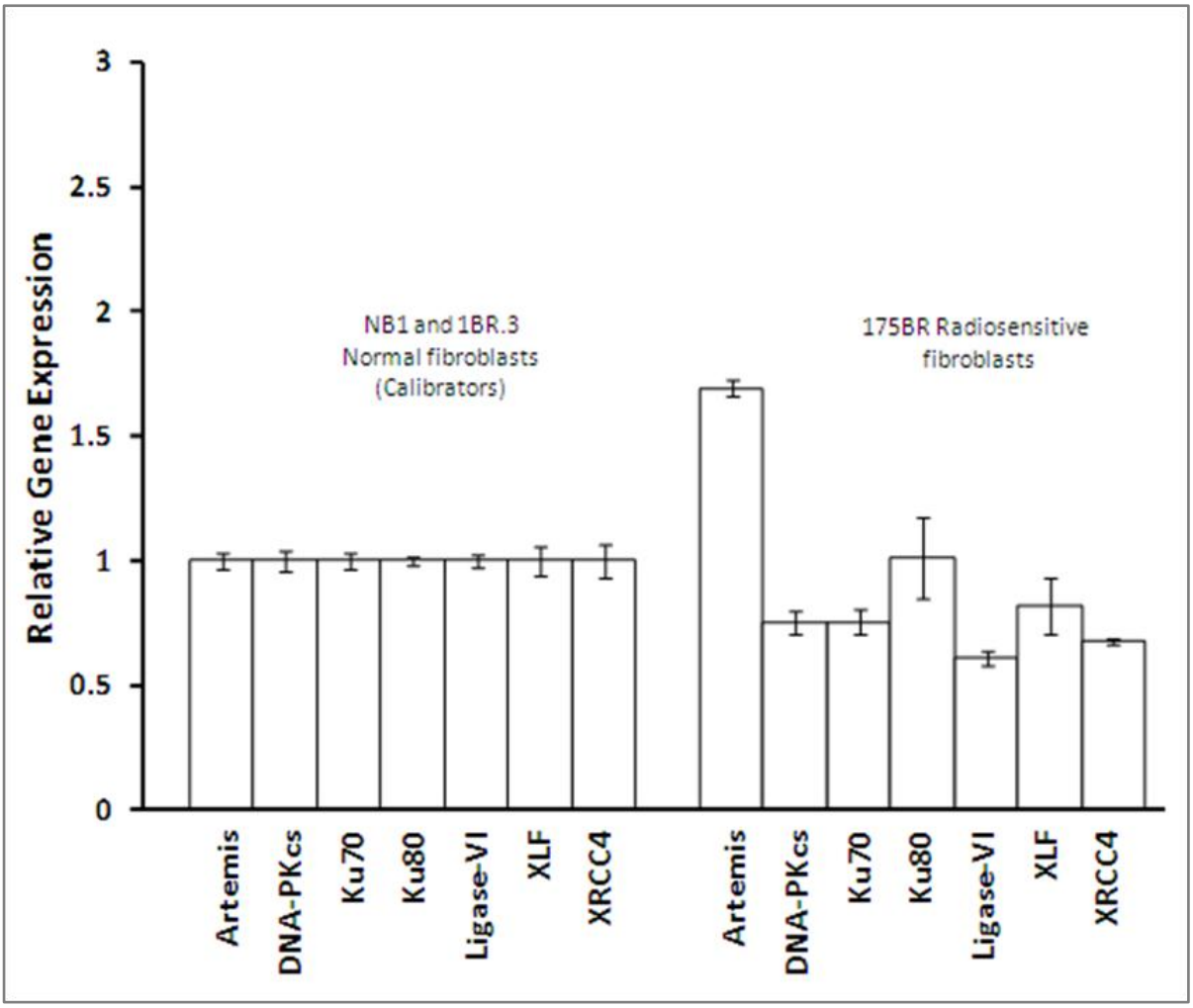

This figure shows the data for the 175BR radiosensitive cell line and is presented in an identical manner to that of Figure 4.8. Also the P value for 175BR cell line is 0.007.

While the expression of the *Artemis* is considerably higher in both cell lines a marginal decrease in DNA-PKcs, Ku70, Ku80 and XRCC4 and a marginal increase in Ligase-IV and XLF were observed in 84BR or decrease in DNA-PKcs, Ku70, Ku80, Ligase-IV XLF and XRCC4 were observed in 175BR cells. Although, the dramatic increase in the *Artemis* expression is more striking than the marginal fluctuation observed in the expression of the remaining NHEJ repair genes is also worth mentioning as any change in gene expression could be the consequence of some form of defect or abnormality of that gene or of its regulation of gene expression.

4.4 - Discussion

In previous Chapters we have hypothesised from the clonogenic and the H2AX assays that the cellular radiosensitivity seen in clinically radiosensitive patient 84BR and the patient 175BR may be due to a defect in the NHEJ repair pathway as HR pathway was found to be functioning normally.

Then, in this chapter we tried to unveil the defect in NHEJ repair pathway which may be responsible for the radiosensitivity observed at clinical and cellular level in radiosensitive patients. Hence, to determine this defect, if any in the NHEJ repair genes, a qRT-PCR assay was conducted, which enabled us to study the level of gene expression of some of the key genes found in NHEJ repair pathway.

The key genes under investigation were the Ku70, Ku80, DNAPKcs, XRCC4, XLF, Ligase IV and *Artemis*. Since the previous studies have clearly shown that any defects in any component of NHEJ pathway can lead to hypersensitivity to IR, genome instability, immunodeficiency and cancer (Bassing and Alt 2004) the next prudent decision in our research was to detect the level of NHEJ repair genes as to disclose the reason for the radiosensitivity seen in 84BR and 175BR cells.

Based on the study by Mohrin *et al.,* (2010), and Chiou *et al.,* (2007) also the fact that the real time PCR is the golden standard for gene expression was the preferred choice for the analysis of the key NHEJ genes in two radiosensitive patient cell lines.
As discussed in previous chapters certain diseases are known to be associated with defective genes in NHEJ repair pathway. Defects leading to a reduction in functional

Artemis endonuclease activity are particularly noteworthy. At the cellular level this manifests extreme radiosensitivity. In human subjects, Artemis deficiency results in RS-SCID. RS-SCID is characterised clinically by extreme radiosensitivity and by a complete absence of T and B cells due to a failure of the receptor recombination stage of V(D)J recombination (Dvorak and Cowan 2010). Attempts to correct the deficiency in cells by transduction with lentiviral gene expression vectors containing the *Artemi*s cDNA has led to over-expression of Artemis in a number of mammalian cell types (Multhaup *et al.,* 2010). While such findings have significant implications for the role of gene therapy approaches for the treatment of SCID, it also reveals a potentially novel mechanism which may explain radiosensitivity in human cell types.

Chapter 5 - Artemis over-expression and Apoptosis in Radiosensitive cells

5.1 - Introduction

As described in Chapter 1 the key proteins involved in NHEJ repair pathway are; Ku70, Ku80, DNA-PKcs, Artemis, XLF, XRCC4 and Ligase IV. The Ku70 is associated with Ku80 to form a Ku heterodimer that binds to DNA ends with high affinity (Smider *et al.,* 1994). Upon binding to DNA ends, the Ku heterodimer recruits DNA-PKcs to the sites of DSB (West *et al.,* 1998). The DNA-PKcs protein becomes autophosphorylated and functions as a scaffold to bridge the broken DNA ends in a synaptic complex (DeFazio *et al.,* 2002). The DNA-PKcs also provides binding sites for other NHEJ proteins such as nuclease Artemis (Ma *et al.,* 2002), which is required for trimming of the DNA ends or XRCC4/DNAligase IV complex involved in re-joining step of NHEJ (O'Driscoll *et al.,* 2001).

The *Artemis* gene is also required for V(D)J recombination during T-cell and B-cell development. In order to get each V (D) J segments to join together the DNA must form a DSB. Also since the two ends of the broken DNA molecule generated by DSB are rarely compatible Artemis complexes with DNA-PKcs to create a hairpin opening which is one of the crucial stages of V(D)J recombination (Ma *et al.,* 2002).

Artemis deficiency in human subjects results in SCID which is characterised clinically by extreme radiosensitivity and by a complete absence of T and B cells due to a failure of the receptor recombination stage of V(D)J recombination (Dvorak and Cowan 2010). Attempts to correct the deficiency in cells by transduction with lentiviral gene expression vectors containing the *Artemis* cDNA has led to over-expression of

Artemis in a number of mammalian cell types (Multhaup *et al.,* 2010). However, over-expression has also resulted in a loss of cell viability, associated with increased DNA damage and elevated apoptosis as a result of abnormal activity of the Artemis endonuclease inducing DNA breaks (Multhaup *et al.,* 2010).

While such findings have significant implications for the role of gene therapy approaches for the treatment of SCID, it also reveals a potentially novel mechanism which may explain radiosensitivity in human cell types. To support this assertion, we have characterised two radiosensitive human fibroblast cell lines (175BR and 84BR) derived from different cancer patients in which we observed a two-fold increase in the expression of *Artemis* as determined by qRT-PCR analysis. This over-expression in *Artemis* was also associated with:

- Enhanced cellular radiosensitivity (observed with clonogenic assays conducted with radiation).
- A possible defect in NHEJ repair pathway (observed with clonogenic asays conducted with HN2).
- A reduction in the repair of DNA DSBs (observed with H2AX DSB repair assay).

Although, radiosensitivity is associated with deficiency in Artemis the study by Moshous *et al.,* (2001) and by Multhaup *et al.,* (2010) opted us to review the relationship between Artemis over-expression, DNA damage repair defect, radiosensitivity and apoptosis in radiosensitive human fibroblasts (84BR and 175BR).

5.2 - Materials and Method

5.2.1- Transfection of NB1-Tert cells with *Artemis* cDNA

The *Artemis* cDNA expression construct was purchased from Origene Inc (Rockville, MD, USA) which was provided in the expression plasmid pCMV6-XL5 (under control of the cytomegalovirus promoter). This plasmid was supplied without a selectable marker to identify transfected cells. Therefore the NB1-Tert cells were co-transfected with pCMV6-XL5 and pPur plasmid (Clontech, Hant, UK).

Figure 5.1 - Map of pCMV6-XL5.

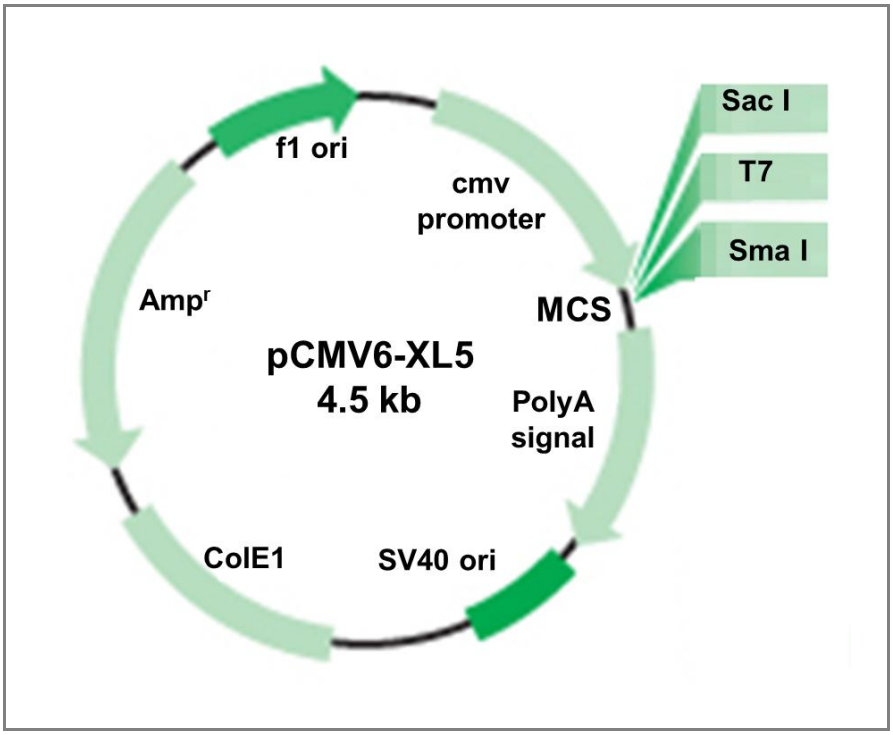

The pCMV-XL5 (4.5 kb) contains: a polylinker also known as the multiple cloning site (MCS), for cloning of the gene of interest; Cytomegalovirus (CMV), a promoter for the expression of cloned cDNA; an ampicillin-resistance gene (amp^r), for selective amplification; the SV40 ori for replication in mammalian cells; f1 ori, the filamentous phage origin of replication, for recovery of single-stranded plasmids.

To overcome the absence of a selectable marker to identify *Artemis* transfected cells, the pCMV6-XL5 plasmid was co-transfected with the pPur plasmid shown below. The puromycin resistance gene was used as a selectable marker to identify the transfected cells.

Figure 5.2- Map of Plasmid pPur.

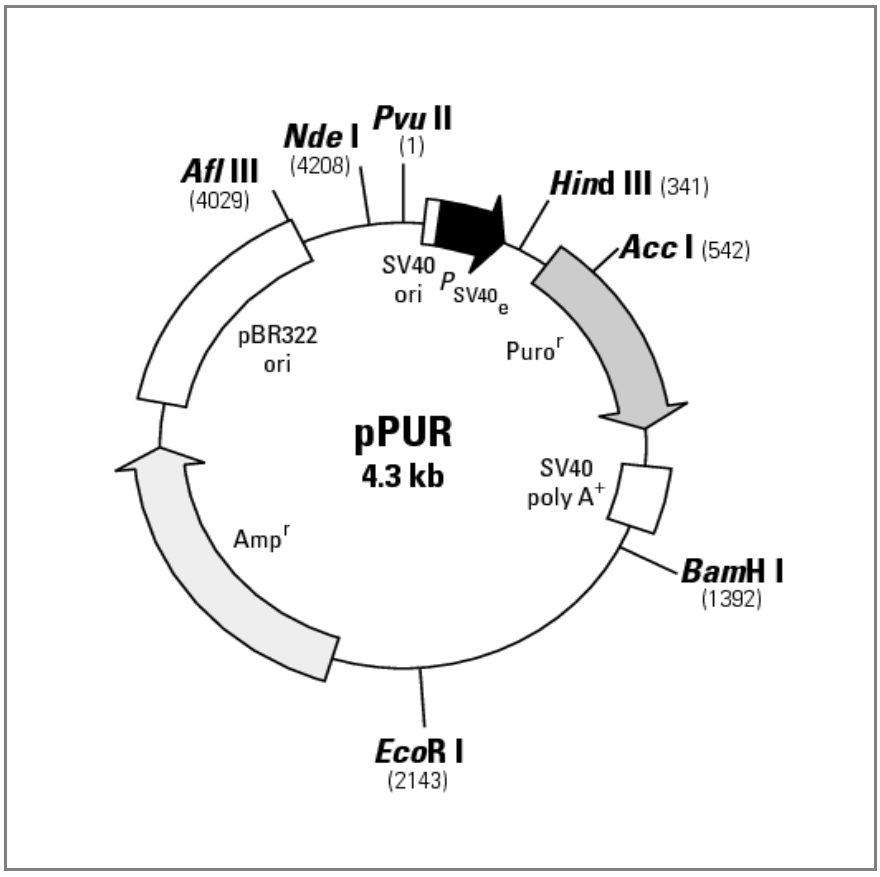

The 4.3 kb pPUR is a selection vector which contains; Puro^r gene that confers resistance to puromycin, pBR322 origin of replication for propagation in *E.coli* and Amp^r gene for selection of transformed E.coli cells in cultures containing ampicillin.

5.2.2- Maxi Preparation of Plasmid DNA

5.2.2.1 - Transformation of E.coli

The pCMV6.XL5 plasmid containing the *Artemis* cDNA was transferred into chemically competent DH5α cells (Invitrogen, Paisley, Scotland) for amplification. Three µl (10ng) of plasmid was mixed in 100µl thawed DH5α competent bacteria cells, gently swirled and incubated on ice for 15 minutes. The bacterial cells were heat shocked at 42ºC for 2 minutes. One ml SOC medium was added to the mixture, mixed gently and transferred to a fresh Eppendorf tube. The SOC media was made by adding 20g of Bacto-tryptone, 5g of Bacto yeast extract, 2ml of 5M NaCI, 2.5ml of 1M KCI, 10ml of 1M $MgCI_2$, 10ml of 1M $MgSO_4$, 20ml of 1M glucose added to 900ml of dH_2O (all reagents purchased from Fisher Scientific). Once mixed, the volume was adjusted to 1L with dH_2O and immediately autoclaved. Transformed *E.coli* were transferred to a sterile 15ml tube and incubated for 1 hour in 200rpm in the orbital incubator shaker (Gallenkamp, Holly, Misigan, USA) at 37ºC. After 1 hour incubation 100µl and 200µl aliquots of the transformed sample were spread with a sterile spreader onto two separate pre made Luria-Bertani (LB) agar plates containing 100µg/ml ampicillin. The plates were left to dry in sterile air under the flame of Bunsen burner. The plates were inverted in the incubator (Gallenkamp, Holly, Misigan, USA) at 37ºC for overnight incubation. The next day the bacteria growth was visible on the surface of the LB agar plates, the plates were either kept at 20ºC or a colony of bacteria was picked with a sterile loop and streaked in a fresh LB agar plate containing ampicillin and incubated further at 37ºC for overnight. This step was repeated three times for three days to get single small colonies.

5.2.2.2 - Growing Large Volume of Transformed Bacteria

Once single small colonies were achieved, the colonies were picked with a sterile loop in the centre to avoid picking satellites and inoculated in a 10ml LB culture medium containing 100µg/ml ampicillin. The transformed bacterial cells were incubated for 6-8 hours at 37ºC with vigorous shaking at 200rpm. The next day the bacteria culture became very turbid; this culture was re-inoculated in 1L of LB media and further incubated at 37ºC with vigorous shaking at 200rpm for overnight. One ml aliquots of cell culture in 80% glycerol were frozen at -80ºC.

5.2.2.3 - Purification of Plasmid DNA

Before commencing the maxi prep the RNAse was added to the P1 buffer then the P1 and the P3 buffers were stored at 4ºC until used. The following steps were then conducted using the QIAGEN plasmid maxi kit to extract the plasmid DNA from the bacteria culture.

i. Bacteria culture, harvest and lysis

The 1L of saturated bacterial culture grown in LB media was pelleted by centrifugation (Sigma 6k10, Meadowrose, UK) at 6000xg for 15 minutes at 4ºC. The bacterial pellet was homogenously re-suspended in 10ml re-suspension Buffer P1 (100µg/ml RNase A, 50mM Tris-HCI and 10mM EDTA, pH 8) buffer. To the cells, 10ml of lysis Buffer P2 (0.2 M NaOH in 1% SDS) was added then mixed vigorously by inverting for 4-6 times and incubated at RT for 5 minutes. To the viscous lysate 10ml ice-cold Neutralisation Buffer P3 (2.55M potassium acetate, pH 4.8) was added to neutralise the lysing effect of Buffer P2, and, after thoroughly mixing the lysate was incubated on ice for 20 minutes.

ii. Bacterial lysate clearing

The lysate was centrifuged at 16000 x g for 30 minutes at 4ºC then transferred to a fresh tube and re-centrifuged for 15 minutes to clear off any remaining pellet. The clear supernatant containing plasmid DNA was transferred to a fresh tube.

iii. Bind, wash and elute plasmid DNA on QIAGEN-tip

The QIAGEN tip was equilibrated by applying 10ml QBT Buffer (750mM NaCI, 50 mM Mops, 15% ethanol and 0.15% Triton X-100, pH 7) and allowing the column to empty by gravity flow. The supernatant containing plasmid DNA was applied to the active QIAGEN tip and allowed to enter the resin by gravity flow. The QIAGEN tip was washed twice with 30ml of QC buffer (1M NaCI, 50mM Mops, 15% ethanol, pH 7) by allowing the buffer run through the QIAGEN tip by gravity flow. The DNA was eluted with 15ml elution QF buffer (1.25M NaCI, 50mM Mops, 15% ethanol, pH 8.2) into a clean 50ml vessel.

iv. Precipitate, wash and re-dissolve plasmid DNA

The DNA was precipitated by adding 10.5ml RT isopropanol (0.7 volume of elution buffer) to the eluted DNA. The DNA was centrifuged at 16000 x g for 30 minutes at 4ºC, and the supernatant was discarded. The DNA pellet was washed twice in 3ml RT 70% ethanol to remove the remaining salts from the preparation. The floating pellet was briefly spun at 13000 x g for 5 minutes, the methanol was discarded and the pellet was air dried for 5-10 minutes. The pellet was then re-dissolved in 750µl Tris-EDTA (TE) buffer (10mM Tris-CI (Sigma Aldrich, Germany) 1Mm EDTA (Fisher Scientific, New Jersey, USA) at pH 8.0. The DNA suspension was left at RT for few hours to allow the DNA to solubilise in TE buffer before storing at -20ºC.

5.2.3- Analysis of Purified Plasmid DNA

The plasmid DNA was diluted in 1:100 (1µl DNA plus 99µl H_2O) dilution and 1:10 (10µl DNA plus 90µl H_2O) dilution with DEPC treated water in two separate cuvettes. The UV spectrophotometer (Eppendorf, BioPhotometer) was turned on 15 minutes prior to use. The spectrophotometer was blanked with DEPC treated water. The concentration of the plasmid DNA was determined by measuring the absorbance at 260nm (A_{260}) on the spectrophotometer. An absorbance of 1 unit at 260nm corresponds to 50µg of DNA per ml. Therefore, the concentration of the purified plasmid DNA was calculated by using the following equation:

DNA concentration (µg/ml) = (A_{260}) x (dilution factor) x (50 µg/ml DNA)

Total yield = DNA concentration x volume of sample in ml

Then the purity of DNA was calculated by measuring the ratio between the absorbance values at 260 and 280 nm (260/280).

5.2.4- Agarose Gel Analysis of Purified Plasmid DNA

The purified plasmid DNA was run on a 1% agarose gel to assess the quality of the DNA and to confirm that the DNA sample is free from RNA contamination. The samples were run at 40V for 50 minutes, and visualised under UV transilluminator. An image of the DNA run was captured with the image acquisition end analysis system.

5.2.5- Co-transfection of NB1-Tert cells with pCMV6-XL5 *Artemis* cDNA

Co-transfection of NB1-Tert cells with pCMV6-XL5 plasmid containing *Artemis* cDNA was performed with Genejuice lipid transfection reagent (Novagen, Ltd). Twenty micrograms of each plasmid in 100μl of serum free medium containing 3μl of Genejuice reagent was added to the $1X10^6$ cells in 10ml of complete DMEM. The mixture was left on cells for 5 hours then the media was changed and the cells were incubated at 37ºC for 24 hours. The successfully transfected cells were selected in 20μg/ml puromycin. The selection and medium refreshment were repeated once a week, for 4 weeks until distinct colonies were ready to be picked. A puromycin-resistant clone was also isolated in which the cells were transfected with pPur only without pCMV6-XL5 plasmid.

5.2.6- Isolation and Freezing of NB1-Tert Transfectants

Puromycin resistant clones were collected by ring cloning and expanded into culture. The culture were transferred to 50mm Petri dishes containing 5ml complete medium supplemented with 20μg/ml puromycin and incubated at 37ºC in a humidified atmosphere of 10% CO_2 in air. When cells reached to approximately 80% confluence aliquots of clones were frozen in liquid nitrogen for future use. When the puromycin resistant clones were subjected to further analysis an aliquot was gently thawed at 37ºC prior to use.

5.2.7- Clonogenic assay – Surviving fraction at 2 Gy gamma irradiation

The NB1-Tert cells and those transfected with the *Artemis* cDNA and pPur only were subjected to clonogenic assays to determine the γ-radiation sensitivity in each of the various clones selected. The procedure for clonogenic assay (see Chapter 3) was also employed here. The response of all five clones to γ-radiation was compared to that of non-transfected parental NB1-Tert cells.

5.2.8- Quantitation of Artemis Protein Expression in Cells

The Artemis protein expression in the fibroblast cell lines (NB1, 1BR.3, 84BR and 175BR) and the NB1-Tert cell line transfected with *Artemis* was determined using the immunocytochemistry and imaging flow cytometry assay. Cells growing as monolayers were trypsinised and washed twice in 10ml of ice cold PBS. Following fixation in 3.7% paraformaldehyde in PBS at 4ºC for 15 minutes, cells were washed in PBS and fixed in 50:50 vol:vol methanol acetone for 10 minutes at 4ºC. Cells were rehydrated and permeabilised in tris buffered saline (TBS) containing 0.1% Tween 20 after which the cells were stained with a rabbit polyclonal anti-artemis antibody at a dilution of 1/100 in permeabilisation buffer containing 5% goat serum (Abcam, Cambridge, UK). Following two washes in permeabilisation buffer, a goat anti-rabbit Alexa Fluor^{488} conjugated secondary antibody (Invitrogen) was added at a dilution of 1/1000 for 1 hr at RT. Cells were washed three times in permeabilisation buffer and re-suspended in 100μl Accumax flow cytometry buffer (PAA Ltd.) containing 5μM Draq 5 (to visualise the nuclear region). Images of 10,000 cells were captured using the Imagestream and the level of Artemis expression in cells was determined by calculating the average Alexa Fluor^{488}-associated fluorescence in the nuclei of the cells.

5.2.9- Apoptosis Assay

The level of apoptosis in untreated and cells irradiated with 2Gy gamma radiation was determined by immunocytochemistry and imaging flow cytometry using a FITC Annexin-V Apoptosis detection kit (BD Pharmingen Ltd., Oxford, UK) according to the manufacturer's instructions. In brief either untreated or cells irradiated with 2Gy gamma radiation were recovered into a suspension by trypsinisation and washed twice in PBS. Cells were resuspended into 500μl of binding buffer to which was added 5μl annexin V-FITC and 5μl of propidium iodide. Cells were incubated for 10 minutes at RT in the dark and levels of apoptosis were determined by counting 5,000 cells using the Imagestream imaging flow cytometer with a 488nm laser at a power setting of 40m Watts (Amnis Corporation, Seattle, Washington, USA). Images of all cells were visualised using the Ideas™ analysis software programme of the Imagestream (Bourton *et al.,* 2012). Here cells are first gated for single cells, cells in focus, followed by identification of apoptotic cells. Apoptotic cells were gated and enumerated by identifying those cells that exhibited FITC and propidium iodide staining. Staining patterns in all cells was visually confirmed by assessing the appearance of the cells using the Image Gallery of the Ideas™ software package.

5.2.10- Sample loading and data analysis

Levels of apoptosis were determined by counting 5,000 cells using the Imagestream™ imaging flow cytometer with a 488nm laser at a power setting of 40m Watts (Amnis Corporation, Seattle, Washington, USA). Images of all cells were visualised using the Ideas™ analysis software programme of the Imagestream *e.g.* (Bourton *et al.,* 2012). Here cells are first gated for single cells; cells in focus followed by cells that exhibit the following patterns of fluorescence. Early apoptotic cells were

gated and enumerated by identifying those cells that exhibited FITC fluorescence located at the membrane region of the cells. A membrane mask was created using the Mask Manager function of the Ideas™ software. Late apoptotic cells were enumerated by gating those cells that exhibited both intracellular FITC and propidium iodide staining. Staining patterns in all cells was visually confirmed by assessing the appearance of the cells using the Image gallery of the Ideas™ software package.

5.3 - Results

5.3.1 - Detection of plasmid Quality with Agarose gel

The pPur and pCMV6-XL5 plasmids containing full length *Artemis* cDNA were amplified in *E.coli* and purified with Qiagen MaxiPrep kit. Once the plasmids were purified approximately 200 to 400ng of plasmids were run on a 1% agarose gel to detect the quality of the plasmids. The image Figure 5.3 illustrates the agarose gel analysis of pCMV6-XLF *Artemis* cDNA and pPUR plasmids. The pCMV6-XL5 plasmid did not contain any selectable marker required for identification of transfected cells and isolation of the resulting colonies. To overcome this problem, the full length *Artemis* cDNA was co-transfected into recipient NB1-Tert cells with the pPur plasmid conferring resistance to puromycin.

Figure 5.3 - Agarose gel analysis of the purified plasmids.

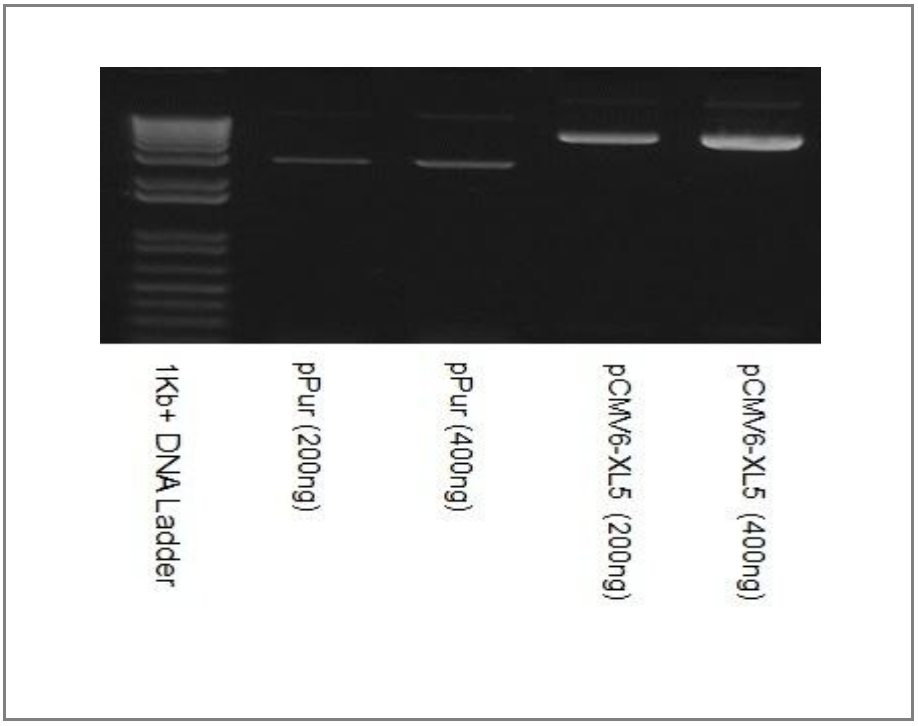

The pPUR plasmid cDNA is 4.3 Kb and the pCMV6-XL5 plasmid containing full length *Artemis* cDNA is 4.5 Kb. The plasmids were purified using the Qiagen maxi columns and run on 1% agarose gel.

5.3.2 - Artemis Expression in Cells

With the aid of pCMV6-XL5 and pPur plasmids the *Artemis* full length cDNA was transferred into NB1-Tert cells. In total six puromycin resistant clones were isolated. The level of Artemis expression in cells was measured by the method of imaging flow cytometry in conjunction with immunocytochemistry. Cells growing as monolayers were trypsinised and stained with antibodies to detect Artemis. Images of 10,000 cells were captured with imaging flow cytometry and using a series of pre-determined analysis routines in the Ideas™ software (Amnis Inc.) (*e.g.,* Bourton *et al*., 2011) the average level of nuclear fluorescence attributable to Artemis expression was calculated. The data are summarised in Table 5.1.

Table 5.1 - Artemis expression in all cell lines determined by imaging flow cytometry.

Cell line	Artemis Expression	Cell line	Artemis Expression
NB1	1.00	NB1-Tert	1.00
1BR.3	1.00	Vector only	0.64
84BR	2.06	Clone 1	1.81
175BR	2.09	Clone 2	2.08
		Clone 3	1.65
		Clone 4	2.02
		Clone 5	2.25
		Clone 6	1.05

Artemis expression was determined by calculating the average Artemis associated fluorescence in the nuclei of 10,000 cell images. Artemis expression (fluorescence) in NB1-Tert parental cells or normal fibroblast cells is assigned a value of 1.0 (relative fluorescence). Fluorescence in all other cell lines was expressed in relation to the relative fluorescence in normal cells or parental cells.

In the NB1 and 1BR.3 normal fibroblast cells the average nuclear fluorescence attributable to Artemis expression was averaged and given a value of 1.0. Expression of Artemis in the 84BR and 175BR was expressed in relation to levels in the normal fibroblast cells. We demonstrate that the 84BR and 175BR cells display a 2.06 and 2.09-fold increase in nuclear Artemis expression. These data support our observations of elevated Artemis expression derived from the qRT-PCR experiments.

Artemis expression in the NB1-Tert parental cells was derived as explained above. Artemis expression in the vector-only transfected cells and in clone 6 reveals a largely unchanged level of Artemis expression. However in clones 1-5 there is an increased level of Artemis expression in the nuclei of these cells. This ranged from a 1.65-fold increased level of expression in clone 3 to a 2.25-fold elevated expression in clone 5. A representative image of Artemis staining of cells, derived from imaging flow cytometry is shown in Figure 5.4.

Figure 5.4 - Representative images of NB1-Tert cells stained for Artemis.

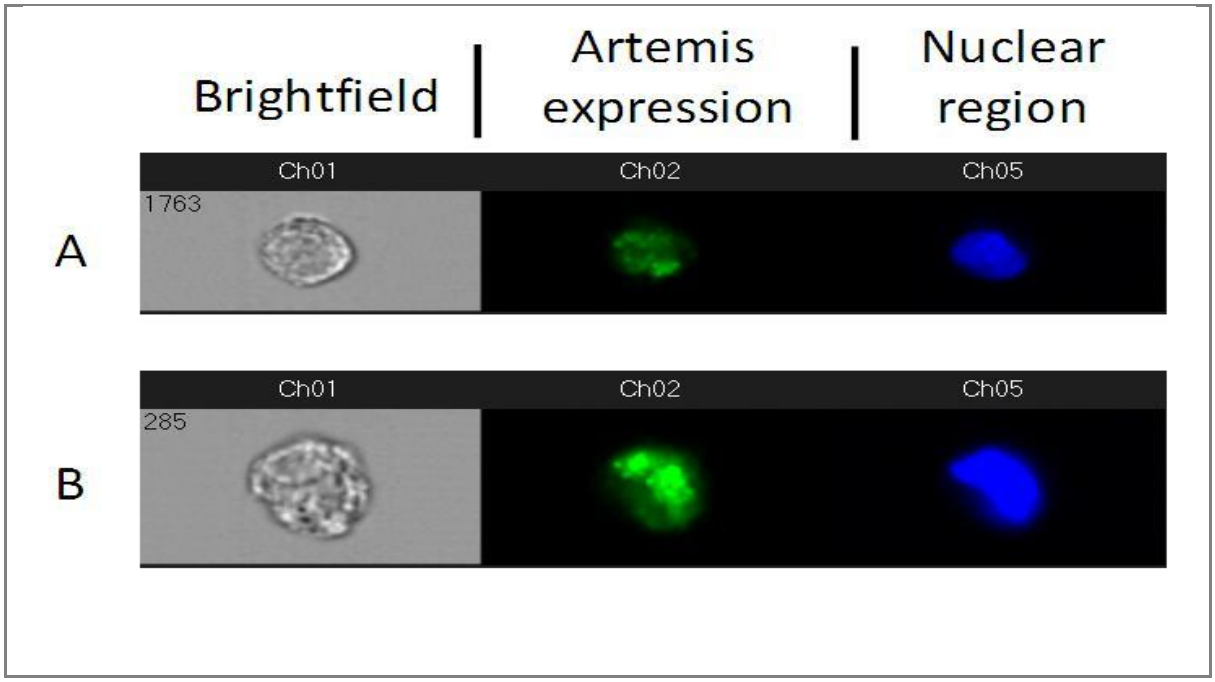

A brightfield image is shown in the left column. The centre column shows Alexa Fluor^{488} staining for Artemis and the right column shows the Draq 5 staining of the nuclear region of the cell. Row A shows NB1-Tert parental cells. Row B shows elevated Artemis expression in NB1-Tert clone 2 which has been transfected to over-express the Artemis protein.

5.3.3 - Radiation Sensitivity of Artemis-Transfected NB1-Tert Cells

Clonogenic cell survival in the *Artemis*-transfected NB1-Tert cells following exposure to 0, 2, 4, 6 and 8 Gy gamma radiation is shown in Figure 5.5. In the parental NB1-Tert cells and those transfected with the pPur plasmid together with a single clone (clone 6) of *Artemis* transfected cells, there is a similar and normal level of survival. However, in NB1-Tert clones 1 to 5 (that are over-expressing *Artemis*), there is marked reduction in the clonogenic cell survival following exposure to increasing

doses of gamma radiation. In the single clone 6 in which the radiation response was unaltered, it is likely that here the cells were transfected with the pPur plasmid only and failed to acquire the *Artemis* gene during the co-transfection process.

Figure 5.5 - The γ-radiation sensitivity of *Artemis* transfectants.

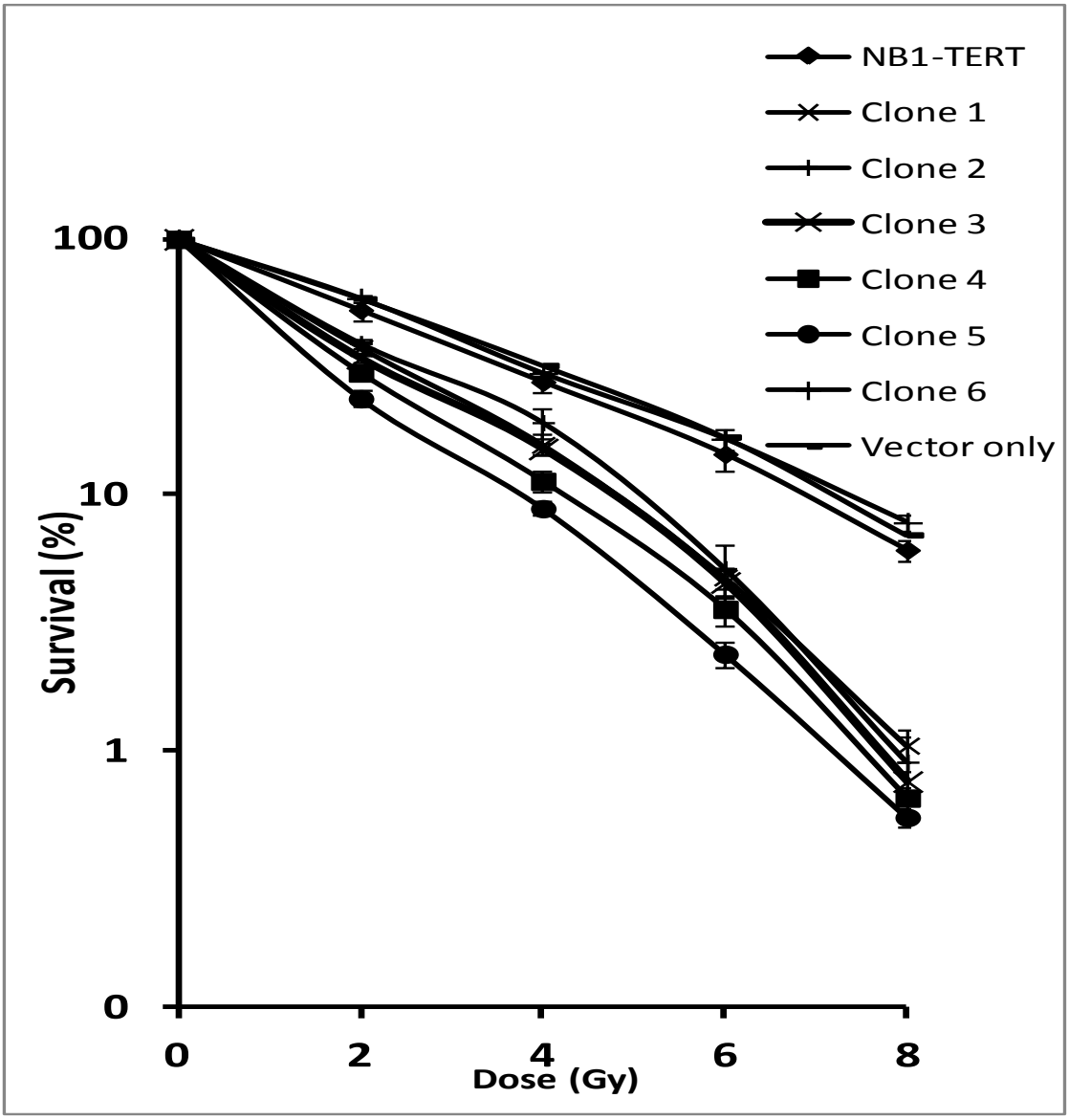

The survival of the NB1-Tert cells transfected with *Artemis* following exposure to 0, 2, 4, 6 and 8 Gy gamma radiation. The NB1-Tert cells were transformed with *Artemis* cDNA and the transfected clones as well as non-transfected clones were diluted and irradiated with different doses of γ-radiation, as explained in Chapter 1. Surviving colonies were then fixed, stained and colonies counting 50 or more were counted. Survival of each clones were normalised to plating efficiency of unirradiated control cells. Data are derived from three independent experiments and error bars shown represent standard error of the mean. The P value is <0.05.

5.3.4 - Elevated Apoptosis in *Artemis*-Transfected NB1-Tert Cells

Apoptosis in NB1-Tert cells transfected to over-express Artemis was measured by imaging flow cytometry. In five of six clones we demonstrated a significantly increased level of apoptosis when compared to non-transfected cells and cells transfected with the pPur vector only. In clone 6 we did not observe elevated apoptosis. Interestingly, this clone was not observed to have elevated Artemis expression; this is likely due to the failure to transfect with the *Artemis* cDNA during co-transfection.

Figure 5.6 - Apoptosis in NB1-Tert cells transfected to over-express the Artemis protein.

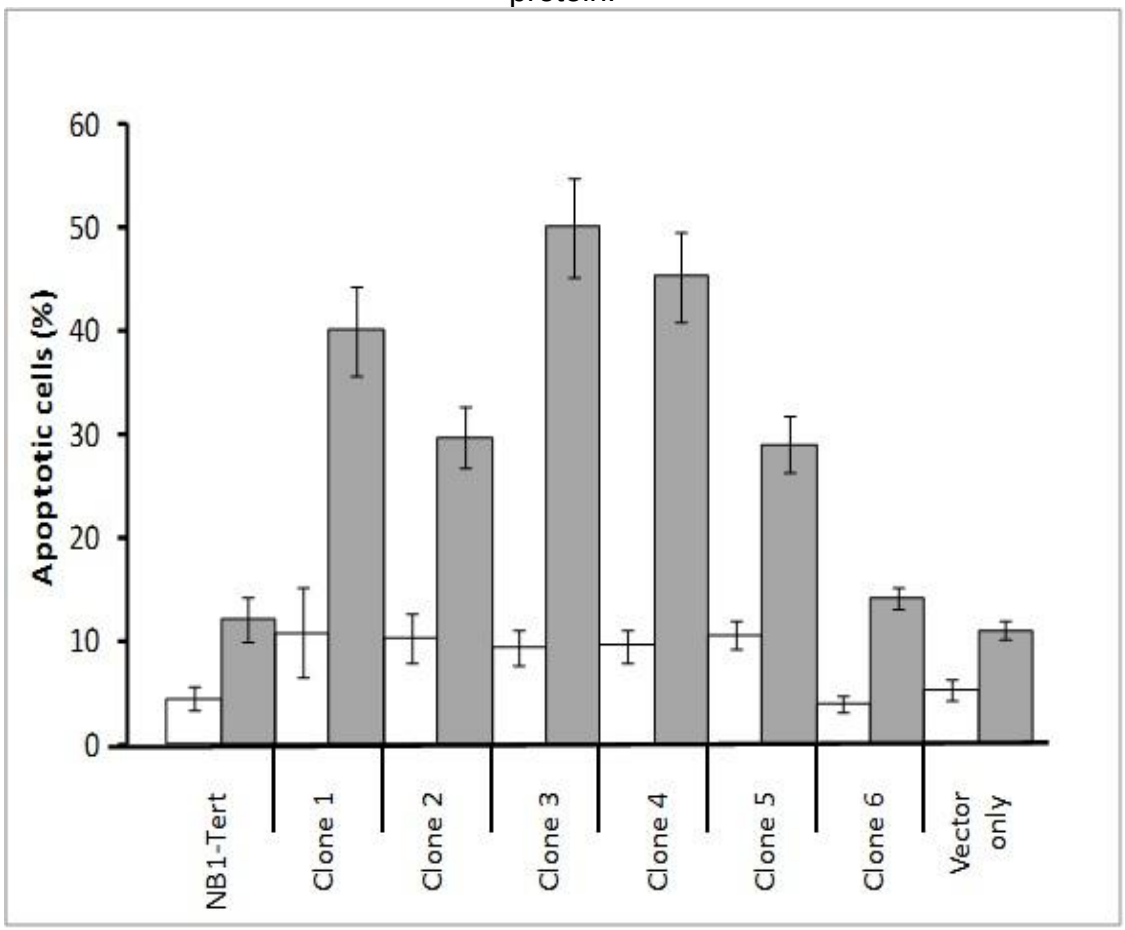

Data are derived from analysing the images of not less than 5000 cells. Standard deviation bars are included and shown on the graph. White bars are untreated cells. Grey bars are cells treated with a 2 Gy gamma radiation. The P value is < 0.05.

Figure 5.7- Non-apoptotic and cells at different stages of apoptosis.

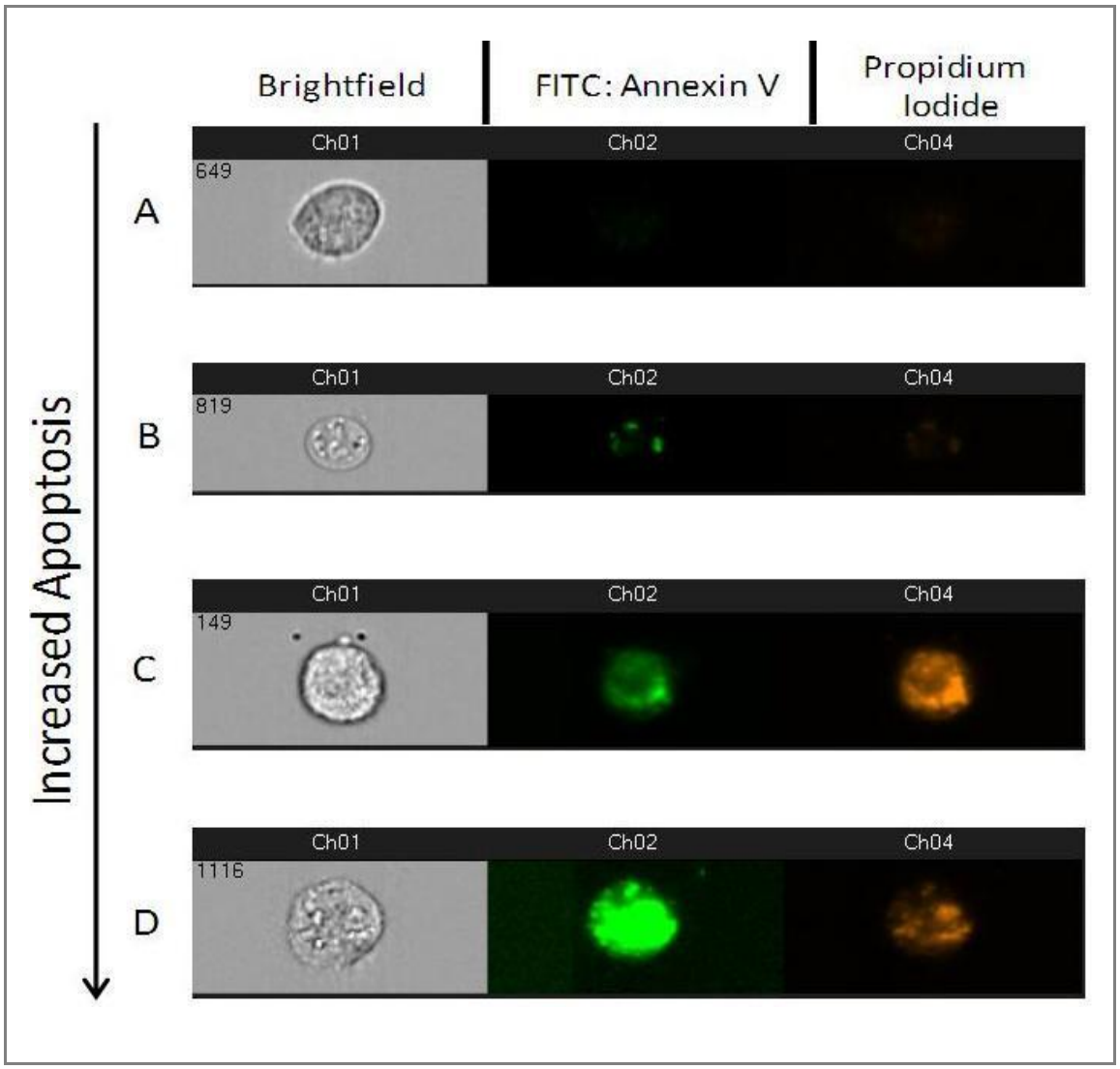

Images derived from Imagestream analysis shows a brightfield image together with an image of Annexin V staining (FITC) and an image of the nucleus stained with PI. A: A normal cell with spherical nucleous and no sign of apoptosis, B: Shrunken cell with light fluorescence as a sign of early apoptosis, C: cell beginning to bleb and intense green fluorescence indicates apoptosis, D: Cell membrane breaking and intense fluorescence indicating high level of apoptosis.

5.3.5 - Apoptosis in radiation hypersensitive patient cells

The data in Figure 5.6 shows that in the repair normal NB1 and 1BR.3 cells the levels of apoptosis in un-irradiated cells (determined by the number of cells positive for Annexin V and propidium iodide staining) is 5.00% and 3.31% of all cells. Following 2 Gy gamma radiation the levels of radiation-induced apoptosis increases to 8.65% and 11.50% respectively for each cell line. In the radiation-sensitive 84BR and 175BR fibroblasts, apoptosis levels in un-irradiated cells are 8.65% and 10.32% respectively. Following 2Gy irradiation these levels increase to 24.54% and 30.60% respectively. These data indicate that spontaneous levels of apoptosis in the radiosensitive cell lines are higher than in the repair-competent NB1 and 1BR.3 cells. Moreover, a similar and significantly increased level of apoptosis is observed in the 84BR and 175BR cell lines compared to the repair competent fibroblasts ($P < 0.05$, Student's unpaired t-test).

Figure 5.8 - Apoptosis in patient and in control cells.

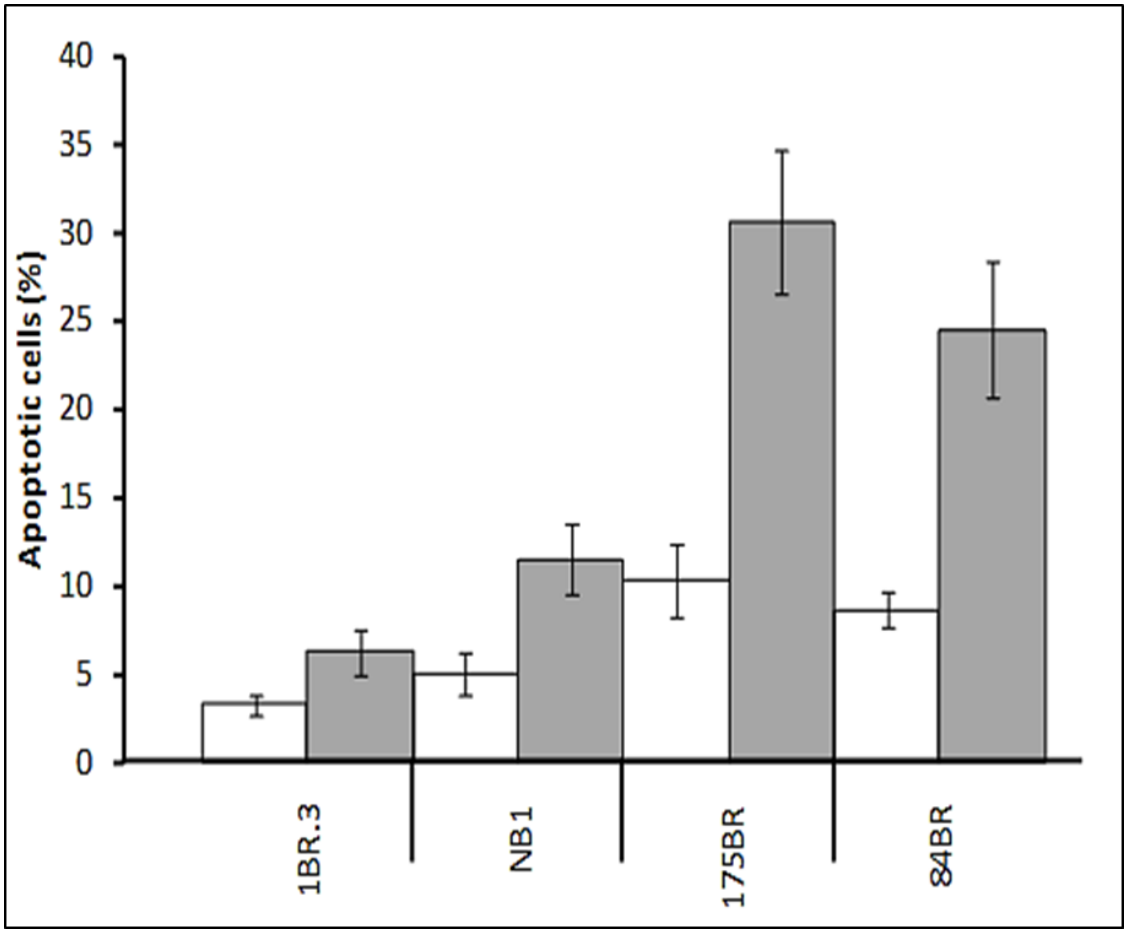

Here the apoptosis level in NB1 and 1BR.3 repair normal cell lines compared with the radiosensitive 84BR and 175BR cell lines prior (white bars) and following 2Gy gamma radiation (grey bars) is illustrated. Apoptosis was determined by Annexin V and propidium iodide staining and data are derived from imaging flow cytometry using the Imagestream whereby images of 5000 or more cells were captured and apoptotic cells determined. Standard deviation bars are included and shown on the graphs. The P value is < 0.05.

5.4 - Discussion

In previous chapters, it was demonstrated that the 84BR and 175BR patient cell lines were hypersensitive to the lethal effects of γ-radiation. However, a normal response to DNA cross-linking agent (nitrogen mustard), as explained in Chapter 3, which requires collaboration of NHEJ and HR, indicated that the likely defective pathway controlling the hypersensitivity was NHEJ. The qRT-PCR analysis of key genes associated with NHEJ DNA repair revealed a 1.5-2 fold over-expression of the *Artemis* endonuclease in both 175BR and 84BR patient cells. Thus, the likelihood of radiosensitivity as a result of *Artemis* over expression in these cells. To investigate further this hypothesis and subsequently to reveal the defect in *Artemis* gene, the NB1-Tert cells were co-transfected with full length *Artemis* cDNA. The pCMV6.XL5 vector did not carry any selectable marker, thus the full length *Artemis* cDNA was co-transfected with plasmid pPur into NB1-Tert cells and the transfectant capable of growing and producing clones in puromycin were isolated. In total six clones were identified. The use of imaging flow cytometry revealed the highest Artemis expression, ranging between 1.65 to 2.25 fold, in clones 1-5, while in clone 6 there was largely unchanged level of Artemis expression. It is likely that the clone 6 was co-transfected with pPur only thus the reason why the Artemis expression was largely unchanged.

The radiosensitivity of these clones was examined through γ-irradiation clonogenic assay. Different clones containing *Artemis* cDNA were irradiated with increasing doses of γ-irradiation. Non-transfected NB1-Tert cell line served as control in this experiment. The γ-irradiation survival curve showed that the NB1-Tert clones 1 to 5 had a marked reduction in the clonogenic cell survival following exposure to

increasing doses of gamma radiation, suggesting that the radiosensitivity in these clones may be associated with the over-expression of *Artemis* gene. Thus, further supporting the association of high *Artemis* expression detected in Chapter 4 with qRT-PCR, with radiosensitivity in175BR and 84BR patients.

One explanation as to why those cells with high expression of Artemis, (the five NB1-Tert clones and the two patient cell lines (175BR and 84BR) displayed much higher cellular radiosensitivity in comparison to the controls, might be due to the fact that the more Artemis is being made, the higher is the nuclease activity (i.e. the trimming of the DNA ends) during the NHEJ repair of DSBs of DNA. Therefore, as the nuclease activity increases more DNA is un-specifically trimmed and less XRCC4 and Ligase IV proteins are available for the ligation and sealing of the DNA ends. The un-specific cutting of the DNA therefore, resulted in a defect in the ability of both patient cells to repair the DSBs caused by IR. This may then have resulted in high sensitivity to radiation in cells with high expression of Artemis.

While we demonstrate radiosensitivity associated with Artemis over-expression in the two cell lines and that this result is concordant with that of (Multhaup *et al.,* 2010), others have not demonstrated similar findings. For example, over-expression of functional Artemis in the 48BR normal fibroblast cell line results in increased radioresistance. However an Artemis construct deleted at the C-terminus thus removing endonuclease activity of the protein results in a dominant negative phenotype whereby the 48BR fibroblasts are rendered sensitive to the lethal effects of radiation and radiomimetic drugs (Mohapatra *et al.,* 2011). The apparent disparity of these findings are unclear but it may be speculated that cell line specific

differences in DNA repair and gene expression may underpin the differences in radiation survival following *Artemis* transfection. Alternatively, over-expression of an endonuclease such as Artemis beyond a critical level may lead to cytotoxicity rather than resistance to radiation.

Also in five of six clones and the two radiation-sensitive fibroblasts (84BR and 175BR) the apoptosis was elevated after gamma radiation exposure. Thus, the data indicate that the spontaneous levels of apoptosis in the radiosensitive cell lines are higher than in the repair-competent NB1, 1BR.3 and NB1-Tert cells.

To reiterate, our findings together with the results of others (e.g. Mohapatra *et al.,* 2011) indicate that both increased and reduced levels of Artemis expression can result in cellular radiosensitivity. While the level of over-expression in the 84BR and 175BR cell lines is approximately 1.5-2 fold, we do observe elevated apoptosis and a failure to efficiently repair DNA DSB before and following radiation exposure. Therefore, we hypothesise that the increased expression of the Artemis protein appears to act in a dominant negative manner and can result in elevated sensitivity to IR and elevated apoptosis.

Chapter 6 - General Discussion

In this research, the cellular radiosensitivity in two human fibroblast cell lines (84BR and 175BR) has been identified. The 84BR fibroblast cell line was derived from a non-affected skin biopsy of radiosensitive breast cancer patient (Arlett *et al*., 1989). The 175BR cell line as derived from a non-affected skin biopsy from an individual with multiple tumours of independent histological origin and was a kind gift from Professor Bruce Ponder (Cambridge Research Institute, Cambridge, UK).

The breast cancer patient is an adult female who has over-reacted to radiotherapy. Also on the RTOG scale this patient was categorised as class three patient with severe odema, swelling and persistent fibrosis (Cox *et al.,* 1995). The clinical hyper sensitivity to radiotherapy in 84BR patient was also confirmed at cellular level by two independent studies conducted by Arlett *et al.,* (1989) and Alsbeih *et al.,* (1996).

According to the family pedigree, provided by Professor Bruce Ponder, and the patient information provided by Dr C.F Arlett, the patient 175BR is an adult male and multiple tumours existed amongst other members of his family. However, there is no evidence of clinical radiosensitivity and over-reaction to radiotherapy in this patient.

Other cell lines used in this project were the NB1 and 1.BR3 normal diploid fibroblast cell lines as described in Bridger and Kill (2004) and Arlett et al., 1988 and the immortal NB1-Tert cell line was established during this research.

The clonogenic assays were conducted by exposure of cells to IR and the DNA cross-linking agent (nitrogen mustard). The clonogenic assay conducted with IR had

two fold purposes; to detect the hypersensitivity of both patient cells to γ-radiation, and to confirm the findings of Arlett *et al.,* (1989) and Alsbeih *et al.,* (1996) which supports the radiosensitivity of 84BR patient cells at cellular level. The results of clonogenic assay with IR demonstrated that both the 84BR and 175BR patient cells were 1.5-2 fold more sensitive to the lethal effects of IR, than two fibroblast cell lines 1BR.3 and NB1 derived from repair normal individuals.

The exposure of cells to γ-radiation can result in single strand breaks single strand breaks together with sugar and base oxidations. The damage to DNA is recognised and repaired by specific DNA repair pathways. The three enzymatically distinct pathways that repair DNA DSBs are: NHEJ, HR, and SSA. While the NHEJ is the main pathway of IR-induced DSB repair in eukaryotic cells the HR is the principle mechanism in prokaryotic cells.

To determine the defective DSB repair pathway responsible for γ-radiation sensitivity of 84BR and 175BR cell lines, these cells were treated with increasing doses of HN2. As exposure of HN2 on patient cells revealed similar response to that of control cells, the possibility of defective HR was excluded thus, the results implied a defect in NHEJ pathway.

The DSBs in 84BR and 175BR cells were detected by immunofluorescence assay where the cells treated with γ-irradiation and the ability of the cells to repair DSBs were measured with anti γ-H2AX antibody. The DSB repair in these cells were measured on the basis of clearance of γ-H2AX foci against repair time and compared to that of control cell lines. Immunofluorescence assay showed that in 84BR and

175BR cells the majority of the γ-H2AX foci were still present after 24 hour exposure to IR, which suggested defective DSB repair. The majority of γ-H2AX foci in control cell lines (NB1 and 1.BR3) were cleared thus, indicated the efficient repair of DSBs. The persistence of γ-H2AX foci even at 24hr post irradiation in patient cells and enhanced radiosensitivity in patient cell lines was associated with a failure to effectively repair DNA DSBs following radiation exposure.

The next step of this research involved detection of NHEJ repair defect which may have been responsible for the radiosensitivity seen in both patients. To identify the NHEJ defective gene the qRT-PCR assay was conducted. This assay enabled us to study the level of gene expression of some of the key genes (Ku70, Ku80, DNAPKcs, XRCC4, XLF, Ligase IV and *Artemis*) found in NHEJ repair pathway. Quantitative PCR analysis of key genes associated with NHEJ DNA repair revealed a 1.5-2 fold over-expression of the *Artemis* endonuclease, which is a key component of the NHEJ repair pathway. In the absence of detecting any other defect in the cells other than an abnormal over-expression of *Artemis*, it was necessary to determine how such a phenotype might be responsible for the radiation hypersensitivity of the two cell lines

A study by Multhaup *et al*., (2010) investigating the use of lentivral vectors for the gene therapy of RS-SCID demonstrated that over-expression of the Artemis protein was associated with reduced cell survival, increased DNA damage and elevated apoptosis. Similarly, we hypothesised from our observations that in the cell lines described in this study, that increased expression of the Artemis endonuclease might be acting as a dominant negative leading to abnormal and illegitimate DNA DSBs

due to the unregulated action of the protein thus contributing to increased radiosensitivity.

The expression of Artemis protein in fibroblast cell lines (NB1, 1BR.3, 84BR and 175BR) and clones of NB1.Tert cells transfected with *Artemis* was determined using immunocytochemistry and imaging flow cytometry. A 2.06 and 2.09-fold increase in nuclear Artemis was detected thus, confirming the observations of elevated *Artemis* expression detected by RT-qPCR experiments. Also the Artemis expression ranged from 1.65-fold increased level in clone 3 to 2.25-fold elevated expression in clone 5.

As in Multhaup *et al.,* (2010) study to determine the effect of over-expression of Artemis in those fibroblast cells the apoptosis assay was conducted. The levels of apoptosis in untreated and cells irradiated with 2Gy gamma radiation were determined by immunocytochemistry and imaging flow cytometry. In the repair normal NB1 and 1BR.3 cells the levels of apoptosis in un-irradiated cells was 5.00% and 3.31% of all cells. After treating the cells to 2Gy gamma radiation the levels of radiation induced apoptosis increased to 8.65% and 11.50% respectively for each cell line. In the radiation-sensitive 84BR and 175BR fibroblasts, apoptosis levels in un-irradiated cells were 8.65% and 10.32% respectively. Following 2Gy irradiation these levels increased to 24.54% and 30.60% respectively. Thus the results indicate a much higher spontaneous levels of apoptosis in the radiosensitive cell lines when compared to repair-component NB1 and 1BR.3 cell lines.

Similarly the apoptosis in NB1-Tert cells transfected to over-express *Artemis* was also significantly increased when compared to non-transfected cells and cells transfected with the pPur vector only.

The clonogenic cell survival in the *Artemis* transfected NB1-Tert clones 1 to 5 (that are over-expressing *Artemis*), a marked reduction in the clonogenic cell survival was also confirmed following exposure to increasing doses of gamma radiation.

Thus, the increased endonuclease activity associated with over-expression of Artemis is associated with higher levels of DNA DSB, radiosensitivity and elevated apoptosis in two radio-hypersensitive cell lines (175BR and 84BR) as well as those NB1-Tert clones 1 to 5 with high expression of Artemis. These data reveal a potentially novel mechanism responsible for radiosensitivity in human cells.

From these observations we propose a novel mechanism of cellular radiation hypersensitivity whereby the increased expression of the Artemis endonuclease promotes illegitimate DNA DSB leading to elevated DNA damage and elevated apoptosis associated with clinical and cellular radiosensitivity. Also the prolonged H2AX foci in patient cells are not only due to deficiency in repairing DSBs. Also the foci may be the result of new breaks being created due to an excess of the Artemis nuclease.

Future Work

Since the over-expression of Artemis resulted in radiosensitivity in two patient cell lines (84BR and 175BR) and in NB1-Tert cells transfected to induce high expression of *Artemis* in clonogenic assay the gene knockdown would ideally bring the level of *Artemis* expression to a normal level. One suggestion is that normal level of *Artemis* expression may restore normal radiosensitivity in the cells. Thus, a restoration of normal radiosensitivity might lead to efficient DSB repair and automatically a reduction in apoptosis levels in those cells.

Also, it would be interesting to see if over-expression of Artemis in DNA-PKcs defective cells would cause radiosensitivity as described in this thesis. The cell lines XP14BRneo17 (Abbaszadeh *et al.,* 2010) and the MO59J (Anderson *et al.,* 2001) are defective in DNA-PKcs. Therefore, over-expression of Artemis in these cell lines may not render the cells sensitive to radiation due to the necessity for DNA-PKcs phosphorylation of Artemis. This would also address this question as to whether other kinases have the ability to activate Artemis in the absence of DNA-PKcs.

Finally, we have demonstrated a dominant negative effect of Artemis over-expression in two fibroblast cell lines derived from cancer patient and in the cell line NB1-Tert transfected to over-express Artemis. It may be conceded that this is a limited number of cell types. Therefore, it would be a useful enterprise to determine the effect in a wider variety of cell types from normal individuals and in cells derived from different types of cancer. Moreover, the critical level of Artemis expression in cells which results in radiosensitivity needs to be addressed. For example, it was demonstrated that a twofold over-expression of Artemis results in radiosensitivity. It

would be useful to create a range of cell lines with increasing and decreasing levels of Artemis to determine which level of protein expression induces radiation resistance and sensitivity.

References

Abbaszadeh, F., P. H. Clingen, C. F. Arlett, P. N. Plowman, E. C. Bourton, M. Themis, E. M. Makarov, R. F. Newbold, M. H. Green and C. N. Parris (2010). "A novel splice variant of the DNA-PKcs gene is associated with clinical and cellular radiosensitivity in a patient with xeroderma pigmentosum." J Med Genet **47**(3): 176-181.

Ahnesorg, P., P. Smith and S. P. Jackson (2006). "XLF interacts with the XRCC4-DNA ligase IV complex to promote DNA nonhomologous end-joining." Cell **124**(2): 301-313.

Alsbeih, M. G., B. Fertil, C. F. Arlett and E. P. Malaise (1996). "High split-dose recovery in hypersensitive human fibroblasts: a case of induced radioresistance?" Int J Radiat Biol **69**(2): 225-239.

Anderson, C. W., J. J. Dunn, P. I. Freimuth, A. M. Galloway and M. J. Allalunis-Turner (2001). "Frameshift mutation in PRKDC, the gene for DNA-PKcs, in the DNA repair-defective, human, glioma-derived cell line M059J." Radiat Res **156**(1): 2-9.

Annunziato, A. T. (2008). "DNA Packaging: Nucleosomes and Chromatin."

Arlett CF, C. J., Green MHL Ed. (1989). Radiosensitive individuals in the population. In Low Dose Radiation: Biological Bases of Risk Assessment. Taylor Francis, London, Baverstock KF, Stather JW.

Arlett, C. F., J. Cole and M. Green, Eds. (1989). Radiosensitive individuals in the population. In Low Dose Radiation: Biological Bases of Risk Assessment. Taylor Francis, London, Baverstock KF, Stather JW.

Arlett, C. F., M. H. Green, A. Priestley, S. A. Harcourt and L. V. Mayne (1988). "Comparative human cellular radiosensitivity: I. The effect of SV40 transformation and immortalisation on the gamma-irradiation survival of skin derived fibroblasts from normal individuals and from ataxia-telangiectasia patients and heterozygotes." Int J Radiat Biol **54**(6): 911-928.

Arlett, C. F., P. N. Plowman, P. B. Rogers, C. N. Parris, F. Abbaszadeh, M. H. Green, T. J. McMillan, C. Bush, N. Foray and A. R. Lehmann (2006). "Clinical and cellular ionizing radiation sensitivity in a patient with xeroderma pigmentosum." Br J Radiol **79**(942): 510-517.

Aurias, A., J. L. Antoine, R. Assathiany, M. Odievre and B. Dutrillaux (1985). "Radiation sensitivity of Bloom's syndrome lymphocytes during S and G2 phases." Cancer Genet Cytogenet **16**(2): 131-136.

Bakhshi, S., K. M. Cerosaletti, P. Concannon, E. V. Bawle, J. Fontanesi, R. A. Gatti and K. Bhambhani (2003). "Medulloblastoma with adverse reaction to radiation therapy in nijmegen breakage syndrome." J Pediatr Hematol Oncol **25**(3): 248-251.

Bassing, C. H. and F. W. Alt (2004). "The cellular response to general and programmed DNA double strand breaks." DNA Repair (Amst) **3**(8-9): 781-796.

Bassing, C. H., W. Swat and F. W. Alt (2002). "The mechanism and regulation of chromosomal V(D)J recombination." Cell **109 Suppl**: S45-55.

Beucher, A., J. Birraux, L. Tchouandong, O. Barton, A. Shibata, S. Conrad, A. A. Goodarzi, A. Krempler, P. A. Jeggo and M. Lobrich (2009). "ATM and Artemis promote homologous recombination of radiation-induced DNA double-strand breaks in G2." EMBO J **28**(21): 3413-3427.

Bilsland, E. and J. A. Downs (2005). "Tails of histones in DNA double-strand break repair." Mutagenesis **20**(3): 153-163.
Bohr, V. A. and G. L. Dianov (1999). "Oxidative DNA damage processing in nuclear and mitochondrial DNA." Biochimie **81**(1-2): 155-160.
Boland, C. R. and A. Goel (2010). "Microsatellite instability in colorectal cancer." Gastroenterology **138**(6): 2073-2087 e2073.
Bourton, E. C., P. N. Plowman, S. A. Zahir, G. U. Senguloglu, H. Serrai, G. Bottley and C. N. Parris (2012). "Multispectral imaging flow cytometry reveals distinct frequencies of gamma-H2AX foci induction in DNA double strand break repair defective human cell lines." Cytometry A **81**(2): 130-137.
Brandt, V. L. and D. B. Roth (2004). "V(D)J recombination: how to tame a transposase." Immunol Rev **200**: 249-260.
Bridger, J. M. and I. R. Kill (2004). "Aging of Hutchinson-Gilford progeria syndrome fibroblasts is characterised by hyperproliferation and increased apoptosis." Exp Gerontol **39**(5): 717-724.
Burma, S., B. P. Chen and D. J. Chen (2006). "Role of non-homologous end joining (NHEJ) in maintaining genomic integrity." DNA Repair (Amst) **5**(9-10): 1042-1048.
Chadwick, K., Leenhouts, HP (1994). "DNA double strand breaks from two single strand breaks and cell cycle radiation sensitivity. ." Radiation Protection Dosimetry **52**: 363-366.
Chan, D. W., B. P. Chen, S. Prithivirajsingh, A. Kurimasa, M. D. Story, J. Qin and D. J. Chen (2002). "Autophosphorylation of the DNA-dependent protein kinase catalytic subunit is required for rejoining of DNA double-strand breaks." Genes Dev **16**(18): 2333-2338.
Chen, L., K. Trujillo, P. Sung and A. E. Tomkinson (2000). "Interactions of the DNA ligase IV-XRCC4 complex with DNA ends and the DNA-dependent protein kinase." J Biol Chem **275**(34): 26196-26205.
Cheng, K. C., D. S. Cahill, H. Kasai, S. Nishimura and L. A. Loeb (1992). "8-Hydroxyguanine, an abundant form of oxidative DNA damage, causes G----T and A----C substitutions." J Biol Chem **267**(1): 166-172.
Chiou, S. S., J. L. Huang, Y. S. Tsai, T. F. Chen, K. W. Lee, S. H. Juo, Y. J. Jong, C. H. Hung, T. T. Chang and C. S. Lin (2007). "Elevated mRNA transcripts of non-homologous end-joining genes in pediatric acute lymphoblastic leukemia." Leukemia **21**(9): 2061-2064.
Chistiakov, D. A., N. V. Voronova and A. P. Chistiakov (2009). "Ligase IV syndrome." Eur J Med Genet **52**(6): 373-378.
Chrzanowska, K. H., H. Gregorek, B. Dembowska-Baginska, M. A. Kalina and M. Digweed (2012). "Nijmegen breakage syndrome (NBS)." Orphanet J Rare Dis **7**: 13.
Chun, H. H. and R. A. Gatti (2004). "Ataxia-telangiectasia, an evolving phenotype." DNA Repair (Amst) **3**(8-9): 1187-1196.
Clingen, P. H., C. F. Arlett, J. A. Hartley and C. N. Parris (2007). "Chemosensitivity of primary human fibroblasts with defective unhooking of DNA interstrand cross-links." Exp Cell Res **313**(4): 753-760.
Collins, A. R. (2004). "The comet assay for DNA damage and repair: principles, applications, and limitations." Mol Biotechnol **26**(3): 249-261.
Cox, J. D., J. Stetz and T. F. Pajak (1995). "Toxicity criteria of the Radiation Therapy Oncology Group (RTOG) and the European Organization for Research and

Treatment of Cancer (EORTC)." Int J Radiat Oncol Biol Phys **31**(5): 1341-1346.
D'Haene, B., J. Vandesompele and J. Hellemans (2010). "Accurate and objective copy number profiling using real-time quantitative PCR." Methods **50**(4): 262-270.
Dai, Y., B. Kysela, L. A. Hanakahi, K. Manolis, E. Riballo, M. Stumm, T. O. Harville, S. C. West, M. A. Oettinger and P. A. Jeggo (2003). "Nonhomologous end joining and V(D)J recombination require an additional factor." Proc Natl Acad Sci U S A **100**(5): 2462-2467.
David, S. S., V. L. O'Shea and S. Kundu (2007). "Base-excision repair of oxidative DNA damage." Nature **447**(7147): 941-950.
de Laat, W. L., N. G. Jaspers and J. H. Hoeijmakers (1999). "Molecular mechanism of nucleotide excision repair." Genes Dev **13**(7): 768-785.
DeFazio, L. G., R. M. Stansel, J. D. Griffith and G. Chu (2002). "Synapsis of DNA ends by DNA-dependent protein kinase." EMBO J **21**(12): 3192-3200.
Delia, D., S. Mizutani, S. Panigone, E. Tagliabue, E. Fontanella, M. Asada, T. Yamada, Y. Taya, S. Prudente, S. Saviozzi, L. Frati, M. A. Pierotti and L. Chessa (2000). "ATM protein and p53-serine 15 phosphorylation in ataxia-telangiectasia (AT) patients and at heterozygotes." Br J Cancer **82**(12): 1938-1945.
Demuth, I. and M. Digweed (2007). "The clinical manifestation of a defective response to DNA double-strand breaks as exemplified by Nijmegen breakage syndrome." Oncogene **26**(56): 7792-7798.
Derveaux, S., J. Vandesompele and J. Hellemans (2010). "How to do successful gene expression analysis using real-time PCR." Methods **50**(4): 227-230.
Dianov, G., C. Bischoff, J. Piotrowski and V. A. Bohr (1998). "Repair pathways for processing of 8-oxoguanine in DNA by mammalian cell extracts." J Biol Chem **273**(50): 33811-33816.
Dianov, G. L. (2011). "Base excision repair targets for cancer therapy." Am J Cancer Res **1**(7): 845-851.
Dianov, G. L. and J. L. Parsons (2007). "Co-ordination of DNA single strand break repair." DNA Repair (Amst) **6**(4): 454-460.
Dvorak, C. C. and M. J. Cowan (2010). "Radiosensitive severe combined immunodeficiency disease." Immunol Allergy Clin North Am **30**(1): 125-142.
Eastham, A. M., J. Atkinson and C. M. West (2001). "Relationships between clonogenic cell survival, DNA damage and chromosomal radiosensitivity in nine human cervix carcinoma cell lines." Int J Radiat Biol **77**(3): 295-302.
Ellis, N. A., J. Groden, T. Z. Ye, J. Straughen, D. J. Lennon, S. Ciocci, M. Proytcheva and J. German (1995). "The Bloom's syndrome gene product is homologous to RecQ helicases." Cell **83**(4): 655-666.
Fagbemi, A. F., B. Orelli and O. D. Scharer (2011). "Regulation of endonuclease activity in human nucleotide excision repair." DNA Repair (Amst) **10**(7): 722-729.
Fehlauer, F., S. Tribius, U. Holler, D. Rades, A. Kuhlmey, A. Bajrovic and W. Alberti (2003). "Long-term radiation sequelae after breast-conserving therapy in women with early-stage breast cancer: an observational study using the LENT-SOMA scoring system." Int J Radiat Oncol Biol Phys **55**(3): 651-658.
Fousteri, M. and L. H. Mullenders (2008). "Transcription-coupled nucleotide excision repair in mammalian cells: molecular mechanisms and biological effects." Cell Res **18**(1): 73-84.

Frankenburg, D., M. Frankenburg-Schwager, D. Blocher and R. Harbich (1981). "Evidence for DNA Double-Strand Breaks as the Critical Lesions in Yeast Cells Irradiated with Sparsely or Densly Ionizing Radiation under Oxic or Anoxic Conditions." Radiation Research **88**: 524-532.

Friedberg, E. C. (2001). "How nucleotide excision repair protects against cancer." Nat Rev Cancer **1**(1): 22-33.

Friesner, J. D., B. Liu, K. Culligan and A. B. Britt (2005). "Ionizing radiation-dependent gamma-H2AX focus formation requires ataxia telangiectasia mutated and ataxia telangiectasia mutated and Rad3-related." Mol Biol Cell **16**(5): 2566-2576.

Fullgrabe, J., N. Hajji and B. Joseph (2010). "Cracking the death code: apoptosis-related histone modifications." Cell Death Differ **17**(8): 1238-1243.

Gatti, R. A. (2001). "The inherited basis of human radiosensitivity." Acta Oncol **40**(6): 702-711.

German, J. (1995). "Bloom's syndrome." Dermatol Clin **13**(1): 7-18.

Girard, P. M., N. Foray, M. Stumm, A. Waugh, E. Riballo, R. S. Maser, W. P. Phillips, J. Petrini, C. F. Arlett and P. A. Jeggo (2000). "Radiosensitivity in Nijmegen Breakage Syndrome cells is attributable to a repair defect and not cell cycle checkpoint defects." Cancer Res **60**(17): 4881-4888.

Goodarzi, A. A., Y. Yu, E. Riballo, P. Douglas, S. A. Walker, R. Ye, C. Harer, C. Marchetti, N. Morrice, P. A. Jeggo and S. P. Lees-Miller (2006). "DNA-PK autophosphorylation facilitates Artemis endonuclease activity." EMBO J **25**(16): 3880-3889.

Guda, K., L. Natale and S. D. Markowitz (2007). "An improved method for staining cell colonies in clonogenic assays." Cytotechnology **54**(2): 85-88.

Gunderson, K. and G. Chu (1991). "Pulsed-field electrophoresis of megabase-sized DNA." Mol Cell Biol **11**(6): 3348-3354.

Hada, M. and A. G. Georgakilas (2008). "Formation of clustered DNA damage after high-LET irradiation: a review." J Radiat Res **49**(3): 203-210.

Hastak, K., R. K. Paul, M. K. Agarwal, V. S. Thakur, A. R. Amin, S. Agrawal, R. M. Sramkoski, J. W. Jacobberger, M. W. Jackson, G. R. Stark and M. L. Agarwal (2008). "DNA synthesis from unbalanced nucleotide pools causes limited DNA damage that triggers ATR-CHK1-dependent p53 activation." Proc Natl Acad Sci U S A **105**(17): 6314-6319.

Hefferin, M. L. and A. E. Tomkinson (2005). "Mechanism of DNA double-strand break repair by non-homologous end joining." DNA Repair (Amst) **4**(6): 639-648.

Hegi, M. E., L. Liu, J. G. Herman, R. Stupp, W. Wick, M. Weller, M. P. Mehta and M. R. Gilbert (2008). "Correlation of O6-methylguanine methyltransferase (MGMT) promoter methylation with clinical outcomes in glioblastoma and clinical strategies to modulate MGMT activity." J Clin Oncol **26**(25): 4189-4199.

Helleday, T. (2003). "Pathways for mitotic homologous recombination in mammalian cells." Mutat Res **532**(1-2): 103-115.

Helleday, T., J. Lo, D. C. van Gent and B. P. Engelward (2007). "DNA double-strand break repair: from mechanistic understanding to cancer treatment." DNA Repair (Amst) **6**(7): 923-935.

Higuchi, R., G. Dollinger, P. S. Walsh and R. Griffith (1992). "Simultaneous amplification and detection of specific DNA sequences." Biotechnology (N Y) **10**(4): 413-417.

Hoeller, U., K. Borgmann, M. Bonacker, A. Kuhlmey, A. Bajrovic, H. Jung, W. Alberti and E. Dikomey (2003). "Individual radiosensitivity measured with lymphocytes may be used to predict the risk of fibrosis after radiotherapy for breast cancer." Radiother Oncol **69**(2): 137-144.

Holthusen, H. (1936). "Erfahrungen uber die Vertraglichkeitsgrenze fur Rontgenstrahlen und deren Nutzanwendung zur Verhutung von Schaden. ." Strahlenther **57**: 254-269.

Hsieh, P. and K. Yamane (2008). "DNA mismatch repair: molecular mechanism, cancer, and ageing." Mech Ageing Dev **129**(7-8): 391-407.

Ip, S. C., U. Rass, M. G. Blanco, H. R. Flynn, J. M. Skehel and S. C. West (2008). "Identification of Holliday junction resolvases from humans and yeast." Nature **456**(7220): 357-361.

Jackson, S. P. (2002). "Sensing and repairing DNA double-strand breaks." Carcinogenesis **23**(5): 687-696.

Jackson, S. P. and J. Bartek (2009). "The DNA-damage response in human biology and disease." Nature **461**(7267): 1071-1078.

Jeppesen, D. K., V. A. Bohr and T. Stevnsner (2011). "DNA repair deficiency in neurodegeneration." Prog Neurobiol **94**(2): 166-200.

Jiricny, J. (2006). "The multifaceted mismatch-repair system." Nat Rev Mol Cell Biol **7**(5): 335-346.

Jiricny, J. and G. Marra (2003). "DNA repair defects in colon cancer." Curr Opin Genet Dev **13**(1): 61-69.

Jiricny, J. and M. Nystrom-Lahti (2000). "Mismatch repair defects in cancer." Curr Opin Genet Dev **10**(2): 157-161.

Jones, J. M., M. Gellert and W. Yang (2001). "A Ku bridge over broken DNA." Structure **9**(10): 881-884.

Junop, M. S., M. Modesti, A. Guarne, R. Ghirlando, M. Gellert and W. Yang (2000). "Crystal structure of the Xrcc4 DNA repair protein and implications for end joining." EMBO J **19**(22): 5962-5970.

Kaina, B., G. P. Margison and M. Christmann (2010). "Targeting O(6)-methylguanine-DNA methyltransferase with specific inhibitors as a strategy in cancer therapy." Cell Mol Life Sci **67**(21): 3663-3681.

Kobayashi, N., K. Agematsu, K. Sugita, M. Sako, S. Nonoyama, A. Yachie, S. Kumaki, S. Tsuchiya, H. D. Ochs, Y. Fukushima and A. Komiyama (2003). "Novel Artemis gene mutations of radiosensitive severe combined immunodeficiency in Japanese families." Hum Genet **112**(4): 348-352.

Krejci, L., V. Altmannova, M. Spirek and X. Zhao (2012). "Homologous recombination and its regulation." Nucleic Acids Res **40**(13): 5795-5818.

Kuhne, M., E. Riballo, N. Rief, K. Rothkamm, P. A. Jeggo and M. Lobrich (2004). "A double-strand break repair defect in ATM-deficient cells contributes to radiosensitivity." Cancer Res **64**(2): 500-508.

Lavin, M. F. and Y. Shiloh (1997). "The genetic defect in ataxia-telangiectasia." Annu Rev Immunol **15**: 177-202.

Lee, S. H. and C. H. Kim (2002). "DNA-dependent protein kinase complex: a multifunctional protein in DNA repair and damage checkpoint." Mol Cells **13**(2): 159-166.

Lempiainen, H. and T. D. Halazonetis (2009). "Emerging common themes in regulation of PIKKs and PI3Ks." EMBO J **28**(20): 3067-3073.

Leonard, S. S., G. K. Harris and X. Shi (2004). "Metal-induced oxidative stress and signal transduction." Free Radic Biol Med **37**(12): 1921-1942.

Leuther, K. K., O. Hammarsten, R. D. Kornberg and G. Chu (1999). "Structure of DNA-dependent protein kinase: implications for its regulation by DNA." EMBO J **18**(5): 1114-1123.
Li, G. M. (2008). "Mechanisms and functions of DNA mismatch repair." Cell Res **18**(1): 85-98.
Li, X. and W. D. Heyer (2008). "Homologous recombination in DNA repair and DNA damage tolerance." Cell Res **18**(1): 99-113.
Li, Y., D. Y. Chirgadze, V. M. Bolanos-Garcia, B. L. Sibanda, O. R. Davies, P. Ahnesorg, S. P. Jackson and T. L. Blundell (2008). "Crystal structure of human XLF/Cernunnos reveals unexpected differences from XRCC4 with implications for NHEJ." EMBO J **27**(1): 290-300.
Lu, H., K. Schwarz and M. R. Lieber (2007). "Extent to which hairpin opening by the Artemis:DNA-PKcs complex can contribute to junctional diversity in V(D)J recombination." Nucleic Acids Res **35**(20): 6917-6923.
Ma, Y., U. Pannicke, H. Lu, D. Niewolik, K. Schwarz and M. R. Lieber (2005). "The DNA-dependent protein kinase catalytic subunit phosphorylation sites in human Artemis." J Biol Chem **280**(40): 33839-33846.
Ma, Y., U. Pannicke, K. Schwarz and M. R. Lieber (2002). "Hairpin opening and overhang processing by an Artemis/DNA-dependent protein kinase complex in nonhomologous end joining and V(D)J recombination." Cell **108**(6): 781-794.
Ma, Y., K. Schwarz and M. R. Lieber (2005). "The Artemis:DNA-PKcs endonuclease cleaves DNA loops, flaps, and gaps." DNA Repair (Amst) **4**(7): 845-851.
Mansilla-Soto, J. and P. Cortes (2003). "VDJ recombination: Artemis and its in vivo role in hairpin opening." J Exp Med **197**(5): 543-547.
Market, E. and F. N. Papavasiliou (2003). "V(D)J recombination and the evolution of the adaptive immune system." PLoS Biol **1**(1): E16.
Meyn, M. S. (1995). "Ataxia-telangiectasia and cellular responses to DNA damage." Cancer Res **55**(24): 5991-6001.
Misteli, T. and E. Soutoglou (2009). "The emerging role of nuclear architecture in DNA repair and genome maintenance." Nat Rev Mol Cell Biol **10**(4): 243-254.
Mladenov, E. and G. Iliakis (2011). "Induction and repair of DNA double strand breaks: the increasing spectrum of non-homologous end joining pathways." Mutat Res **711**(1-2): 61-72.
Mohapatra, S., M. Kawahara, I. S. Khan, S. M. Yannone and L. F. Povirk (2011). "Restoration of G1 chemo/radioresistance and double-strand-break repair proficiency by wild-type but not endonuclease-deficient Artemis." Nucleic Acids Res **39**(15): 6500-6510.
Mohrin, M., E. Bourke, D. Alexander, M. R. Warr, K. Barry-Holson, M. M. Le Beau, C. G. Morrison and E. Passegue (2010). "Hematopoietic stem cell quiescence promotes error-prone DNA repair and mutagenesis." Cell Stem Cell **7**(2): 174-185.
Moshous, D., I. Callebaut, R. de Chasseval, B. Corneo, M. Cavazzana-Calvo, F. Le Deist, I. Tezcan, O. Sanal, Y. Bertrand, N. Philippe, A. Fischer and J. P. de Villartay (2001). "Artemis, a novel DNA double-strand break repair/V(D)J recombination protein, is mutated in human severe combined immune deficiency." Cell **105**(2): 177-186.
Moshous, D., L. Li, R. Chasseval, N. Philippe, N. Jabado, M. J. Cowan, A. Fischer and J. P. de Villartay (2000). "A new gene involved in DNA double-strand break repair and V(D)J recombination is located on human chromosome 10p." Hum Mol Genet **9**(4): 583-588.

Mozaffarieh, M., A. Schoetzau, M. Sauter, M. Grieshaber, S. Orgul, O. Golubnitschaja and J. Flammer (2008). "Comet assay analysis of single-stranded DNA breaks in circulating leukocytes of glaucoma patients." Mol Vis **14**: 1584-1588.

Multhaup, M., A. D. Karlen, D. L. Swanson, A. Wilber, N. V. Somia, M. J. Cowan and R. S. McIvor (2010). "Cytotoxicity associated with artemis overexpression after lentiviral vector-mediated gene transfer." Hum Gene Ther **21**(7): 865-875.

Munshi, A., M. Hobbs and R. E. Meyn (2005). "Clonogenic cell survival assay." Methods Mol Med **110**: 21-28.

Murphy, S., A. Hayward, G. Troup, E. J. Devor and T. Coons (1980). "Gene enrichment in an American Indian population: an excess of severe combined immunodeficiency disease." Lancet **2**(8193): 502-505.

Musio, A., V. Marrella, C. Sobacchi, F. Rucci, L. Fariselli, S. Giliani, G. Lanzi, L. D. Notarangelo, D. Delia, R. Colombo, P. Vezzoni and A. Villa (2005). "Damaging-agent sensitivity of Artemis-deficient cell lines." Eur J Immunol **35**(4): 1250-1256.

Nakamura, T. M., L. L. Du, C. Redon and P. Russell (2004). "Histone H2A phosphorylation controls Crb2 recruitment at DNA breaks, maintains checkpoint arrest, and influences DNA repair in fission yeast." Mol Cell Biol **24**(14): 6215-6230.

Nocentini, S. (1995). "Comet assay analysis of repair of DNA strand breaks in normal and deficient human cells exposed to radiations and chemicals. Evidence for a repair pathway specificity of DNA ligation." Radiat Res **144**(2): 170-180.

Noordzij, J. G., N. S. Verkaik, M. van der Burg, L. R. van Veelen, S. de Bruin-Versteeg, W. Wiegant, J. M. Vossen, C. M. Weemaes, R. de Groot, M. Z. Zdzienicka, D. C. van Gent and J. J. van Dongen (2003). "Radiosensitive SCID patients with Artemis gene mutations show a complete B-cell differentiation arrest at the pre-B-cell receptor checkpoint in bone marrow." Blood **101**(4): 1446-1452.

O'Driscoll, M., K. M. Cerosaletti, P. M. Girard, Y. Dai, M. Stumm, B. Kysela, B. Hirsch, A. Gennery, S. E. Palmer, J. Seidel, R. A. Gatti, R. Varon, M. A. Oettinger, H. Neitzel, P. A. Jeggo and P. Concannon (2001). "DNA ligase IV mutations identified in patients exhibiting developmental delay and immunodeficiency." Mol Cell **8**(6): 1175-1185.

O'Driscoll, M. and P. Jeggo (2002). "Immunological disorders and DNA repair." Mutat Res **509**(1-2): 109-126.

O'Sullivan, D. J. (2000). "Methods for analysis of the intestinal microflora." Curr Issues Intest Microbiol **1**(2): 39-50.

Olive, P. L. and J. P. Banath (2006). "The comet assay: a method to measure DNA damage in individual cells." Nat Protoc **1**(1): 23-29.

Olive, P. L. and R. E. Durand (2005). "Heterogeneity in DNA damage using the comet assay." Cytometry A **66**(1): 1-8.

Olive, P. L., P. J. Johnston, J. P. Banath and R. E. Durand (1998). "The comet assay: a new method to examine heterogeneity associated with solid tumors." Nat Med **4**(1): 103-105.

Pannicke, U., M. Honig, I. Schulze, J. Rohr, G. A. Heinz, S. Braun, I. Janz, E. M. Rump, M. G. Seidel, S. Matthes-Martin, J. Soerensen, J. Greil, D. K. Stachel, B. H. Belohradsky, M. H. Albert, A. Schulz, S. Ehl, W. Friedrich and K. Schwarz (2010). "The most frequent DCLRE1C (ARTEMIS) mutations are based on homologous recombination events." Hum Mutat **31**(2): 197-207.

Paterson, M. C., A. K. Anderson, B. P. Smith and P. J. Smith (1979). "Enhanced radiosensitivity of cultured fibroblasts from ataxia telangiectasia heterozygotes manifested by defective colony-forming ability and reduced DNA repair replication after hypoxic gamma-irradiation." Cancer Res **39**(9): 3725-3734.

Paull, T. T., E. P. Rogakou, V. Yamazaki, C. U. Kirchgessner, M. Gellert and W. M. Bonner (2000). "A critical role for histone H2AX in recruitment of repair factors to nuclear foci after DNA damage." Curr Biol **10**(15): 886-895.

Pavy, J. J., J. Denekamp, J. Letschert, B. Littbrand, F. Mornex, J. Bernier, D. Gonzales-Gonzales, J. C. Horiot, M. Bolla and H. Bartelink (1995). "EORTC Late Effects Working Group. Late effects toxicity scoring: the SOMA scale." Radiother Oncol **35**(1): 11-15.

Pfaffl, M. W. (2001). "A new mathematical model for relative quantification in real-time RT-PCR." Nucleic Acids Res **29**(9): e45.

Pfaffl, M. W. and M. Hageleit (2001). "Validities of mRNA quantification using recombinant RNA and recombinant DNA external calibration curves in real-time RT-PCR." Biotechnology Letters **23**(4): 275-282.

Poinsignon, C., D. Moshous, I. Callebaut, R. de Chasseval, I. Villey and J. P. de Villartay (2004). "The metallo-beta-lactamase/beta-CASP domain of Artemis constitutes the catalytic core for V(D)J recombination." J Exp Med **199**(3): 315-321.

Ramsden, D. A. and M. Gellert (1998). "Ku protein stimulates DNA end joining by mammalian DNA ligases: a direct role for Ku in repair of DNA double-strand breaks." EMBO J **17**(2): 609-614.

Ramsden, D. A., B. D. Weed and Y. V. Reddy (2010). "V(D)J recombination: Born to be wild." Semin Cancer Biol **20**(4): 254-260.

Rasimas, J. J., P. A. Dalessio, I. J. Ropson, A. E. Pegg and M. G. Fried (2004). "Active-site alkylation destabilizes human O6-alkylguanine DNA alkyltransferase." Protein Sci **13**(1): 301-305.

Redon, C., D. Pilch, E. Rogakou, O. Sedelnikova, K. Newrock and W. Bonner (2002). "Histone H2A variants H2AX and H2AZ." Curr Opin Genet Dev **12**(2): 162-169.

Riballo, E., S. E. Critchlow, S. H. Teo, A. J. Doherty, A. Priestley, B. Broughton, B. Kysela, H. Beamish, N. Plowman, C. F. Arlett, A. R. Lehmann, S. P. Jackson and P. A. Jeggo (1999). "Identification of a defect in DNA ligase IV in a radiosensitive leukaemia patient." Curr Biol **9**(13): 699-702.

Richardson, C., N. Horikoshi and T. K. Pandita (2004). "The role of the DNA double-strand break response network in meiosis." DNA Repair (Amst) **3**(8-9): 1149-1164.

Ridgway, P., C. Maison and G. Almouzni. (2002). "Functional organization of the genome: chromatin " Atlas of Genetics and Cytogenetics in Oncology and Haematology.

Robertson, A. B., A. Klungland, T. Rognes and I. Leiros (2009). "DNA repair in mammalian cells: Base excision repair: the long and short of it." Cell Mol Life Sci **66**(6): 981-993.

Rogakou, E. P., C. Boon, C. Redon and W. M. Bonner (1999). "Megabase chromatin domains involved in DNA double-strand breaks in vivo." J Cell Biol **146**(5): 905-916.

Rogakou, E. P., D. R. Pilch, A. H. Orr, V. S. Ivanova and W. M. Bonner (1998). "DNA double-stranded breaks induce histone H2AX phosphorylation on serine 139." J Biol Chem **273**(10): 5858-5868.

Rothkamm, K., I. Kruger, L. H. Thompson and M. Lobrich (2003). "Pathways of DNA double-strand break repair during the mammalian cell cycle." Mol Cell Biol **23**(16): 5706-5715.

Rotman, G. and Y. Shiloh (1999). "ATM: a mediator of multiple responses to genotoxic stress." Oncogene **18**(45): 6135-6144.

Saintigny, Y., K. Makienko, C. Swanson, M. J. Emond and R. J. Monnat, Jr. (2002). "Homologous recombination resolution defect in werner syndrome." Mol Cell Biol **22**(20): 6971-6978.

Sandoval, N., M. Platzer, A. Rosenthal, T. Dork, R. Bendix, B. Skawran, M. Stuhrmann, R. D. Wegner, K. Sperling, S. Banin, Y. Shiloh, A. Baumer, U. Bernthaler, H. Sennefelder, M. Brohm, B. H. Weber and D. Schindler (1999). "Characterization of ATM gene mutations in 66 ataxia telangiectasia families." Hum Mol Genet **8**(1): 69-79.

Scharer, O. D. (2003). "Chemistry and biology of DNA repair." Angew Chem Int Ed Engl **42**(26): 2946-2974.

Scott, S. P. and T. K. Pandita (2006). "The cellular control of DNA double-strand breaks." J Cell Biochem **99**(6): 1463-1475.

Shin, D. S., C. Chahwan, J. L. Huffman and J. A. Tainer (2004). "Structure and function of the double-strand break repair machinery." DNA Repair (Amst) **3**(8-9): 863-873.

Silber, J. R., M. S. Bobola, A. Blank and M. C. Chamberlain (2012). "O(6)-Methylguanine-DNA methyltransferase in glioma therapy: Promise and problems." Biochim Biophys Acta **1826**(1): 71-82.

Smider, V., W. K. Rathmell, M. R. Lieber and G. Chu (1994). "Restoration of X-ray resistance and V(D)J recombination in mutant cells by Ku cDNA." Science **266**(5183): 288-291.

Smith, G. C. and S. P. Jackson (1999). "The DNA-dependent protein kinase." Genes Dev **13**(8): 916-934.

Stahlberg, A., N. Zoric, P. Aman and M. Kubista (2005). "Quantitative real-time PCR for cancer detection: the lymphoma case." Expert Rev Mol Diagn **5**(2): 221-230.

Tauchi, H., S. Matsuura, J. Kobayashi, S. Sakamoto and K. Komatsu (2002). "Nijmegen breakage syndrome gene, NBS1, and molecular links to factors for genome stability." Oncogene **21**(58): 8967-8980.

TJ, P. P. a. M. (1990). "Use of the Tetrazolium Assay in Measuring the Response of Human Tumor Cells to Ionizing Radiation." Cancer Research **50**: 1392-1396.

Turley, H., L. Wu, M. Canamero, K. C. Gatter and I. D. Hickson (2001). "The distribution and expression of the Bloom's syndrome gene product in normal and neoplastic human cells." Br J Cancer **85**(2): 261-265.

Ulsh, B. A. (2010). "Checking the foundation: recent radiobiology and the linear no-threshold theory." Health Phys **99**(6): 747-758.

Valko, M., D. Leibfritz, J. Moncol, M. T. Cronin, M. Mazur and J. Telser (2007). "Free radicals and antioxidants in normal physiological functions and human disease." Int J Biochem Cell Biol **39**(1): 44-84.

van der Burg, M., H. Ijspeert, N. S. Verkaik, T. Turul, W. W. Wiegant, K. Morotomi-Yano, P. O. Mari, I. Tezcan, D. J. Chen, M. Z. Zdzienicka, J. J. van Dongen and D. C. van Gent (2009). "A DNA-PKcs mutation in a radiosensitive T-B-SCID patient inhibits Artemis activation and nonhomologous end-joining." J Clin Invest **119**(1): 91-98.

van der Burg, M., J. J. van Dongen and D. C. van Gent (2009). "DNA-PKcs deficiency in human: long predicted, finally found." Curr Opin Allergy Clin Immunol **9**(6): 503-509.
Varon, R., C. Vissinga, M. Platzer, K. M. Cerosaletti, K. H. Chrzanowska, K. Saar, G. Beckmann, E. Seemanova, P. R. Cooper, N. J. Nowak, M. Stumm, C. M. Weemaes, R. A. Gatti, R. K. Wilson, M. Digweed, A. Rosenthal, K. Sperling, P. Concannon and A. Reis (1998). "Nibrin, a novel DNA double-strand break repair protein, is mutated in Nijmegen breakage syndrome." Cell **93**(3): 467-476.
Verbeek, B., T. D. Southgate, D. E. Gilham and G. P. Margison (2008). "O6-Methylguanine-DNA methyltransferase inactivation and chemotherapy." Br Med Bull **85**: 17-33.
Vichai, V. and K. Kirtikara (2006). "Sulforhodamine B colorimetric assay for cytotoxicity screening." Nat Protoc **1**(3): 1112-1116.
Voigt, W. (2005). "Sulforhodamine B assay and chemosensitivity." Methods Mol Med **110**: 39-48.
Ward, J. F. (1985). "Biochemistry of DNA lesions." Radiat Res Suppl **8**: S103-111.
Weemaes, C. M., T. W. Hustinx, J. M. Scheres, P. J. van Munster, J. A. Bakkeren and R. D. Taalman (1981). "A new chromosomal instability disorder: the Nijmegen breakage syndrome." Acta Paediatr Scand **70**(4): 557-564.
West, R. B., M. Yaneva and M. R. Lieber (1998). "Productive and nonproductive complexes of Ku and DNA-dependent protein kinase at DNA termini." Mol Cell Biol **18**(10): 5908-5920.
Weterings, E. and D. C. van Gent (2004). "The mechanism of non-homologous end-joining: a synopsis of synapsis." DNA Repair (Amst) **3**(11): 1425-1435.
Willers, H., J. Dahm-Daphi and S. N. Powell (2004). "Repair of radiation damage to DNA." Br J Cancer **90**(7): 1297-1301.
Williams, V. M., M. Filippova, U. Soto and P. J. Duerksen-Hughes (2011). "HPV-DNA integration and carcinogenesis: putative roles for inflammation and oxidative stress." Future Virol **6**(1): 45-57.
Wiseman, H. and B. Halliwell (1996). "Damage to DNA by reactive oxygen and nitrogen species: role in inflammatory disease and progression to cancer." Biochem J **313 (Pt 1)**: 17-29.
Wogan, G. N., S. S. Hecht, J. S. Felton, A. H. Conney and L. A. Loeb (2004). "Environmental and chemical carcinogenesis." Semin Cancer Biol **14**(6): 473-486.
Wood, R. D. (1997). "Nucleotide excision repair in mammalian cells." J Biol Chem **272**(38): 23465-23468.
Wood, R. D., M. Mitchell, J. Sgouros and T. Lindahl (2001). "Human DNA repair genes." Science **291**(5507): 1284-1289.
Wyman, C., D. Ristic and R. Kanaar (2004). "Homologous recombination-mediated double-strand break repair." DNA Repair (Amst) **3**(8-9): 827-833.
Xu, Y. and D. Baltimore (1996). "Dual roles of ATM in the cellular response to radiation and in cell growth control." Genes Dev **10**(19): 2401-2410.
Yasaei, H. and P. Slijepcevic (2010). "Defective Artemis causes mild telomere dysfunction." Genome Integr **1**(1): 3.
Yung, W. K. (1989). "In vitro chemosensitivity testing and its clinical application in human gliomas." Neurosurg Rev **12**(3): 197-203.

Appendix

The two papers published during this project are attached in the next page.